6-2016

Mechanisms of Immune Activation and Suppression by Parasitic Wasps of *Drosophila*

Johnny R. Ramroop
Graduate Center, City University of New York

Mechanisms of Immune Activation and Suppression by Parasitic Wasps of *Drosophila*

By

Johnny R. Ramroop

A dissertation submitted to the Graduate Faculty in Biology in partial fulfillment of the requirements for the degree of Doctor of Philosophy.

THE CITY UNIVERSITY OF NEW YORK

2016

This manuscript has been read and accepted for the Graduate Facility in Biology in satisfaction of the dissertation requirement for the degree of Doctor of Philosophy.

Shubha Govind, Ph.D.

_____	_____
Date	Chair of the Examining Committee

Laurel A. Eckhardt, Ph.D.

_____	_____
Date	Executive Officer

Supervisory Committee:

Mark Pezzano, Ph.D

Linda Spatz, Ph.D

Diana Bratu, Ph.D.

Eric Lai, Ph.D

THE CITY UNIVERSITY OF NEW YORK

Abstract

Mechanisms of Immune Activation and Suppression by Parasitic Wasps of *Drosophila*

By

Johnny R. Ramroop

Advisor: Dr. Shubha Govind

Thesis Overview

Drosophila melanogaster has served as an excellent model organism to study the molecular processes of innate immunity. Flies essentially lack adaptive immunity and the innate immune system is often divided into the humoral and cellular responses (LEMAITRE and HOFFMANN 2007). The humoral arm involves the production of antimicrobial peptides, secreted from the fat body, to combat bacterial and fungal infections. The cellular response involves the production of hemocytes (blood cells: crystal cells, plasmatocytes, and lamellocytes) in the larval lymph gland, in the sessile pools, and in circulation (GOLD and BRUCKNER 2014). Microbial pathogens are phagocytosed by plasmatocytes whereas larger parasites such as parasitic wasp eggs are neutralized by egg encapsulation, principally by lamellocytes. The innate immune response is vital for survival against the abundant pathogens and parasites in their natural habitats. The range of microbial as well as Hymenoptera species that attack their Diptera hosts is

vast. These pathogens and parasitoids have evolved strategies to either evade or suppress host immune responses (KEEBAUGH 2013).

This thesis contains two chapters. In Chapter 1, we focused on the mechanisms underlying host defense in response to specialist wasps of *D. melanogaster*, *Leptopilina boulardi*. Chapter 1 is already published (SMALL *et al.* 2014) and I shared first authorship with Dr. Small.

Previous experiments demonstrated that Notch (N) signaling is essential for crystal cell specification and differentiation (DUVIC *et al.* 2002; LEBESTKY *et al.* 2003), and also promotes lamellocyte differentiation (DUVIC *et al.* 2002). The N ligand, Serrate is expressed in the posterior signaling center (PSC), a non-hematopoietic cell population, also called the niche. Through direct contact, the PSC activates N signaling in the developing hematopoietic cells and instructs them to become crystal cells (LEBESTKY *et al.* 2003). *L. boulardi* infection promotes lamellocyte but inhibits crystal cell differentiation (KRZEMIEN *et al.* 2010). ROS production is also activated in the PSC upon wasp infection (SINENKO *et al.* 2011). In Chapter 1, we demonstrate a second function for N signaling: *L. boulardi* parasitization inactivates N signaling in the developing lymph gland lobes; reduction of N signaling correlates with lamellocyte differentiation. We also demonstrate an unexpected link between N signaling and ROS in restricting differentiation of hematopoietic progenitors (SMALL *et al.* 2014).

In chapter 2, we focused on strategies that the generalist parasitic wasp *L. heterotoma* employs to actively suppress the hosts' immune responses. Building on previous work that showed that *L. boulardi* infection activates NF-κB signaling in the PSC (GUEGUEN *et al.* 2013), we examined changes in the PSC and hematopoietic progenitors after *L. heterotoma* infection and found reduction in gene expression in the PSC, presence of VLPs around (but not within)

PSC cells, and significant reduction in the progenitor population. Consistent with previous results (CHIU 2002), this reduction correlates with Caspase activation in plasmatocytes and lysis of lamellocytes, within the lymph gland and circulating hemocyte populations. These responses are mediated by virus-like particles (VLPs) produced in the *L. heterotoma* venom.

L. heterotoma VLPs have 4-8 spikes and the spike-to-spike distance is roughly 300 nm (RIZKI and RIZKI 1990). A mouse polyclonal antibody against VLPs was generated previously in our lab and immuno-electron microscopy (EM) experiments localized this protein's origin to secretory cells of the venom gland (CHIU *et al.* 2006). The p40 protein is also present in large amounts in the lumen of the venom gland where VLPs undergo biogenesis and assembly (MORALES *et al.* 2005)(CHIU *et al.* 2006). VLPs are ultimately deposited into the host hemocoel during the egg laying process (CHIU *et al.* 2006). Immuno-EM of purified mature VLPs localizes p40 to the VLP spike surface and spike termini. p40 is also present in plasmatocytes and lamellocytes of host cells. Proteomic analyses of *L. heterotoma* VLPs reveal more than 150 proteins, some of which are not expressed in *L. boulardi* (Govind lab, unpub. results).

In Chapter 2, we show (1) differential effects of *L. boulardi* (lamellocyte differentiation, activation of gene expression in the PSC) and *L. heterotoma* (cell death, repression of gene expression in PSC) on lymph gland homeostasis; (2) the subcellular localization of p40 (punctate and vesicular in plasmatocytes, nuclear in lamellocytes); (3) Rab5-dependent entry into plasmatocytes but not in lamellocytes; (4) an immune function for the PSC. Molecular characterization of p40 revealed a protein with signal sequence, a central helical domain, and C-terminal transmembrane domain. The central helical domain share structural similarity with proteins of the SipD/IpaD family, normally present on tips of Gram negative bacterial type three secretion system needles. Incubation of bacterial extracts with live lamellocytes resulted in

alteration in cell morphology. We hypothesize a direct role for p40 in mediating VLP entry into lamellocytes. These studies constitute the first detailed investigation of any VLP protein and begin to uncover mechanisms of active immune suppression by VLPs. They also contribute to our understanding of the biotic nature of VLPs.

CHIU, H., GOVIND, S., 2002 Natural infection of *D. melanogaster* by virulent parasitic wasps induces apoptotic depletion of hematopoietic precursors. Cell Death Differ 9: 1379-1381.

CHIU, H., J. MORALES and S. GOVIND, 2006 Identification and immuno-electron microscopy localization of p40, a protein component of immunosuppressive virus-like particles from Leptopilina heterotoma, a virulent parasitoid wasp of Drosophila. J Gen Virol 87: 461-470.

DUVIC, B., J. A. HOFFMANN, M. MEISTER and J. ROYET, 2002 Notch signaling controls lineage specification during Drosophila larval hematopoiesis. Curr Biol 12: 1923-1927.

GOLD, K. S., and K. BRUCKNER, 2014 Drosophila as a model for the two myeloid blood cell systems in vertebrates. Exp Hematol 42: 717-727.

KEEBAUGH, E. S., SCHLENKE, T.A., 2013 Insights from natural host–parasite interactions: The Drosophila model. Dev Comp Immunol In press.

LEBESTKY, T., S. H. JUNG and U. BANERJEE, 2003 A Serrate-expressing signaling center controls Drosophila hematopoiesis. Genes Dev 17: 348-353.

LEMAITRE, B., and J. HOFFMANN, 2007 The host defense of Drosophila melanogaster. Annu Rev Immunol 25: 697-743.

RIZKI, R. M., and T. M. RIZKI, 1990 Parasitoid virus-like particles destroy Drosophila cellular immunity. Proc Natl Acad Sci U S A 87: 8388-8392.

SMALL, C., J. RAMROOP, M. OTAZO, L. H. HUANG, S. SALEQUE *et al.*, 2014 An unexpected link between notch signaling and ROS in restricting the differentiation of hematopoietic progenitors in Drosophila. Genetics 197: 471-483.

Introduction

Because of deep molecular conservation (ADAMS *et al.* 2000), *D. melanogaster* serves as an excellent model for studying fundamental biological processes, including innate immunity and hematopoiesis. *Drosophila* lacks adaptive immunity and relies primarily on innate immune responses to defend against infectious bacteria, viruses, fungi, and metazoan parasites such as parasitic wasps. Innate immunity in flies is divided into the humoral and cellular responses. Humoral immunity involves secretion of anti-microbial peptides and other proteins from the fat body into the hemolymph. Microbial or wasp infection activates the transcription of specific antimicrobial peptide genes; genetic activation of antimicrobial genes depends on Toll/IMD signaling and functions of the NF-κB family transcription factors (GOVIND 2008; HULTMARK 2003; LEMAITRE and HOFFMANN 2007). Cellular immunity engages the functions of three classes of blood cells or hemocytes that either phagocytose microbes or encapsulate larger, metazoan pathogens (CROZATIER and MEISTER 2007; HULTMARK 2003; LEMAITRE and HOFFMANN 2007). In this thesis, we are concerned with hematopoiesis and hemocyte functions in host defense against natural parasitic wasps of fruit flies. Wasps attack larval stages of their fly hosts(SMALL *et al.* 2012). Wasps differ in their host range and virulence strategies and can either activate one or both arms of the immune system or suppress host defense altogether (HEAVNER *et al.* 2014; LEE *et al.* 2009). A brief introduction to the wasps, cell types, and immune responses follows.

Drosophila and their parasitic wasps

In their natural environment, the cosmopolitan fruit flies of the genus *Drosophila* are attacked by endoparasitoid wasps. While the fly host is armed with innate immunity, the wasps also possess virulence mechanisms to inactivate host immune responses. Thus, both insect species are engaged in a biological arms race for survival (HEAVNER *et al.* 2014). We use a

natural *Drosophila*-wasp host-parasite model system to decipher mechanisms of host defense against larval parasites as well as virulence mechanisms of endoparasitoid wasp species of the genus *Leptopilina* (HEAVNER *et al.* 2014; LEE *et al.* 2009; SMALL *et al.* 2012). Depending on the infecting wasp species and the infected fly species, there can be one of two outcomes. If the host is able to mount a strong immune response, parasitization is unsuccessful, the parasite is sequestered and killed, and the fly continues through its development to eclose in approximately 15 days. If parasitization is successful either because the parasite is armed with virulence mechanisms or the host is immune-compromised; the parasite develops and consumes the developing host, emerging from the host's pupal case in roughly 30 days (MELK and GOVIND 1999; SMALL *et al.* 2012).

Wasps of the *Leptopilina spp*. (ALLEMAND 2002; SCHILTHUIZEN 1998) are popular models for investigating questions in ecology, population biology, and host-parasite interactions. *D. melanogaster* is inarguably the best characterized insect and the most popular host for *Drosophila/Leptopilina* studies. *D. melanogaster* offers a plethora of genetic tools for in-depth studies and also serves as a reference genus for the analysis of gene functions of other *Drosophila/*species attacked by *Leptopilina*. The genomes of a dozen *Drosophila* hosts have been sequenced (ASHBURNER 2007; CLARK *et al.* 2007) providing opportunities to test molecular and evolutionary hypotheses. Artificially selected *D. melanogaster* hosts with high resistance to wasps compete poorly as larvae, feed slowly, and possess higher hemocyte density than controls suggesting tradeoff mechanisms for anti-parasite defense functions (KRAAIJEVELD and GODFRAY 1997; KRAAIJEVELD *et al.* 2001).

L. boulardi is a specialist wasp species and attacks a small range of flies in the melanogaster group including *D. yakuba* (SCHLENKE *et al.* 2007). Infection with *L. boulardi*

strain 17 activates the NF-κB transcription factors Dorsal/Dif and the canonical target gene, *drosomycin* (PADDIBHATLA *et al.* 2010; SCHLENKE *et al.* 2007). Different *L. boulardi* strains exhibit intraspecific differences in virulence and have served to identify venom factors that might underlie variation in wasp success (DUBUFFET *et al.* 2009). The venom of *L. boulardi* contains virus-like particles (VLPs) (GUEGUEN *et al.* 2011; SCHLENKE *et al.* 2007) although no specific virulence function has been attributed to them yet. *L. boulardi* strain 17 is highly virulent on *D. melanogaster* but is not as successful on *D. yakuba*, a fly in the melanogaster group (SCHLENKE *et al.* 2007). In fact, *L. boulardi 17* infection activates the transcription of numerous genes of both the humoral (antimicrobial peptide genes) and the cellular (genes for hematopoiesis and activation and differentiation of hemocytes) immune pathways (LEE *et al.* 2009; SCHLENKE *et al.* 2007). Yet, the parasite venom alters hemocyte shape and function and blocks the wasp egg encapsulation response (COLINET *et al.* 2007; DUBUFFET *et al.* 2009). A *L. boulardi*-specific venom protein called LbGAP has been identified within lamellocytes with altered cell shape, the principal cell type involved in encapsulation (COLINET *et al.* 2007).

In contrast *to L. boulardi*, *L. heterotoma*, a generalist parasitic wasp, is successful on a wider host range and overcomes both cellular and humoral responses (SCHLENKE *et al.* 2007). Overall, *L. heterotoma* attack is not followed by significant changes in gene expression (SCHLENKE *et al.* 2007). In fact, cells of the cellular arm, both progenitors and mature plasmatocytes and lamellocytes are killed or lysed (CHIU and GOVIND 2002; RIZKI and RIZKI 1984; RIZKI and RIZKI 1994). *L. heterotoma* VLPs produced in the long gland of the venom gland (FERRARESE *et al.* 2009) are morphologically similar to *L. boulardi* VLPs (GUEGUEN *et al.* 2011) and are thought to be responsible for hemocyte lysis (RIZKI and RIZKI 1984; RIZKI and RIZKI 1990; RIZKI and RIZKI 1994). Thus, *L. boulardi* and *L. heterotoma*, although

phylogenetically related, utilize different infection strategies. *L. victoriae*, a sister species to *L. heterotoma* (ALLEMAND 2002) shares virulence properties and VLP functions with *L. heterotoma* VLPs (CHIU and GOVIND 2002; CHIU *et al.* 2006; MORALES *et al.* 2005). The most abundant proteins of *L. heterotoma* and *L. victoriae* VLPs have been shown to possess virulence function(CHIU *et al.* 2006). VLP structure and function are investigated in this thesis.

Drosophila hematopoiesis and blood cells

Drosophila larvae have an open circulatory system and hemocytes are present in three main hematopoietic compartments; circulating (free floating, clusters of sessile population (LEITAO and SUCENA 2015) (MAKHIJANI *et al.* 2011), and lymph gland (larval hematopoietic organ (FOSSETT 2013). There are three hemocyte cell types; plasmatocytes, crystal cells and lamellocytes (Figure 1). Plasmatocytes are the most abundant, representing approximately 95% of the total hemocyte population. They are phagocytic and engulf dead cells/tissue as well as microbial pathogens. Crystal cells are less abundant, making up approximately 5% of the total hemocyte population. They express pro-phenoloxidase that is involved in melanization reaction and wound healing. Lamellocytes are rarely found in healthy third instar larvae and their differentiation is induced by wasp infection. Lamellocytes are large, adhesive cells that encapsulate and melanize foreign parasites that are too large to be phagocytosed by plasmatocytes (GOLD and BRUCKNER 2014; GOVIND 2008; LANOT *et al.* 2001; SORRENTINO *et al.* 2002).

Drosophila hematopoiesis occurs in two waves: (1) an early primitive wave during embryogenesis that results in the production of plasmatocytes and crystal cells and (2) a definitive wave that occurs during larval development. Hemocytes from both hematopoietic waves persist until adult flies (HOLZ *et al.* 2003). A cascade of transcription factor activities

controls hematopoietic lineage development and fate choice (Figure 1). The GATA family protein, Serpent, and Friend-of-GATA U-shaped are important in the initial hematopoietic specification step (LEBESTKY *et al.* 2000). Notch signaling and Lozenge specify crystal cell differentiation (DUVIC *et al.* 2002; LEBESTKY *et al.* 2003) (TERRIENTE-FELIX *et al.* 2013). Glial cell missing (Gcm 1 and Gcm2) (ALFONSO and JONES 2002) and PDGF/VEGF Receptor (PVR) (JUNG *et al.* 2005) mediate plasmatocytes specification. A number of signaling pathways, transcription factors as well as reactive oxygen species control hemocyte development in a context and stage-specific manner (Figure 1).

Plasmatocytes and lamellocytes are over represented in the hemocoel of some mutants such as larvae carrying the *hopscotch*$^{Tum\text{-}l}$ ((*hop*$^{Tum\text{-}l}$) mutation. A point mutation causes constitutive activation of the JAK kinase *hopscotch* and leads to hyperproliferation of circulating and lymph gland hemocytes and the formation of melanotic tumors (LUO *et al.* 1995). These cell types can be distinguished by differences in antigenic markers or with specific endogenous reporters [(Figure 2 (EVANS *et al.* 2014; GOLD and BRUCKNER 2014; KURUCZ *et al.* 2007b)].

At the third instar stage, the lymph gland contains a pair of large anterior lobes and two sets of smaller posterior lobes that flank the dorsal vessel (Figure 3). The anterior lobe contains three main regions: the posterior signaling center (PSC), the medullary zone (MZ) and the cortical zone (CZ) (Figure 3). The PSC or niche is a cluster of approximately 25-50 cells located at the base of the anterior lobes and provides the microenvironment for hemocyte quiescence/differentiation (BENMIMOUN *et al.* 2015; CROZATIER *et al.* 2004; KRZEMIEN *et al.* 2007; LEBESTKY *et al.* 2003; MANDAL *et al.* 2007). Stem-like progenitors in the MZ cycle slowly, relative to cells in the cortical zone are multipotent (JUNG *et al.* 2005; MINAKHINA and STEWARD 2010). The cortex or (CZ) contains mature differentiated cells that are mitotically

active (JUNG *et al.* 2005) (Figure 3). Mature cells in the CZ are released into circulation during metamorphosis or following an immune challenge (LANOT *et al.* 2001).

Several cell-specific genes are expressed in different regions of the lymph gland. Serrate, Antennapedia and Collier are expressed in the PSC (CROZATIER *et al.* 2004; JUNG *et al.* 2005; MANDAL *et al.* 2007). Domeless, the JAK/STAT receptor, is expressed in the medulla (EVANS 2007), Peroxidasin (Pxn) is expressed in mature plasmatocytes, Lozenge (Lz) and Pro-phenoloxidase are expressed in mature crystal cells, both populate the cortex of the lymph gland (JUNG *et al.* 2005). An enhancer in the *misshapen* (*msn*) gene (TOKUSUMI *et al.* 2009) and integrin β PS (STOFANKO *et al.* 2008) are expressed in lamellocytes. Antibodies against the antigens expressed in these cell types distinguish their identity; P1 (Nimrod C) for plasmatocytes (KURUCZ *et al.* 2007a), ProPO for crystal cells and integrin β for lamellocytes. These cell types can also be stained with phalloidin also reveal different cell sizes and shape to differentiate them; lamellocytes being the largest and most highly stained (EVANS *et al.* 2014).

Notch signaling in *Drosophila* hematopoiesis

Notch signaling is a juxtacrine signaling pathway (GAZAVE *et al.* 2009; RADTKE *et al.* 2005). The Notch receptor is activated after ligand-receptor interaction. Two sequential proteolytic cleavages follow. The first cleavage by the metalloprotease TACE (tumor necrosis factor α-converting enzyme) occurs within the extracellular domain. The extracellular subunit of the receptor is trans-endocytosed along with the ligand into the nearby signal sending cell and targeted for degradation. The second cleavage occurs within the transmembrane domain by the γ-secretase activity of the multi-protein complex of presenilins, which includes Nicastrin, APH-1 and PEN-2. The Notch (NICD) then translocates into the nucleus and binds to the transcription factor Supressor of Hairless. This replaces corepressors with coactivators leading to

transcriptional activation (GAZAVE *et al.* 2009; RADTKE *et al.* 2005). Serrate mediated Notch signaling from the PSC signals progenitors to differentiate into crystal cells (DUVIC *et al.* 2002; LEBESTKY *et al.* 2003). Post parasitization lamellocyte differentiation occurs at the expense of crystal cells (KRZEMIEN *et al.* 2010).

Noncanonical and ligand-independent Notch signaling promotes hemocyte survival. Contact between signal-sending and -receiving cells maintains active Notch signaling. Cells in circulation circumvent this need through noncanonical Notch activation via stabilization of the Notch receptor in the endocytic pathway. This is mediated by Hif-α in the absence of ligand binding resulting in the expansion of the mature crystal cell population (MUKHERJEE *et al.* 2011).

Methods

The UAS-GAL4 system is one of the many powerful tools used in *Drosophila* genetics (BLAIR 2003; BRAND and PERRIMON 1993). This binary expression system consists of two components (1) the yeast GAL4 transcriptional activator expressed in a tissue specific manner under the control of an endogenous promoter/enhancer or one that is engineered 5' to the GAL4 coding sequence; and (2) an "overexpression" construct or inhibitory RNA construct transgene under the control of the yeast *UAS* (upstream activation sequence and binding site for GAL4) promoter. This versatile system can be used to misexpress a gene in a cell and/or tissue of choice. Reporter genes such as *GFP* or *lacZ* when expressed under the control of GAL4 mark the desired cell population. Similarly, cells whose functions are sought may be eliminated by ablation by expressing a pro-apoptotic gene. The UAS and GAL4 strains used in this study are listed under the Methods sections for each chapter.

Genetic mosaic techniques are used to study the effects of loss-of-function or gain-of-function mutations that may cause early embryonic or larval lethality allowing gene function

analysis in later developmental stages (BLAIR 2003). These techniques limit the mutation to only a subset of cells within a tissue or organ at the desired developmental stage. Clonal analyses are frequently used to gauge the precise phenotype of a mutation at the cellular level and reveals autonomous/non-autonomous gene action in a specific biological process. In this study, we made FLP-out clones (STRUHL and BASLER 1993) to produce loss-of-function clones for Notch, using an RNAi construct. FLP recombinase binds to the FRT sequences and mediates recombination (STRUHL and BASLER 1993). Mitotic recombination generates GFP-marked clones under the control of a heat shock sensitive *hsp70* regulatory sequence. Exposing developmentally-synchronized 4-day old larvae (genotype *hs-flp; actinFRTstopFRT Gal4, UAS-mcd8GFP*) to heat shock (37^{o}C for 15 minutes) activates mitotic recombination in *cis* and allows the actin promoter to drive GFP expression. Daughter cells of the cell in which recombination occurred are GFP-positive. Clones can be induced by heat shock, without (control cells), or with (experimental cells with the interfering RNA), at different time points. Similarly, the FLP/FRT system can be used to similarly to generate clones that overexpress protein or that express mutanted protein. Clones are characterized by examining the expression of cell specific markers, or changes in cell morphology, or cell viability. If the mutant phenotype coincides with the mutant clones, the gene function is considered to be cell autonomous.

Genetic mosaics to study gene function in developing tissues can also be produced by the twin clone method (BLAIR 2003; XU and RUBIN 1993). This technique involves FRTs placed in *trans* at the same locus of homologous chromosomes. The FRT is inserted into proximal locations (close to the centromere) on the chromosome arm bearing the loss-of-function mutation. The FLP recombinase is produced by heat shock (*hsp70* regulatory sequence drives the coding sequence of FLP recombinase). If there are two FRTs in identical positions on

homologous chromosomes but the animal is heterozygous for the mutation in question, then recombination between these FRT sites (BLAIR 2003; XU and RUBIN 1993) produces sister clones (cells homozygous for the mutation and cells with two wild type copies) in a heterozygous background. Markers such as *lacZ*, linked to the FRT with the wild type allele for example, can be used to distinguish the different clone cell populations. Homozygous mutant clones will carry zero copies of *lacZ* and will not express beta-galactosidase, whereas cells in the wild type clone will carry and express two copies of *lacZ* (XU and RUBIN 1993).

Conclusion

This thesis is divided into two chapters. Chapter 1 focuses on the role of Notch signaling in lamellocyte differentiation in response to *L. boulardi*. This work was published in Genetics in 2014 with other co-authors. Their contributions are noted in the acknowledgements and with Figure legends. The second chapter focuses on the characterization of VLP protein p40 and its possible function in immune suppression by *L. heterotoma*. The main findings from both chapters are summarized in the thesis abstract.

Figure 1. Plasticity in hematopoietic development

A simplified view hematopoietic lineages and hemocyte types in fly larvae. The GATA transcription factor Serpent, when bound to the coregulator Friend of GATA (GATA:FOG complex) controls cell fate choice through interactions with other transcription factors and Notch, JAK-STAT, BMP, hedgehog, JNK, EGFR, wingless, or NF-κB signaling pathways. Reactive oxygen species also influence the quiescence versus differentiation decision. The genetic mechanisms underlying cell fate choice is context-specific, depending on the developmental stage and hematopoietic compartment. Plasmatocytes can transdifferentiate into either lamellocytes or crystal cells. For more details see (FOSSETT 2013; GOLD and BRUCKNER 2014; LEBESTKY *et al.* 2000; LEITAO and SUCENA 2015; MINAKHINA and STEWARD 2010; MINAKHINA *et al.* 2011; OWUSU-ANSAH and BANERJEE 2009; SINENKO *et al.* 2012; STOFANKO 2010).

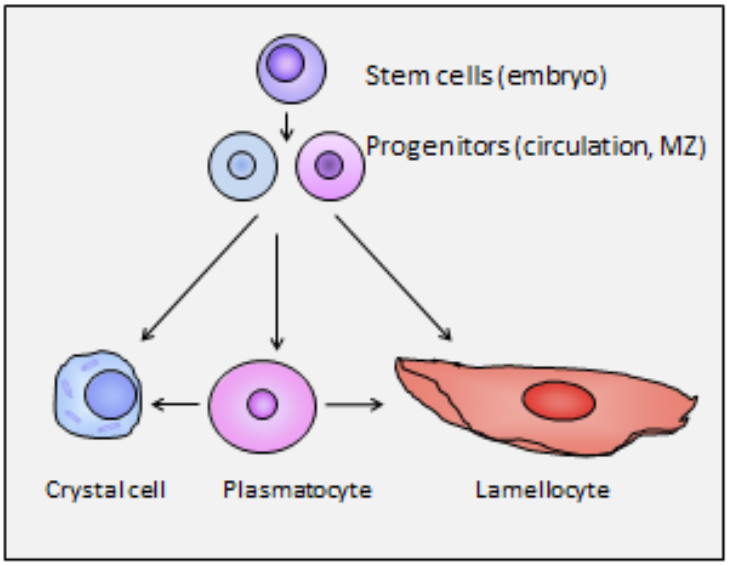

Maria Otazo helped with this schematic.

Figure 2. *hopscotch*$^{Tumorous\text{-}lethal}$ (*hop*$^{Tum\text{-}l}$) larvae provide a ready source of plasmatocytes and lamellocytes

Circulating hemocyte population in the *hop*$^{Tum\text{-}l}$ mutant background. *hop*$^{Tum\text{-}l}$ *msn-GAL4*; *UAS-mCD8-GFP* uses the *misshapen* promoter (TOKUSUMI *et al.* 2009) to label lamellocytes by mCD8-GFP expression. GFP-negative cells express the P1 antigen (Nimrod C--red) (KURUCZ *et al.* 2007a) in this mutant background. Plasmatocytes predominate in the circulating population of wild type animals and lamellocytes are rarely seen.

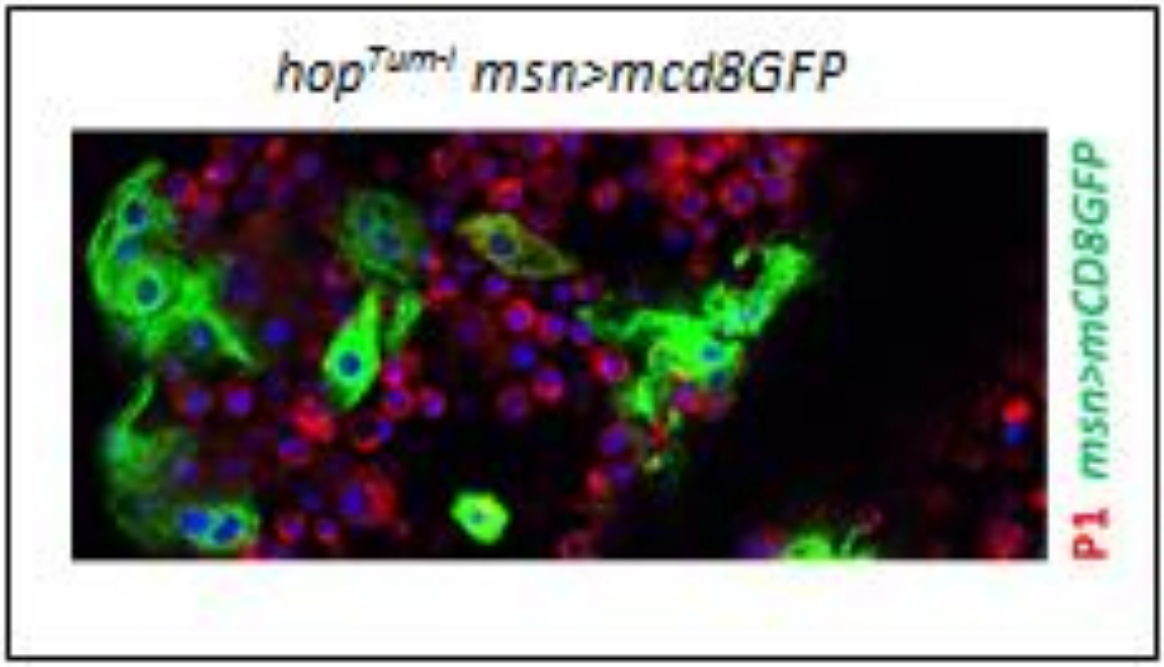

Figure 3. Schematic of the third instar lymph gland

The three regions of the lymph gland in the anterior lobes: PSC- posterior signaling center, MZ- medullary zone or medulla (with quiescent prohemocyte progenitors), and CZ- cortical zone or cortex (with mature differentiated hemocytes) are shown. Region-specific markers include; *Antp-Gal4* (for PSC), *Domeless-Gal4* (for MZ) and *Hml-Gal4* (for cells in the CZ). A triple-fluorescence reporter line (EVANS *et al.* 2014) identifies the three lymph gland regions: *Hml-DsRed* (CZ), *dome MESO-EBFP2* (MZ) and *hh-GFP* (PSC). Posterior lobes do not show such regionalization and harbor immature progenitors.

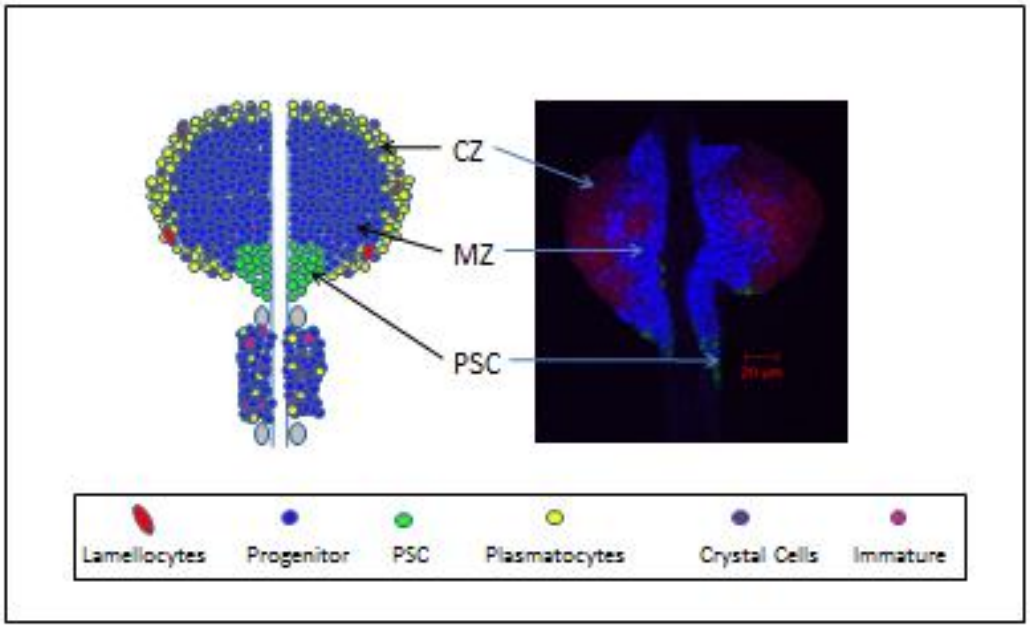

Literature Cited

ADAMS, M. D., S. E. CELNIKER, R. A. HOLT, C. A. EVANS, J. D. GOCAYNE *et al.*, 2000 The genome sequence of Drosophila melanogaster. Science 287: 2185-2195.

ALFONSO, T. B., and B. W. JONES, 2002 gcm2 promotes glial cell differentiation and is required with glial cells missing for macrophage development in Drosophila. Dev Biol 248: 369-383.

ALLEMAND, R., LEMAITRE, C., FREY, F., BOULETREAU, M., VAVRE, F., NORLANDER, G., VAN ALPHEN, J., CARTON, Y., 2002 Phylogeny of six African Leptopilina species (Hymenoptera: Cynipoidea, Figitidae), parasitoids of Drosophila, with description of three new species. Ann Soc entomol Fr (n.s.) 38: 319-332.

ASHBURNER, M., 2007 Drosophila Genomes by the Baker's Dozen. Preface. Genetics 177: 1263-1268.

BENMIMOUN, B., C. POLESELLO, M. HAENLIN and L. WALTZER, 2015 The EBF transcription factor Collier directly promotes Drosophila blood cell progenitor maintenance independently of the niche. Proc Natl Acad Sci U S A 112: 9052-9057.

BLAIR, S. S., 2003 Genetic mosaic techniques for studying Drosophila development. Development 130: 5065-5072.

BRAND, A. H., and N. PERRIMON, 1993 Targeted gene expression as a means of altering cell fates and generating dominant phenotypes. Development 118: 401-415.

CHIU, H., and S. GOVIND, 2002 Natural infection of D. melanogaster by virulent parasitic wasps induces apoptotic depletion of hematopoietic precursors. Cell Death Differ 9: 1379-1381.

CHIU, H., J. MORALES and S. GOVIND, 2006 Identification and immuno-electron microscopy localization of p40, a protein component of immunosuppressive virus-like particles from Leptopilina heterotoma, a virulent parasitoid wasp of Drosophila. J Gen Virol 87: 461-470.

CLARK, A. G., M. B. EISEN, D. R. SMITH, C. M. BERGMAN, B. OLIVER *et al.*, 2007 Evolution of genes and genomes on the Drosophila phylogeny. Nature 450: 203-218.

COLINET, D., A. SCHMITZ, D. DEPOIX, D. CROCHARD and M. POIRIE, 2007 Convergent use of RhoGAP toxins by eukaryotic parasites and bacterial pathogens. PLoS Pathog 3: e203.

CROZATIER, M., and M. MEISTER, 2007 Drosophila haematopoiesis. Cell Microbiol 9: 1117-1126.

CROZATIER, M., J. M. UBEDA, A. VINCENT and M. MEISTER, 2004 Cellular immune response to parasitization in Drosophila requires the EBF orthologue collier. PLoS Biol 2: E196.

DUBUFFET, A., D. COLINET, C. ANSELME, S. DUPAS, Y. CARTON *et al.*, 2009 Variation of Leptopilina boulardi success in Drosophila hosts: what is inside the black box? Adv Parasitol 70: 147-188.

DUVIC, B., J. A. HOFFMANN, M. MEISTER and J. ROYET, 2002 Notch signaling controls lineage specification during Drosophila larval hematopoiesis. Curr Biol 12: 1923-1927.

EVANS, C. J., T. LIU and U. BANERJEE, 2014 Drosophila hematopoiesis: Markers and methods for molecular genetic analysis. Methods 68: 242-251.

EVANS, C. J., SINENKO, S.A., MANDAL, L., MARTINEZ-AGOSTO, J.A., HARTENSTEIN,V. AND BANERJEE, UE, 2007 *Genetic Dissection of Hematopoiesis Using Drosophila as a Model System*.

FERRARESE, R., J. MORALES, D. FIMIARZ, B. A. WEBB and S. GOVIND, 2009 A supracellular system of actin-lined canals controls biogenesis and release of virulence factors in parasitoid venom glands. J Exp Biol 212: 2261-2268.

FOSSETT, N., 2013 Signal transduction pathways, intrinsic regulators, and the control of cell fate choice. Biochim Biophys Acta 1830: 2375-2384.

GAZAVE, E., P. LAPEBIE, G. S. RICHARDS, F. BRUNET, A. V. ERESKOVSKY *et al.*, 2009 Origin and evolution of the Notch signalling pathway: an overview from eukaryotic genomes. BMC Evol Biol 9: 249.

GOLD, K. S., and K. BRUCKNER, 2014 Drosophila as a model for the two myeloid blood cell systems in vertebrates. Exp Hematol 42: 717-727.

GOVIND, S., 2008 Innate immunity in Drosophila: Pathogens and pathways. Insect Sci 15: 29-43.

GUEGUEN, G., R. RAJWANI, I. PADDIBHATLA, J. MORALES and S. GOVIND, 2011 VLPs of Leptopilina boulardi share biogenesis and overall stellate morphology with VLPs of the heterotoma clade. Virus Res 160: 159-165.

HEAVNER, M. E., A. D. HUDGINS, R. RAJWANI, J. MORALES and S. GOVIND, 2014 Harnessing the natural - parasitoid model for integrating insect immunity with functional venomics. Curr Opin Insect Sci 6: 61-67.

HOLZ, A., B. BOSSINGER, T. STRASSER, W. JANNING and R. KLAPPER, 2003 The two origins of hemocytes in Drosophila. Development 130: 4955-4962.

HULTMARK, D., 2003 Drosophila immunity: paths and patterns. Curr Opin Immunol 15: 12-19.

JUNG, S. H., C. J. EVANS, C. UEMURA and U. BANERJEE, 2005 The Drosophila lymph gland as a developmental model of hematopoiesis. Development 132: 2521-2533.

KRAAIJEVELD, A. R., and H. C. GODFRAY, 1997 Trade-off between parasitoid resistance and larval competitive ability in Drosophila melanogaster. Nature 389: 278-280.

KRAAIJEVELD, A. R., E. C. LIMENTANI and H. C. GODFRAY, 2001 Basis of the trade-off between parasitoid resistance and larval competitive ability in Drosophila melanogaster. Proc Biol Sci 268: 259-261.

KRZEMIEN, J., L. DUBOIS, R. MAKKI, M. MEISTER, A. VINCENT *et al.*, 2007 Control of blood cell homeostasis in Drosophila larvae by the posterior signalling centre. Nature 446: 325-328.

KRZEMIEN, J., J. OYALLON, M. CROZATIER and A. VINCENT, 2010 Hematopoietic progenitors and hemocyte lineages in the Drosophila lymph gland. Dev Biol 346: 310-319.

KURUCZ, E., R. MARKUS, J. ZSAMBOKI, K. FOLKL-MEDZIHRADSZKY, Z. DARULA *et al.*, 2007a Nimrod, a putative phagocytosis receptor with EGF repeats in Drosophila plasmatocytes. Curr Biol 17: 649-654.

KURUCZ, E., B. VACZI, R. MARKUS, B. LAURINYECZ, P. VILMOS *et al.*, 2007b Definition of Drosophila hemocyte subsets by cell-type specific antigens. Acta Biol Hung 58 Suppl: 95-111.

LANOT, R., D. ZACHARY, F. HOLDER and M. MEISTER, 2001 Postembryonic hematopoiesis in Drosophila. Dev Biol 230: 243-257.

LEBESTKY, T., T. CHANG, V. HARTENSTEIN and U. BANERJEE, 2000 Specification of Drosophila hematopoietic lineage by conserved transcription factors. Science 288: 146-149.

LEBESTKY, T., S. H. JUNG and U. BANERJEE, 2003 A Serrate-expressing signaling center controls Drosophila hematopoiesis. Genes Dev 17: 348-353.

LEE, M. J., M. E. KALAMARZ, I. PADDIBHATLA, C. SMALL, R. RAJWANI *et al.*, 2009 Virulence factors and strategies of Leptopilina spp.: selective responses in Drosophila hosts. Adv Parasitol 70: 123-145.

LEITAO, A. B., and E. SUCENA, 2015 Drosophila sessile hemocyte clusters are true hematopoietic tissues that regulate larval blood cell differentiation. Elife 4.

LEMAITRE, B., and J. HOFFMANN, 2007 The host defense of Drosophila melanogaster. Annu Rev Immunol 25: 697-743.

LUO, H., W. P. HANRATTY and C. R. DEAROLF, 1995 An amino acid substitution in the Drosophila hopTum-l Jak kinase causes leukemia-like hematopoietic defects. EMBO J 14: 1412-1420.

MAKHIJANI, K., B. ALEXANDER, T. TANAKA, E. RULIFSON and K. BRUCKNER, 2011 The peripheral nervous system supports blood cell homing and survival in the Drosophila larva. Development 138: 5379-5391.

MANDAL, L., J. A. MARTINEZ-AGOSTO, C. J. EVANS, V. HARTENSTEIN and U. BANERJEE, 2007 A Hedgehog- and Antennapedia-dependent niche maintains Drosophila haematopoietic precursors. Nature 446: 320-324.

MELK, J. P., and S. GOVIND, 1999 Developmental analysis of Ganaspis xanthopoda, a larval parasitoid of Drosophila melanogaster. J Exp Biol 202: 1885-1896.

MINAKHINA, S., and R. STEWARD, 2010 Hematopoietic stem cells in Drosophila. Development 137: 27-31.

MINAKHINA, S., W. TAN and R. STEWARD, 2011 JAK/STAT and the GATA factor Pannier control hemocyte maturation and differentiation in Drosophila. Dev Biol 352: 308-316.

MORALES, J., H. CHIU, T. OO, R. PLAZA, S. HOSKINS *et al.*, 2005 Biogenesis, structure, and immune-suppressive effects of virus-like particles of a Drosophila parasitoid, Leptopilina victoriae. J Insect Physiol 51: 181-195.

MUKHERJEE, T., W. S. KIM, L. MANDAL and U. BANERJEE, 2011 Interaction between Notch and Hif-alpha in development and survival of Drosophila blood cells. Science 332: 1210-1213.

OWUSU-ANSAH, E., and U. BANERJEE, 2009 Reactive oxygen species prime Drosophila haematopoietic progenitors for differentiation. Nature 461: 537-541.

PADDIBHATLA, I., M. J. LEE, M. E. KALAMARZ, R. FERRARESE and S. GOVIND, 2010 Role for sumoylation in systemic inflammation and immune homeostasis in Drosophila larvae. PLoS Pathog 6: e1001234.

RADTKE, F., A. WILSON and H. R. MACDONALD, 2005 Notch signaling in hematopoiesis and lymphopoiesis: lessons from Drosophila. Bioessays 27: 1117-1128.

RIZKI, R. M., and T. M. RIZKI, 1984 Selective destruction of a host blood cell type by a parasitoid wasp. Proc Natl Acad Sci U S A 81: 6154-6158.

RIZKI, R. M., and T. M. RIZKI, 1990 Parasitoid virus-like particles destroy Drosophila cellular immunity. Proc Natl Acad Sci U S A 87: 8388-8392.

RIZKI, T. M., and R. M. RIZKI, 1994 Parasitoid-induced cellular immune deficiency in Drosophila. Ann N Y Acad Sci 712: 178-194.

SCHILTHUIZEN, M., NORDLANDER, G., STOUTHAMER, R., VAN ALPHEN, J., 1998 Morphological and molecular phylogenetics in the genus Leptopilina (Hymenoptera: Cynipoidea: Eucoilidae). Syst Entomol 23: 253-264.

SCHLENKE, T. A., J. MORALES, S. GOVIND and A. G. CLARK, 2007 Contrasting infection strategies in generalist and specialist wasp parasitoids of Drosophila melanogaster. PLoS Pathog 3: 1486-1501.

SINENKO, S. A., J. SHIM and U. BANERJEE, 2012 Oxidative stress in the haematopoietic niche regulates the cellular immune response in Drosophila. EMBO Rep 13: 83-89.

SMALL, C., I. PADDIBHATLA, R. RAJWANI and S. GOVIND, 2012 An introduction to parasitic wasps of Drosophila and the antiparasite immune response. J Vis Exp: e3347.

SORRENTINO, R. P., Y. CARTON and S. GOVIND, 2002 Cellular immune response to parasite infection in the Drosophila lymph gland is developmentally regulated. Dev Biol 243: 65-80.

STOFANKO, M., S. Y. KWON and P. BADENHORST, 2008 A misexpression screen to identify regulators of Drosophila larval hemocyte development. Genetics 180: 253-267.

STOFANKO, M., KWON, S.Y., BADENHORST, P., 2010 Lineage tracing of lamellocytes demonstrates Drosophila macrophage plasticity. PLoS ONE 5: e14051.

STRUHL, G., and K. BASLER, 1993 Organizing activity of wingless protein in Drosophila. Cell 72: 527-540.

TERRIENTE-FELIX, A., J. LI, S. COLLINS, A. MULLIGAN, I. REEKIE *et al.*, 2013 Notch cooperates with Lozenge/Runx to lock haemocytes into a differentiation programme. Development 140: 926-937.

TOKUSUMI, T., R. P. SORRENTINO, M. RUSSELL, R. FERRARESE, S. GOVIND *et al.*, 2009 Characterization of a lamellocyte transcriptional enhancer located within the misshapen gene of Drosophila melanogaster. PLoS One 4: e6429.

XU, T., and G. M. RUBIN, 1993 Analysis of genetic mosaics in developing and adult Drosophila tissues. Development 117: 1223-1237.

Acknowledgements

I thank my mentor Dr. Shubha Govind, first, for nominating me for the Palefsky Fellowship, which gave me mentoring opportunities at CCNY. Being in Dr. Govind's lab and observing her helped me to develop into a scientist, a collaborator, a teacher and mentor. I am truly inspired by her motivation, drive, determination, enthusiasm, and brilliance.

I thank my committee members: Drs. Diana Bratu, Eric Lai, Mark Pezzano, and Linda Spatz, for their support and feedback. I am grateful to Dr. Shireen Saleque for the opportunity to start my thesis in her lab and for her understanding and support in my transition to the Govind lab. I thank Dr. Saleque for helpful discussions on the Notch and Senseless projects and for freely sharing equipment, reagents, and expertise.

Hsiling Chiu, a former graduate student in the lab assisted with deducing p40 peptide sequences, Drs. Gwen Gueguen and Rong Wang and Georgia Dolios helped decode the *L. heterotoma* VLP proteome. I am grateful to Dr. Shaneen Singh at Brooklyn College and her lab for their long-term collaboration, analysis of the VLP proteome, and computational studies of p40. Mary Ellen Heavner identified the transcript encoding p40 and characterized the p40 gene structure. I thank her for collaborating on the p40 project, sharing data before publication, and for many helpful discussions about our work. She is an amazing person, incredible cook, and a wonderful friend.

I thank Marta Kalamarz, Indira Paddibhatla, Roma Rajwani, and Chiyedza Small for schooling me in fly genetics, lymph gland dissections, and sharing protocols. I thank Roma Rajwani for sharing the *hop*$^{Tum\text{-}l}$ *msn-GAL4; UAS-mCD8-GFP* (recombinant 15.2 line) before publication, Adam Hudgins and Joyce Chan for sharing protocols and results of phagocytosis assays, Gwenaelle Gueguen and Marta Kalamarz for their collaboration on the *PLoS Pathogens*

study, Chiyedza Small, Maria Otazo, and Larry Huang for collaborating on the Notch/ROS study. Larry Huang assembled all the figures in chapter 1. These collaborators and coauthors are also my lasting friends.

Thanks to all members of the Govind lab, past and present, for support and feedback. Past members: Olusola Adeonigbagbe, Adam Hudgins, Mark Lee, Rebecca Moore, Roma Rajwani, and Hamzah Ramawad. Present members: Michelle Batchu, Joyce Chan, Jennifer Chou, Noelle Dziedzic, Mary Ellen Heavner, Silvio Panettieri, Zubaidul Razzak, and Brian Wey. Special thanks to Zoe Papadopol for fly food cooking and maintaining fly stocks. I am also grateful to members of the Saleque lab, Drs. Ananya Sengupta, Divya Singh, and Ghanshyam Upadhyay for technical advice and continued friendship and Dr. Jorge Morales and Daniel Fimiarz of the CCNY microscopy center for help with confocal microscopy.

Other CUNY faculty members offered technical advice and support at different junctures. For this, I thank Drs. J. Angulo, L. Eckhardt, M. Emerson, S. Hoskins, K. Hubbard, C. Li, I. Mano, P. Rockwell, and T. Venkatesh.

I thank the CCNY Biology Department Staff (Christine Klusko, Yolanda Pitt and others) for exceptionally efficient help, the RCMI facilities (Donna Lo) and the RCMI staff for physical and financial support, and Joan Reid at the CUNY Graduate Center for guiding me through the PhD process. I thank my fellow PhD students (also known as CCNY Science Alliance) for their friendship, networking, and many extracurricular activities.

Finally, I thank my family and friends in Trinidad and here in the United States for encouragement, support and faith in me. My late father, Ramdhanee Ramroop, would have been proud, my mother, Kowsil Ramroop, for believing in me (and for endless student loans), my admirable sister, Jenny Cadogan and her family (my niece Rayann Sydney Cadogan, nephew

Jamal Sean Cadogan, and my brother-in-law Ray Cadogan) for continued encouragement and love. I am grateful to my husband, Neal Gartland, for his patience and amazing sense of humor, to his incredible family, Frank and Jean Gartland, Chase Gartland and Dr. Bill Schneider for unconditionally accepting me into their lives.

I am grateful to the members of the *Drosophila* community who provided us with fly stocks, reagents, and information. This work was supported by funds from NIH, NSF, and NASA, and the Palefsky Fellowship.

Table of Contents

List of Figures

Chapter 1: *An Unexpected Link Between Notch Signaling and ROS in Restricting the Differentiation of Hematopoietic Progenitors in Drosophila*

Chapter 2: *Lethal effects of L. heterotoma infection on hematopoiesis and characterization of a SipD/IpaD-like protein from its virus-like particles*

Figures **Page**

Supporting Figures

Chapter 1

An Unexpected Link Between Notch Signaling and ROS in Restricting the Differentiation of Hematopoietic Progenitors in *Drosophila*

Abstract

A fundamental question in hematopoietic development is how multipotent progenitors achieve precise identities, while the progenitors themselves maintain quiescence. In *Drosophila melanogaster* larvae, multipotent hematopoietic progenitors support the production of three lineages, exhibit quiescence in response to cues from a niche, and from their differentiated progeny. Infection by parasitic wasps alters the course of hematopoiesis. Here we address the role of Notch (N) signaling in lamellocyte differentiation in response to wasp infection. We show that *N* activity is moderately high and ubiquitous in all cells of the lymph gland lobes, with crystal cells exhibiting the highest levels. Wasp infection reduces *N* activity, which results in fewer crystal cells and more lamellocytes. Robust lamellocyte differentiation is induced even in *N* mutants. Using RNA interference-knockdown of *N*, *Serrate,* and *Neuralized,* and twin clone analysis of a *N* null allele, we show that all three genes inhibit lamellocyte differentiation. However, unlike its cell-autonomous function in crystal cell development, Notch's inhibitory influence on lamellocyte differentiation is not cell-autonomous. High levels of reactive oxygen species in the lymph gland lobes, but not in the niche, accompany N^{RNAi}-induced lamellocyte differentiation and lobe dispersal. Our results define a novel dual role for Notch signaling in maintaining competence for basal hematopoiesis: while crystal cell development is encouraged, lamellocytic fate remains repressed. Repression of Notch signaling in fly hematopoiesis is important for host defense against natural parasitic wasp infections. These findings can serve as a

model to understand how reactive oxygen species and Notch signals are integrated and interpreted *in vivo*.

Introduction

In mammalian hematopoiesis, multipotent stem cells follow a tightly-regulated developmental program to specify the correct proportions of at least eight mature lineages. A complex set of hierarchical decisions are executed to supply the body with fully functional cells, while also renewing the original stem/progenitor population. Various lines of experimental evidence suggest that signaling pathways and molecular networks of transcription factors constitute key aspects of stem cell regulation (ORKIN and ZON 2008). Functional homologs of many of these signaling pathways and transcription factors are present in *Drosophila* and mutations in their respective fly genes give rise to hematopoietic defects (CROZATIER and MEISTER 2007; FOSSETT 2013; HONTI *et al.* 2013; KRZEMIEN *et al.* 2010a).

The future larval hematopoietic organ in *Drosophila*, called the lymph gland, differentiates from a cluster of embryonic mesodermal cells; Notch limits cardioblast (vascular) development in favor of embryonic lymph gland tissue (MANDAL *et al.* 2004); lymph gland lobe development continues through the first and second larval instars. By the mid third instar, the organ has a pair of anterior lobes, and two sets of smaller posterior lobes, that flank the dorsal vessel. Genetic experiments suggest that progenitors of the three major blood cell types quiesce in the medullary zone or medulla (JUNG *et al.* 2005; KALAMARZ *et al.* 2012; KRZEMIEN *et al.* 2010b; MINAKHINA and STEWARD 2010). The cortex harbors a mixture of maturing and fully-differentiated blood cells. Lineage development in the cortex is tightly regulated. The medulla/cortex boundary is not sharp; cortical cells in an intermediate state of differentiation are closer to the medulla; the terminally-differentiated cells are most peripheral in location (JUNG *et al.* 2005; KALAMARZ *et al.* 2012; KRZEMIEN *et al.* 2010b). Plasmatocytes (90-95%) appear as single cells or in clusters and crystal cells (5-10%) are distributed singly. Crystal cells produce

enzymes for melanization. Like mammalian macrophages, plasmatocytes engulf bacteria and apoptotic cells and make up the majority of circulating cells. Plasmatocytes and crystal cells circulating in the hemolymph have an embryonic origin and represent a developmental compartment that is distinct from the lymph gland [reviewed in (CROZATIER and MEISTER 2007; FOSSETT 2013)]. A non-hematopoietic niche, also referred to as the posterior signaling center (PSC), located at the base of the anterior lobes maintains progenitor quiescence in the anterior lobes (KRZEMIEN *et al.* 2007; LEBESTKY *et al.* 2003; MANDAL *et al.* 2007). It also mediates lamellocyte differentiation but mainly in response to wasp infection via the transcription factor Knot/Collier (CROZATIER *et al.* 2004).

The lymph gland lobes are immune-responsive (LANOT *et al.* 2001; SORRENTINO *et al.* 2002). Parasitic wasps of the *Leptopilina* genus attack second and early third instar larvae. Wasp infection alters the course of basal hematopoiesis and triggers cell division, lamellocyte differentiation, aggregation, and melanization (LEE *et al.* 2009b). Lamellocytes are dedicated to encapsulating wasp eggs. Wasp attack reduces the abundance of crystal cells in the anterior lobes (KRZEMIEN *et al.* 2010b). It also activates NF-κB signaling (GUEGUEN *et al.* 2013) and oxidative stress (SINENKO *et al.* 2012) in the niche. Activated NF-κB signaling in the lobes favors lamellocyte differentiation and inhibits crystal cell development (GUEGUEN *et al.* 2013). The effects of wasp-induced increase in reactive oxygen species is mediated by EGF signaling (SINENKO *et al.* 2012), although its effects on crystal cell development are not known. While it is clear that the lymph gland disperses after wasp infection and some plasmatocytes and lamellocytes arising in the lymph gland transfer into the hemolymph (LANOT *et al.* 2001; SORRENTINO *et al.* 2002; SORRENTINO *et al.* 2004), how wasp attack alters hematopoiesis to promote lamellocyte differentiation in the first place is not well understood.

In this study we analyze the role of Notch signaling in lamellocyte and crystal cell development. Notch signaling is evolutionarily conserved and regulates the diversification of cell fates in animals ranging from flies to mammals (BRAY 2006; KOCH *et al.* 2013). It also plays a role in the maintenance of hematopoietic stem cells (BIGAS *et al.* 2012). In *Drosophila*, Notch's role in crystal cell development is well-documented. It regulates embryonic crystal cell development (BATAILLE *et al.* 2005). In the late embryo, *N* restricts the developmental potential of multipotent progenitors: at restrictive temperature, late stage-16 embryos, N^{ts1} embryos are unable to specify crystal cells (KRZEMIEN *et al.* 2010b). In larval stages, Notch signaling regulates commitment to crystal cell lineage (DUVIC *et al.* 2002; LEBESTKY *et al.* 2003); in pro-crystal cells, the Notch receptor is activated by Serrate (Ser), expressed in the niche cells. Pro-crystal cells express high levels of AML-like transcription factor, Lozenge, and Suppressor of Hairless (*Su(H)*), a transcriptional activator mediating Notch signaling (LEBESTKY *et al.* 2003; TERRIENTE-FELIX *et al.* 2013). Notch and Lozenge select specific target genes to mediate crystal cell development (TERRIENTE-FELIX *et al.* 2013). Ligand-independent non-canonical Notch signaling also promotes crystal cell survival during basal hematopoiesis and hypoxic stress (MUKHERJEE *et al.* 2011).

*N*otch was reported to be essential for wasp-induced differentiation of lamellocytes (DUVIC *et al.* 2002), although the mechanism behind its requirement is not known. We now report an unexpected non cell-autonomous role for Notch signaling in restricting and not promoting differentiation of hematopoietic progenitors into lamellocytes. This inhibition appears to be independent of oxidative stress levels in the niche, although surprisingly, knockdown of *N* leads to increased reactive oxygen species (ROS) production in the lobes. Thus, Notch signaling plays an essential role in host defense against parasites in *Drosophila*. These results highlight an

unexpected pleiotropy for Notch and ROS signaling in regulating the production of alternative lineages during larval hematopoiesis.

Materials and Methods

Stocks, crosses, and wasp infections

HmlΔ-GAL4 (SINENKO *et al.* 2004) was received from S. Bhattacharya. *Dome-GAL4* (GHIGLIONE *et al.* 2002) was a gift from M. Crozatier, *Antp-GAL4* received from S. Minakhina (EMERALD and COHEN 2004). *y w;UAS-mCD8GFP* (SINENKO *et al.* 2004) was incorporated into appropriate *GAL4* backgrounds via standard crosses. UAS-RNAi lines for *Notch* (Valium 1 and 10), *Serrate* (Valium 10) *neuralized* (Valium 10), and *Su(H)* were obtained from the TRiP collection (NI *et al.* 2009; NI *et al.* 2008). *msnf9-cherry* (TOKUSUMI *et al.* 2009) was a gift from R. Schulz. *arm-lacZ 19A/FM7, hs-FLP* (VINCENT *et al.* 1994) was obtained from N. Baker. A chromosome bearing null allele (N^{55e11}, (HEITZLER and SIMPSON 1991) N^{55e11} *FRT19A/FM7* (OHLSTEIN and SPRADLING 2007) was obtained from B. Ohlstein. *UAS-NICD* encoding the Notch intracellular domain (STRUHL and ADACHI 1998) was obtained from K. Irvine. *12X Su(H)-lacZ* (GO *et al.* 1998) was obtained from S. Artavanis-Tsakonas. The *Dome-MESO-GFP* (medulla is GFP-positive) stock was a gift of M. Crozatier. y^1 N^{ts1} and w^a N^{ts2} *rb* flies were obtained from the Bloomington Stock Center.

Females from respective driver stocks containing *y w; UAS-mCD8GFP; Antp-GAL4/TM6 Tb Hu, y w Dome-GAL4/FM7; UAS-mCD8GFP* and *y w; HmlΔGFP/HmlΔGFP*) were crossed to males from respective RNAi stocks *y v/Y;* N^{RNAi}/N^{RNAi} and w^{1118}*/Y; UAS-NICD/TM3*. Third instar animals, selected from 6-8 hour egg-lays and reared at 27^0C, were genotyped by GFP expression. Lymph gland basement membrane dispersal was scored according to (SORRENTINO *et al.* 2002).

For loss-of-function Notch clones (XU and RUBIN 1993), N^{55e11}*FRT19A/FM7* females were crossed to *arm lacZ19A; hs-FLP/TM6 Tb Hu* males to create N^{55e11}/N^{55e11} clones marked by the absence of β-galactosidase. Homozygous wild type N^+/N^+ clones were detected by higher

than background β-galactosidase expression. N^{55e11} mutant clones were generated by 37^0C heat shock of second instar larvae for 30-40 minutes. To induce flp-out clones (STRUHL and BASLER 1993), developmentally-synchronized 4-day old larvae with the hybrid flip-out and Gal4 activation system [*hsp70-flp*; *Actin>CD2>Gal4*] and *UAS-GFP* transgenes or those with an additional *UAS-NICD* transgene, were heat-shocked at 37°C in a water bath for 15 min. N^{RNAi} (Valium 10) flp-out clones were similarly induced with a 1 hr heat shock of developmentally-synchronized mid-to-late second instar animals. After recovery at 25°C, lymph glands were dissected on day 6 from mid third instar larvae, 20 hrs after heat-shock. N^{ts1} or N^{ts2} stocks or progeny from crosses were maintained at 18°C. At the early second larval instar stage, animals were shifted to 29°C through the third instar. Animals were matched for biological age to compare phenotypes. Most mutant males did not emerge; escapers showed notched wings.

Wasp infections were performed as follows: from a six-hour egg-lay, second instar wild type or mutant larvae were subjected to infection by *L. boulardi G486* (SORRENTINO *et al.* 2002) or *L. boulardi Lb17* (SCHLENKE *et al.* 2007) for six to twelve hours, after which wasps were removed and host larvae were allowed to develop to third instar stage. Uninfected controls followed the same growth regimen.

Immunohistochemistry and ROS detection

Unless otherwise specified, mid third instar larvae from 6h or 12 h egg-lays were used in antibody staining experiments. Staining was performed according to (PADDIBHATLA *et al.* 2010) Primary antibodies: mouse anti-Notch (C17.9C6, detects the cleaved product; Developmental Studies Hybridoma Bank, (FEHON *et al.* 1990) 1:10, mouse anti-Nimrod C/P1 and mouse anti-L1/Atilla (1:10) (KURUCZ *et al.* 2007), mouse anti-prophenol oxidase (1:10, Dr T. Trenczek,

University of Giessen), 1:10, anti-integrin βPS (Developmental Studies Hybridoma Bank) 1:10, anti-proPO (CHRISTOPHIDES *et al.* 2002), anti-β galactosidase from Capell (1:2,000 clone analysis) or from Immunology Consultants, Inc (1:200 for N activity). Secondary antibodies: Cy3 AffiniPure Donkey Anti-Chicken (1:500 Jackson Immuno Research) or anti-mouse (1:200 Jackson Immuno Research or 1:500 Invitrogen). Rhodamine-, Alexa Fluor 488-, or Alexa Fluor 647-tagged Phalloidin and nuclear dye Hoechst 33258 (all Invitrogen) were used to examine cell morphology. ROS detection (Invitrogen D11347) was carried out according to (OWUSU-ANSAH and BANERJEE 2009).

Lamellocytes were visualized by (a) their cell shape (filamentous F-actin); or (b) by expression of integrin β PS (STOFANKO *et al.* 2008) ; or (c) Atilla expression (L1;(KURUCZ *et al.* 2007); or (d) by the *misshapen* transcriptional enhancer *msnf9* linked to cherry expression (TOKUSUMI *et al.* 2009). *msnf9-cherry*-positive lamellocytes are also strongly positive for F-actin with Alexa Fluor 488-labeled Phalloidin (data not shown).

Data collection and statistical analysis

Samples were imaged with Zeiss LSM 510 confocal microscope; 0.8 µm -1.5 µm thick optical images were analyzed according to (GUEGUEN *et al.* 2013). Select images were imported into Adobe Photoshop CS5. The eyedropper tool was used to define and extract a signal intensity value from a 5 X 5 square of 25 pixels in random regions of the lobes. Intensity data were collected from 20 cells per lobe in at least 12 animals. Images showing signal saturation were not used for quantification. Niche areas (in μm^2) were measured on confocal images using Path Tool of AxioVision 4.8 software. The average number of niche cells per lobe was scored by manually counting the mCD8-GFP- and Hoechst-positive cells in merged z-stacked images of the niche.

Data were tested for normality before performing statistics using the R software (R-DEVELOPMENT-CORE-TEAM 2010). Sample size, standard deviation, and *p*-values are presented in all graphs.

Results

Notch expression in third instar lymph glands

To examine the expression of the intracellular domain of Notch, we stained lymph glands with anti-NICD. NICD signal is highest in some GFP-negative cells (arrow) while the staining signal is low in cortical *Hml>GFP* cells (Fig. 1A-A''). NICD staining is high in *Dome>mCD8-GFP*-positive cells of the medulla of anterior (Fig. 1B-B'') and posterior lobes (data not shown), as well as *Antp>mCD8GFP*-positive niche cells (Fig. 1C-C''). In none of these populations, is the NICD signal nuclear. We were surprised to find that NICD levels are low or undetectable in lamellocytes induced by wasp attack (Fig. 1D-D") or those in the gain-of-function $hopscotch^{Tumorous\text{-}lethal}$ ($hop^{Tum\text{-}l}$)(LUO *et al.* 1995) background, where ectopic JAK-STAT signaling promotes lamellocyte differentiation in the absence of parasite attack (data not shown). Specificity of NICD staining and successful knockdown of Notch protein was confirmed by staining $Antp>N^{RNAi}$ glands, where the NICD signal was either reduced or not detected in GFP positive niche cells (Fig. S1). Differences in NICD levels and its subcellular localization in the lymph gland suggest different states of *N* activity in different cell populations, and likely distinct functions of *N* in hematopoietic development.

N activities in larval lymph gland lobes

To test if *N*'s influence on progenitor differentiation is more or less ubiquitous, or if *N* activity is localized to crystal cells, we examined *N* activity using specific reporters. We found that a reporter of Notch and Su(H) transcription, *Su(H)-lacZ* (GO *et al.* 1998), is expressed at moderate levels in wild type anterior lobe cells in all three larval stages, although the reporter activity levels are distinctly higher in the third instar lobes (Fig. 2A-D). Additionally, only at the

third instar stage, high *N* target gene activity is also detected in scattered cells (Fig. 2D arrows). A significant fraction of these cells (37.3%; Fig. 6C, C' stars) are also pro-PO-positive, suggesting ontogenetic relationship among the *Su(H)-lacZ*- and pro-PO-positive cell populations. Developmentally, the appearance of mature crystal cells in the lymph gland, positive for Lozenge and Su(H) proteins, coincides with the second-to-third instar molt (LEBESTKY *et al.* 2000).

Ubiquitous moderate activity from the *Su(H)-lacZ* reporter is detected in the N^{ts1} or N^{ts2} lobes reared at permissive 18^{o}C temperature (one *Su(H)-lacZ* copy in N^{ts}/Y males; Fig. 3A, B, E), although high signal in crystal cells is rarely observed in the N^{ts} backgrounds presumably due to the inhibitory effect of the mutation. At non-permissive temperature however, both the moderate ubiquitous and high local *Su(H)-lacZ* signals are reduced in the N^{ts1} and N^{ts2} backgrounds (Fig. 3C-E). Unlike crystal cell differentiation, in N^{ts}/Y lobes, neither the medulla/cortex sizes (assessed by *Dome-MESO-GFP* expression (Fig. 7A, B) nor plasmatocyte development (anti-Nimrod C staining; data not shown) appear to be affected at 29^{o}C. Thus, it appears that, consistent with NICD expression, Notch signaling is widespread in third instar anterior lobes. We hypothesized that the moderate ubiquitous *Notch* activity is needed for selection and patterning, i.e., the distributed appearance of crystal cells in the cortex, in a step prior to their maturation, which requires robust cell autonomous *Notch* activity.

NICD expression promotes development of crystal cell clusters

We first examined Notch's role in crystal cell development. We were surprised to find that NICD expression in the niche (*Antp>NICD*) results in a significant increase in crystal cell number (average 67 crystal cells/lobe in *Antp>NICD* glands, compared to 18 crystal cells/lobe in

control glands, n = 6 lobes for each genotype; $p < 0.05$) (Fig. 4A, B). Many of these crystal cells develop in clusters, a pattern rarely observed in wild type glands. Conversely, RNAi knockdown of *N* via *Antp* led to a significant reduction in crystal cell number (Fig. 4C).

"Flp-out" clones of constitutively-active NICD strongly induced crystal cell fates in third instar lymph glands: All (99%, n = 89 cells) GFP-positive clonal cells expressing NICD are also pro-PO-positive (Fig. 5C-D"), compared to 0.5%, (n = 236 cells) of pro-PO-positive cells in control clones (Fig. 5A-B"). We also observed rare pro-PO-expressing cell clusters in NICD-expressing posterior lobes (Fig. S2C-D'). Crystal cells normally do not develop in posterior lobes (Fig. S2A-B'). Thus, ectopic NICD expression makes all daughter cells unresponsive to their normal internal and external developmental cues and, instead, programs them into crystal cells.

Consistent with the *Antp>NICD* result above (Fig. 4A-C), numerous crystal cells were also found outside the *actin>NICD* "flp-out" clones (Fig. 5D, D''). This observation further supports an indirect positive influence of *N* activity on crystal cell differentiation. In addition, *actin>NICD* "flp-out" lobes contain mature anti-Nimrod C/P1-positive plasmatocytes at the lobe periphery. These plasmatocytes do not express NLS-GFP and are therefore NICD-negative (Fig. 5C, C''). Together, these results not only confirm that high *N* activity is sufficient for crystal cell development as described in previous studies (DUVIC *et al.* 2002; LEBESTKY *et al.* 2003) but also that Notch-mediated non cell-autonomous mechanism patterns the cortex with dispersed crystal cells.

N activity is quenched after wasp infection

To examine if wasp infection might decouple the ubiquitous and localized *N* activities, we infected second instar *Su(H)-lacZ* transgenic animals (wild type for *N*) and stained lymph glands from mid-third instar animals with anti-β galactosidase antibody. We found a significant, two-fold reduction in the ubiquitous signal in lobes of wasp-infected *Su(H)-lacZ* animals compared to lobes from uninfected animals (Fig. 6G). In addition, the number of cells with high *N* activity (some of which also express the pro-PO enzyme (green, arrow)), is significantly reduced (Fig. 6A-F), supporting the idea that moderate ubiquitous *N* activity may be needed to specify crystal cell development, while acquisition of their final fates requires higher *N* activity in the maturing crystal cells, consistent with Notch's cell autonomous role (LEBESTKY *et al.* 2003). The anterior lobes of wasp-infected *Su(H)-lacZ* glands revealed strong lamellocyte differentiation (Fig. 6H, I), raising the possibility that reduction in *N* activity may not compromise lamellocyte differentiation as previously reported (DUVIC *et al.* 2002).

$Notch^{RNAi}$ promotes lamellocyte differentiation

To examine if N^{ts}/Y; *Dome-MESO-GFP*/+ mutant lymph glands support differentiation of lamellocytes, we exposed second instar animals to *L. boulardi*. Unexpectedly, wasp infection of temperature-restricted N^{ts1} or N^{ts2} animals results in robust lamellocyte differentiation and lobe dispersal in mid third-instar animals (Fig. 7A-F).

The expression of Serrate, the Notch ligand, is restricted to few cells of the niche (LEBESTKY *et al.* 2003). To examine if reduction in Notch signaling in this cell population induce lamellocyte differentiation, we conducted cell-specific knockdown using *UAS-*N^{RNAi} in either Valium 1 or Valium 10 vector (NI *et al.* 2009; NI *et al.* 2008) in the niche or cortex, utilizing the

Antp and *Hml* GAL4 drivers, respectively. The driver stock contains the *UAS-GFP* reporter transgene, marking the location of GAL4-positive cells. In each case, lamellocytes were detected in N^{RNAi} lobes, but not in control lobes. Lamellocytes themselves were GFP-negative, and were located in the vicinity of the GFP-positive cells (Fig. 8A-D"), suggesting an inductive relationship. The strongest effects were observed upon knockdown with either Valium 1 or Valium 10 in the niche (Table S1; Fig. 8). As is the case with wasp-infected animals, mature lamellocytes were most often in the cortical zone, rarely at the medulla/cortex junction, and never in the niche or posterior lobes.

Since basement membrane disruption is also a reliable marker for the presence of lamellocytes (SORRENTINO *et al.* 2002; SORRENTINO *et al.* 2004), we inspected the integrity of the basement membrane in both control and N^{RNAi} lobes (Table S1). Basement membrane in the control lobes were largely intact (Fig. 8A, C), but N^{RNAi} lobes were frequently dispersed with disrupted basement membrane (Fig. 8B, D, D', D", Table S1). Lamellocytes were also observed in smear preparations of circulating hemolymph of N^{RNAi} animals (Fig. 8F) but not in control smears (Fig. 8E).With both drivers, knockdown with Valium 10 *UAS-*N^{RNAi} resulted in stronger dispersal relative to Valium 1 *UAS-*N^{RNAi} knockdown. These results imply that lamellocyte precursors are sensitive to *N* activity in neighboring cells.

To further assess the role of Notch signaling in lamellocyte differentiation, we created RNAi knockdown lymph glands where levels of other *N* pathway components, *Ser*, *Neuralized* (*neur*), or *Su(H)* were similarly reduced in the niche. In all cases, supernumerary lamellocytes were induced (Fig. 9 and data not shown). In some *Antp>neur*^{RNAi} glands, ectopic lamellocytes were observed close to the GFP-positive cells (Fig. 9A-B'), but away from the niche. Knockdown of *Ser* (Fig. 9C-D') or *Su(H)* (data not shown) had similar effects.

Thus it appears that *N* pathway components alter cellular properties of the niche, which in turn affects progenitor differentiation. Knockdown of these proteins however affects neither the number of *Antp>mCD8GFP*-positive niche cells, nor the size of the niche (Fig. 9E). In none of these six backgrounds, did we detect actin-rich processes arising from the niche into the progenitor population as reported by others (CROZATIER *et al.* 2007; MANDAL *et al.* 2007; TOKUSUMI *et al.* 2012). Thus, Notch signaling does not affect specification or growth of the niche itself, but instead Notch signaling contributes to the production of a signal needed to maintain lamellocyte progenitor quiescence. RNAi results above (Fig. 8, 9 and Table S1) suggest that this inhibitory influence on lamellocyte differentiation, while stronger in the niche, is not limited to this compartment, and can also be exerted in other parts of the lobe.

Notch's inhibitory influence on lamellocyte differentiation is non cell-autonomous

Non cell-autonomy of *N* was examined in two independent experiments. Flp-out clones, marked with GFP and expressing N^{RNAi} produce descendants that fail to differentiate into lamellocytes. However cells in the vicinity of GFP-positive N^{RNAi} cells (but not neighboring GFP-expressing cells without the N^{RNAi} transgene) show lamellocyte morphology (Fig. 10A, B arrow) and strong lobe dispersal (Fig. 10C, D). We also induced twin clones (XU and RUBIN 1993) in heterozygous N^{55e11}/N^{+} glands. N^{55e11} is a strong loss-of-function allele (DIAZ-BENJUMEA and GARCIA-BELLIDO 1990). In this technique, somatic recombination in heterozygous cells produces daughter cells that are either homozygous mutant (N^{55e11}/N^{55e11}) or wild type (N^{+}/N^{+}). Wild type clones are identified by two copies of the marker protein, β-galactosidase, encoded by the *lacZ* transgene present in *cis* to N^{+}. Fig. 11 shows that integrin β-positive-lamellocytes also express high levels of β-galactosidase. These double-positive cells are

not found within the mutant *N* clone that is negative for the β-galactosidase signal (Fig. 11A-C''). and a majority of newly-differentiated cells are observed in the cortex (Fig. 11). Thus, consistent with the N^{RNAi} experiments, lamellocyte differentiation is non cell-autonomous and a majority of newly-differentiated cells are observed in the cortex (Fig. 11).

Antp>N^{RNAi} leads to changes in ROS levels in lymph gland lobes

Recent work has linked increased ROS levels in the niche to lamellocyte differentiation after wasp infection ((SINENKO *et al.* 2012) and Fig. S3). To examine if reduction in *N* activity has a similar effect on ROS levels, we stained control and *Antp>*N^{RNAi} lymph glands with dihydroethidium (DHE). This cell-permeable probe reacts with cellular superoxide ions to generate oxyethidium (ZHAO *et al.* 2003). The interaction of oxyethidium with nucleic acids is detected as red fluorescence (TARPEY *et al.* 2004). Fig. 12 shows strong red fluorescence in the medulla in control glands, indicating high ROS levels. However, ROS are not detected in the niche and they are low in the cortex, where cells retain the unreacted probe (Fig. 12A, A'', blue). In *Antp>*N^{RNAi} lymph glands, the "high ROS" population (presumed medulla) is depleted (Fig. 12B). However, *Antp>mCD8GFP*-positive cells with N^{RNAi} show no change in ROS levels and exhibit significantly low or no ROS (Fig. 12B''), much like the niche of control lobes (Fig. 12A''). Even NICD expression in the niche did not alter ROS levels in the niche (Fig. 12C''). However, ROS levels are significantly higher in the N^{RNAi} cortex (Fig. 12B) but not in NICD cortex (Fig. 12C). These observations suggest that a ubiquitous effect of *N* signaling is to maintain low ROS in the anterior lobes, which may in turn maintain lamellocyte progenitors in an undifferentiated state.

Discussion

In this study we report a dual role for Notch signaling in larval hematopoiesis: First, Notch appears to play a reciprocal role in the development of crystal cells and in lamellocyte development. Moderate levels of wild type Notch signaling promote crystal cell selection, but, contrary to expectation, support quiescence and not differentiation of lamellocyte progenitors. The inhibitory influence on lamellocyte differentiation is exerted non cell-autonomously and correlates with high oxidative stress in lobes undergoing lamellocyte differentiation and dispersal.

Dual and reciprocal non-autonomous effects of *N* on lineage decision

Division and development of a heterogeneous hematopoietic progenitor population in the third instar medulla is arrested; cortical cells in proximity to the medulla are less fully developed than peripheral cortical cells. Signals from the niche, cortex, and the medulla maintain medullary quiescence, and some of these signals must be modified to release progenitors from their quiescent state (reviewed in (FOSSETT 2013). Our experiments reveal that (1) Notch protein, while ubiquitously expressed, shows considerably variable subcellular localization suggesting different states of *N* activities in the organ (Fig. 1); (2) *N* activity is low and ubiquitous in first and second instar lobes, but increases in the third instar stage as the host becomes competent for defense against parasite attack ((SORRENTINO *et al.* 2002) and Fig. 2); (3) Although reduction in *N* activity does not affect *Antp>GFP* expression, niche size, or the development of the plasmatocyte lineage, it has divergent effects on the other two lineages. While moderate *N* activity encourages the selection and development of individual crystal cell in the lobe cortex, the same activity maintains lamellocyte progenitors in an undifferentiated state (Fig. 4-10).

Lamellocytes themselves do not express high NICD (Fig. 1) and it is quite possible that Notch protein levels are downregulated during the differentiation process.

Notch's autonomous effects on crystal cell development are understood in some detail (LEBESTKY *et al.* 2003; MUKHERJEE *et al.* 2011; TERRIENTE-FELIX *et al.* 2013). Our results suggest that ubiquitous *N* activity in third instar lobes (Fig. 2) in basal hematopoiesis is required for the selection of the correct proportion of crystal cells in the third instar lobe resulting in their dispersed distribution pattern. Other cell signaling mechanisms including Notch signaling itself, build on this *N* activity "pre-pattern" for continued crystal cell development and maturation. Temperature-restricted N^{ts} lobes exhibit normal medulla/cortex zonation (Fig. 7) and produce Nimrod-C-positive plasmatocytes in their correct location (our unpublished results) but are unable to produce crystal cells ((LEBESTKY *et al.* 2003) and Fig. 3). However, forced expression of NICD (or N^{RNAi}) in the niche alone is sufficient to encourage (or discourage) crystal cell development (Fig. 4). More significantly, ectopic NICD expression in mitotic clones alters and overcomes the effects of the normal "pre-pattern" in basal hematopoiesis and programs all clonal cells into crystal cells (Fig. 5).

We were surprised to discover that temperature-restricted N^{ts} lobes are immune competent and can produce lamellocytes (Fig. 7). Thus, reduced *Notch* activity does not compromise lamellocyte differentiation (*i.e.*, *N* may not be needed for lamellocyte differentiation). Instead, under low Notch, lamellocyte progenitors are specified and are developmentally competent. The inhibitory effect of *N* activity on lamellocyte progenitors in the absence of infection is observed upon RNAi knockdown in the niche or cortex (Fig. 8, 9) or removal of *N* function in somatic clones (Fig. 10, 11). We propose that a second role for moderate ubiquitous *N* activity is to generate a signal that shelters lamellocyte progenitors in the

absence of infection. Infection reduces this ubiquitous *N* activity releasing lamellocyte progenitors to mature (Fig. 6).

Are the reciprocal effects of *N* on crystal cells and lamellocytes linked? Recent studies have uncovered unexpected plasticity in hematopoietic development (AVET-ROCHEX *et al.* 2010; HONTI *et al.* 2010; KROEGER *et al.* 2012; STOFANKO *et al.* 2010). Wasp infection induces proliferation and lamellocyte differentiation (KRZEMIEN *et al.* 2010b; SORRENTINO *et al.* 2002), but infection reduces the abundance of crystal cells (KRZEMIEN *et al.* 2010b). Our results provide a mechanism whereby reduction in *N* activity would coordinate alternative fate choice in basal versus activated hematopoiesis; such a switch would allow progenitor reprogramming to tailor host defense to promote wasp egg encapsulation. As such, lymph gland dispersal and release of plasmatocytes and lamellocytes into the hemolymph alters the circulating blood cell population, enhancing the host's immune competence. Our data reveal that Notch plays a critical role in this process. Similar scenarios for Notch mediated restriction of alternative cell fates has been observed at multiple stages of vertebrate hematopoiesis. Notch signaling in zebra fish promotes the production of hematopoietic stem cells at the expense of endothelial cells from a common bi-potent hemangioblast (LEE *et al.* 2009a). Subsequently Notch1 signaling is observed in the mouse thymus, where Notch manages the checkpoint for T-cell commitment at the expense of the B-lineage program; and Notch1 collaborates with GATA-3 to commit progenitors to the T cell lineage (GARCIA-OJEDA *et al.* 2013). Further downstream Notch favors adoption of an αβ over γδ T cell fate (RADTKE *et al.* 2005). Our study expands the recurrent and burgeoning theme of selecting alternative cell fates by activating Notch signaling at crucial lineage branch points in multiple development contexts and in diverse organisms.

N signaling blocks the production of high ROS in anterior lobes

Reduction of Notch signaling appears to influence progenitor quiescence via increased levels of superoxide ions in most lobe cells (Fig. 11). Surprisingly, cells in the lobe but not in the niche where levels of *N* (or *N* pathway components were reduced), show high levels of oxyethidium in response to high superoxide. Thus, it appears that *N* signaling can have systemic effects on the oxidative stress level of the organ. Aberrant increase in cellular ROS is associated with loss of quiescence and precocious differentiation of medullary progenitors (OWUSU-ANSAH and BANERJEE 2009). In addition, the hypoxia protein HIF-α interacts with NICD to promote transcription of target genes that support crystal cell survival (MUKHERJEE *et al.* 2011). Wasp infection induces high ROS in the niche; infection results in the secretion of the epidermal growth factor-like cytokine, Spitz, whose activation of rhomboid and the EGF receptor induces lamellocyte differentiation in the cortex (SINENKO *et al.* 2012). Thus, oxidative stress via ROS has multiple and complex effects on hematopoietic cell quiescence, differentiation or survival. Our results point to the possibility that Notch signaling maintains low oxidative stress in the lobe cortex to preserve lamellocyte progenitor quiescence and promote crystal cell development and survival. The mechanism underlying ROS changes in the cortex remain to be explored.

The developing lymph gland has emerged as a powerful system to study mechanisms governing hematopoietic stem/progenitor cell quiescence and differentiation. We show that *N* activity controls quiescence versus development for divergent lineages. Moderate *N* activity correlates with low ROS levels and lamellocyte quiescence. Experimental evidence suggests that a low-oxygen milieu of the bone marrow protects mammalian hematopoietic stem cells and the supporting niche cells from oxidative stress whereas high ROS correlates with their ability to self renew (ITO *et al.* 2006; PARMAR *et al.* 2007; PICCOLI *et al.* 2005; TOTHOVA *et al.* 2007; WANG

and WAGERS 2011). Primitive hematopoietic stem cells with low ROS exhibit properties of quiescent stem cells which include slow cycling and expression of Notch1 (JANG and SHARKIS 2007). Thus, it is possible that intracellular ROS levels coordinate with signaling pathways to specify quiescence versus proliferation and differentiation. ROS have traditionally been considered to be agents of cell damage and are associated with many human pathologies (BALABAN *et al.* 2005). Recent data link ROS more directly to cellular function and homeostasis via signaling pathways (HAMANAKA *et al.* 2013). Given the extensive conservation of N functions in fly and mammalian hematopoiesis (FOSSETT 2013; KRZEMIEN *et al.* 2010a), our studies open the possibility of more thoroughly understanding how signal transduction and ROS are integrated and how this integration coordinates basal and activated hematopoietic development.

Figures

Figure 1. Notch intracellular domain expression in third instar lymph glands

(**A**) Anti-NICD antibody (red) detects variable N expression in the cortical cells of a mid-third instar lymph gland. (**A'-A''**) Magnification shows weak NICD signal in Hml>GFP-positive cells, whereas some Hml>GFP-negative cells have high punctate cytoplasmic staining (arrow). (**B-B''**) In the medulla, high Anti-NICD staining colocalizes with the *Dome>mCD8GFP* membrane signal (arrow). (**C-C"**) NICD also colocalizes with *Antp>mCD8GFP* signal in an early third instar lymph gland niche (arrow). (**D-D"**) NICD staining is lower or not detected in large lamellocytes (Alexa 488-Phalloidin positive, green) in wild type mid-third instar lymph glands from wasp-infected animals. Lamellocytes are rarely found in uninfected wild type lymph glands (see Fig. 6H). Hoechst (blue) stains DNA.

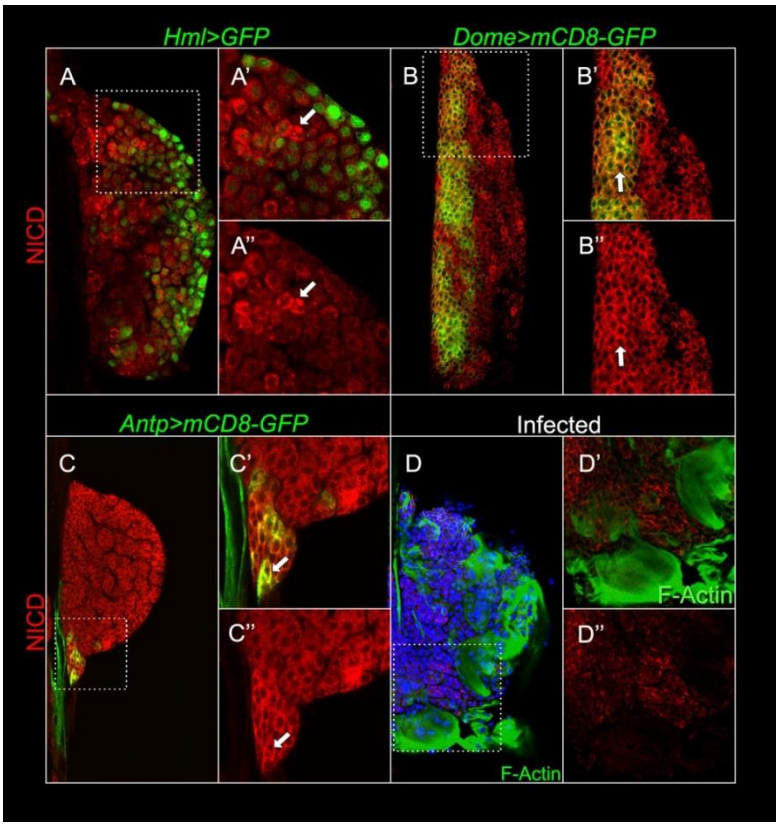

Done by Chiyedza Small. See Small and Ramroop *et al*., 2014

Figure 2. Ubiquitous and localized *N* activities in the larval lymph glands

(**A-D**) Anti-betagalactosidase staining detects moderate ubiquitous expression of *Su(H)-lacZ* reporter transgenes in lobes of first, second, or third instar larvae. In both cases, higher expression is detected in a few scattered cells, presumed crystal cells, in lobes from the third instar animals. (Also see Fig. 6).

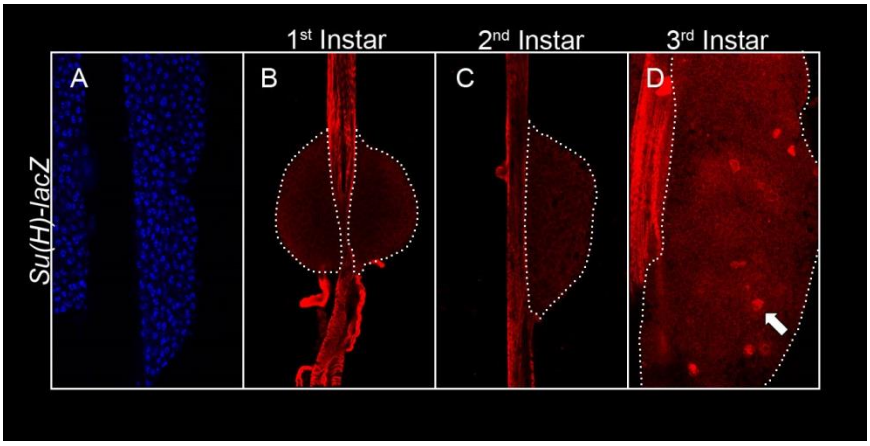

Figure 3. Ubiquitous Notch-reporter activity depends on functional *N* product

Lymph glands from N^{ts2}/Y, *Su(H)-lacZ* larvae at permissive (**A, B**), or non-permissive (**C, D**) temperature, stained with anti β-galactosidase antibody (red). Moderate *N* activity at permissive temperature (**A, B**) is reduced at non-permissive temperature (**C-E**).

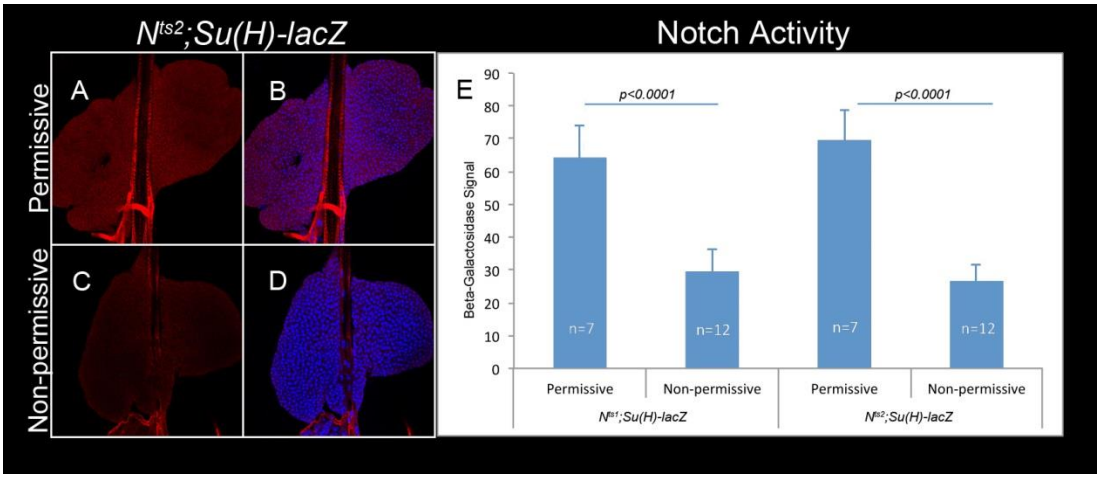

Figure 4. A non cell- autonomous role for *N* in crystal cell development

(**A**) Anterior lobes of *Antp>mCD8GFP* lymph gland stained with anti-pro-PO antibody (red) marks crystal cells in control lobes. (**B**) *Antp>NICD* lobes stained with anti-pro-PO antibody (red) have more crystal cells compared to control lobes. (**C**) A significant reduction in crystal cell number is observed in *Antp>N*^{RNAi} lobes. Samples were taken from mid-third instar animals.

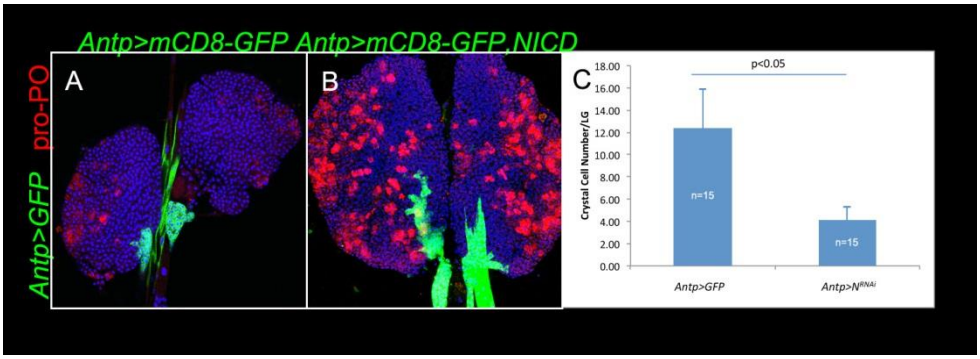

Staining, imaging and quantification were done by Maria Otazo. See Small and Ramroop *et al*., 2014

Figure 5. A cell-autonomous role for *N* in crystal cell development

(**A-B”**) *hsFLP; actin>NLS-GFP* control clones marked with GFP are negative for pro-PO (red). High magnification of the defined areas **A’** and **A”** from panel A and defined areas **B’** and **B”** in panel **B** are shown. (**C-D”**) Most cells in *hsFLP; actin>NLS-GFP, NICD* clones express pro-PO (red), but not Nimrod C (P1). High magnification of the defined areas **C’** and **C”** in panel **C**, and **D’** and **D”** in panel **D** are shown. Hoechst channel is omitted in panels **B** and **D** for clarity.

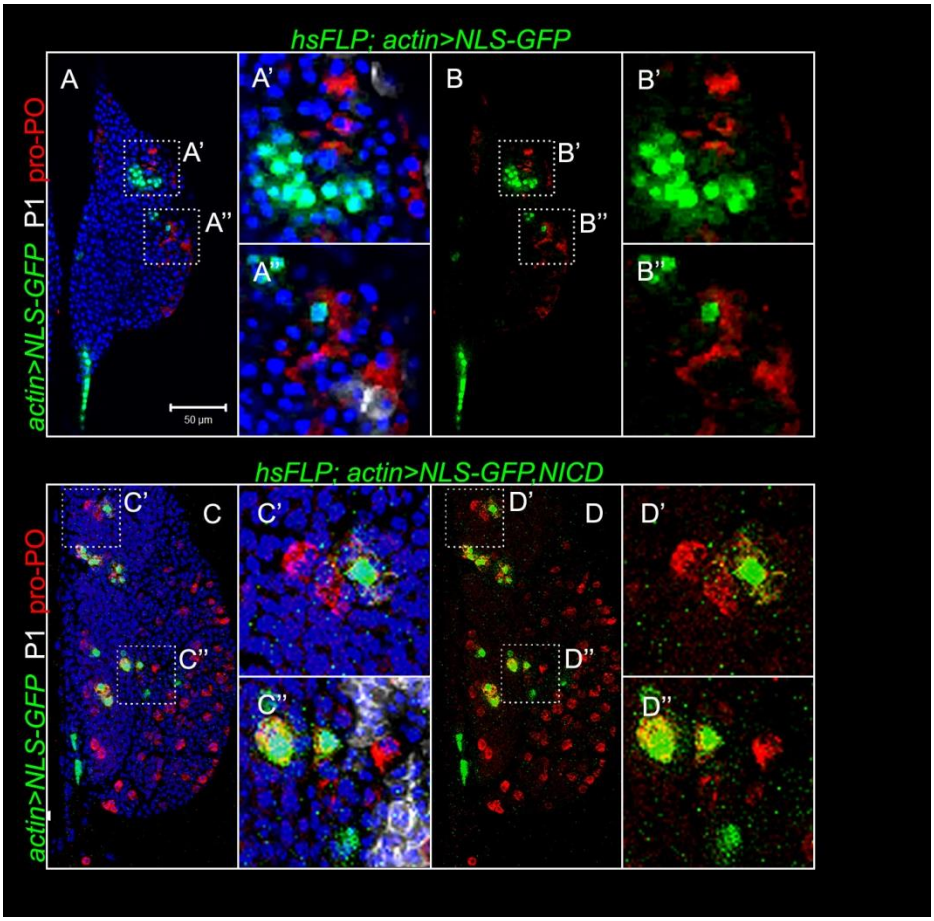

Done by Chiyedza Small. See Small and Ramroop *et al*., 2014

Figure 6. *N* activity is reduced after wasp infection

Anti β-galactosidase antibody (red) -stained lobes from *Su(H)-lacZ* animals co-stained with anti-pro-PO (green) to detect coincidence of high *N* activity in crystal cells (stars). Cells expressing *Su(H)-lacZ* only make up 25.3% of all labeled cells; cells positive for pro-PO only constitute 37.3% of all labeled cells. The remainder labeled cell population (37.3%) are double-positive (n = 406 cells from 20 lobes). Control animals did not experience wasp attack (**A-C'**), or were attacked by wasps (**D-F**) before dissection. Upon infection, *N* activity decreases (**D-G**). (**H, I**) Lamellocyte differentiation in *Su(H)-lacZ* lobes is normal. Anterior lobes from uninfected *Su(H)-lacZ* (H), or infected (I) animal. Lamellocytes are labeled with Phalloidin tagged with Alexa Fluor-647 (white), which also labels the dorsal vessel.

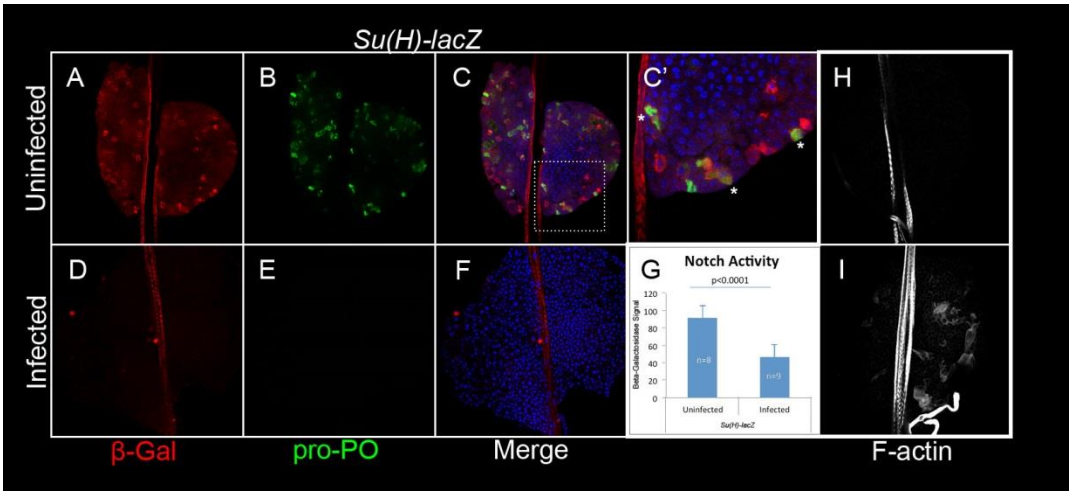

Figure 7. Lymph glands from N^{ts} animals are competent for lamellocyte differentiation

Lymph gland lobes (**A-F**), or circulating cells in the hemolymph (**C-F**, bottom inserts), stained with Rhodamine-Phalloidin to detect the presence of lamellocytes in N^{ts1} (**A-D**) or N^{ts2} (**E, F**) mutants reared at permissive (**A, C**) or non-permissive (**B, D-F**) temperatures.

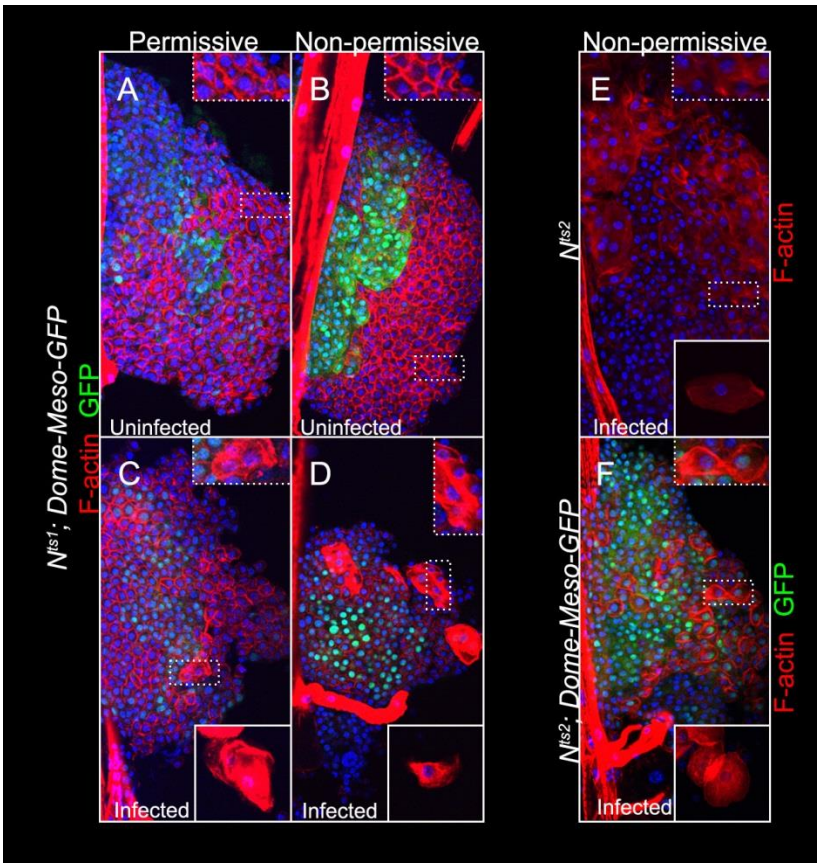

Figure 8. *Notch*^{RNAi} correlates with lamellocyte differentiation

Supernumerary lamellocytes are detected with *msnf9-cherry* reporter (**A, B**) or with Rhodamine Phalloidin (**C, D**), in *Antp>N*^{RNAi} lobes (**B, D-D"**), and not in control lobes (**A, C-C"**). Lamellocyte differentiation accompanies lobe dispersal (right lobes releasing lamellocytes). Hemolymph smears from control (**E**) and *Antp>N*^{RNAi} (**F**) animals stained with Rhodamine Phalloidin.

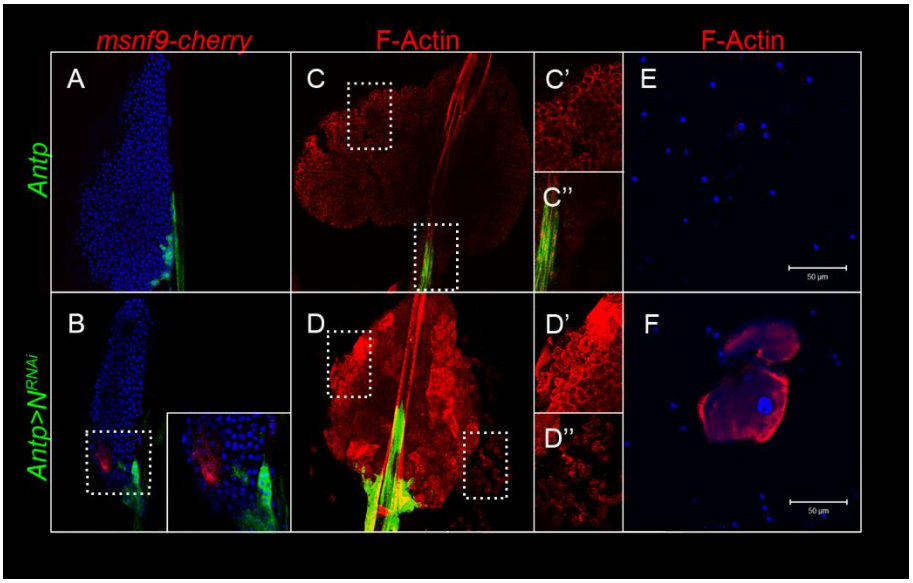

Experiments in panels A-D''was done by Chiyedza Small. See Small and Ramroop *et al*., 2014

Figure 9. Lamellocyte differentiation is induced by *neur*^{RNAi} and *Ser*^{RNAi}

(**A**) Control *Antp>GFP* and (**B, B'**) *Antp>neur*^{RNAi} lymph glands stained with anti-L1 antibody (red). L1-positive lamellocytes are found in the cortex adjacent to satellite niche cells (green). (**C**) Control *Antp>GFP* and *Antp>Ser*^{RNAi} (**D, D'**) lymph glands stained with Rhodamine Phalloidin. F actin-rich lamellocytes (red) are adjacent to the GFP positive niche cells. Hoechst stains DNA (blue). (**E**) Niche size is unaffected by knockdown of N pathway components. Left: Average number of GFP-positive cells per niche ($n \geq 20$) are not significantly different in control (*Antp>mCD8GFP* and *Antp > y w*) lobes and experimental (RNAi of *N*, *Ser*, *neur* and *Su(H)*) lobes. Right: The average area of GFP positive cells per niche ($n \geq 20$) is not significantly different between control and experimental lymph glands.

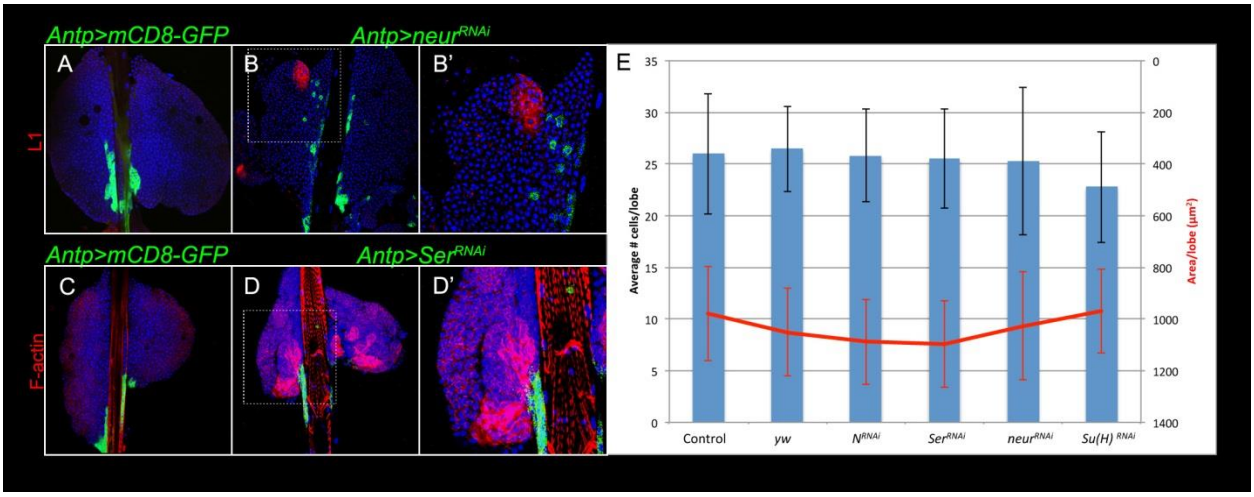

Experiments in panels A-D'done by Chiyedza Small. Quantification and analysis in panel E was done by Johnny Ramroop. See Small and Ramroop *et al*., 2014

Fig. 10. N^{RNAi}-flp-out clones encourage lamellocyte differentiation and lobe dispersal

(**A, C**) Cells that express GFP after somatic recombination with NLS-GFP-positive cells but without N^{RNAi}, do not induce lamellocyte differentiation (A), or lobe dispersal (C). The edge of the lobe in panel C is continuous (arrows) suggesting the presence of an intact basement membrane (**B, D**). Clones with N^{RNAi} induce lamellocytes (B, arrow) and lobe shows a discontinuous edge indicating disrupted basement membrane (D).

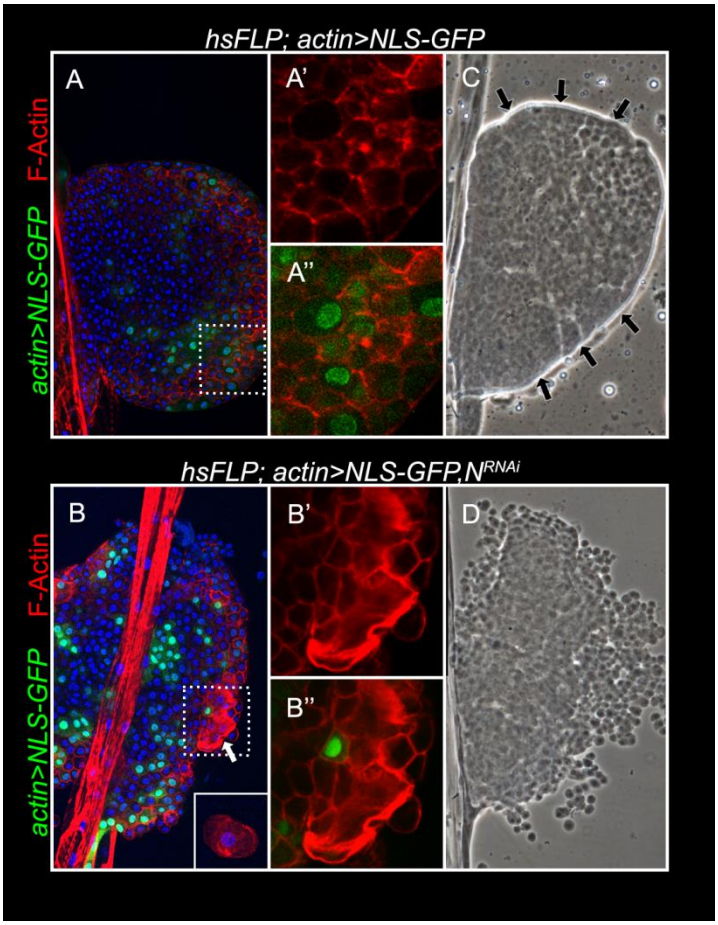

Figure 11. Notch clones reveal non cell-autonomous function in lamellocyte differentiation

(**A**) Schematic of twin clones (genotypes labeled) and lamellocytes in the cortex of an N^{55e11}/N^{+} anterior lobe The schematic corresponds to an analysis of 14 z-stacked confocal images, each of 0.8-µm thickness; merged z-stacks are shown in B-C'' (**B**) A mutant (N^{55e11}/N^{55e11}) clone, marked by the absence of β-galactosidase and a wild type (N^{+}/N^{+}) clone detected by high levels of β galactosidase (red). Lamellocytes positive for integrin β are also β galactosidase-positive (yellow), and these cells are found outside the clone boundary (**B-C''**). The region of interest in panel B is shown at a higher magnification in panels **C-C"**, where double-positive N^{+}/N^{+} lamellocytes with large, thin morphologies are more clearly evident. Hoechst stains DNA (blue).

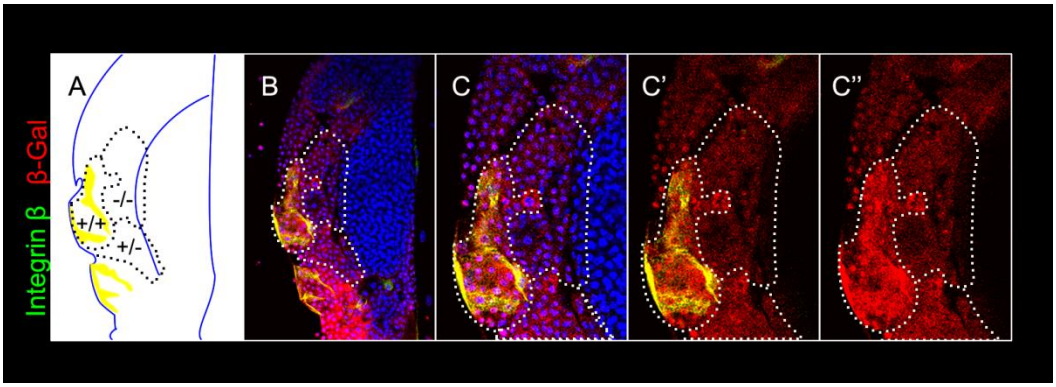

Done by Chiyedza Small. See Small and Ramroop *et al*., 2014

Figure 12. N^{RNAi} induces high levels of ROS in blood cells, but not in the niche

ROS staining of freshly-dissected lymph glands of control (*Antp>mCD8-GFP*, **A-A''**), experimental (*Antp>mCD8-GFP*, N^{RNAi}) (**B-B''**), and (*Antp>mCD8GFP*, N^{IC}) (**C-C''**) animals. High ROS is detected in the medulla and cortex of *Antp>mCD8GFP*, N^{RNAi} lymph glands. ROS levels were low or undetectable in the PSC of all three genotypes (**A'', B'', C''**).

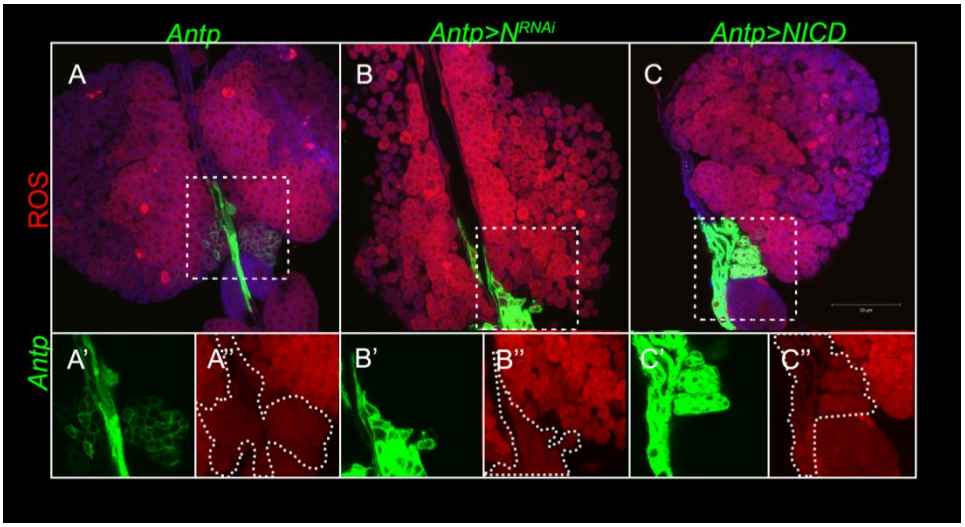

Supporting Figures

Figure S1. Specificity of anti-NICD staining

(**A-A"**) Anti-NICD staining in *Antp>mCD8GFP* background shows N signal (red) in all GFP-positive and GFP-negative cells. (**B-B"**) Reduction of the NICD staining signal is observed in GFP-positive, but not in GFP-negative, *Antp>mCD8GFP; N^{RNAi}* lobe. (**C**) *Antp>mCD8GFP; N^{RNAi}* lobe stained with Alexa Fluor 488–linked Phalloidin to detect F-actin. Cells of lamellocytic morphology and rich in F-actin appear in the vicinity of the niche.

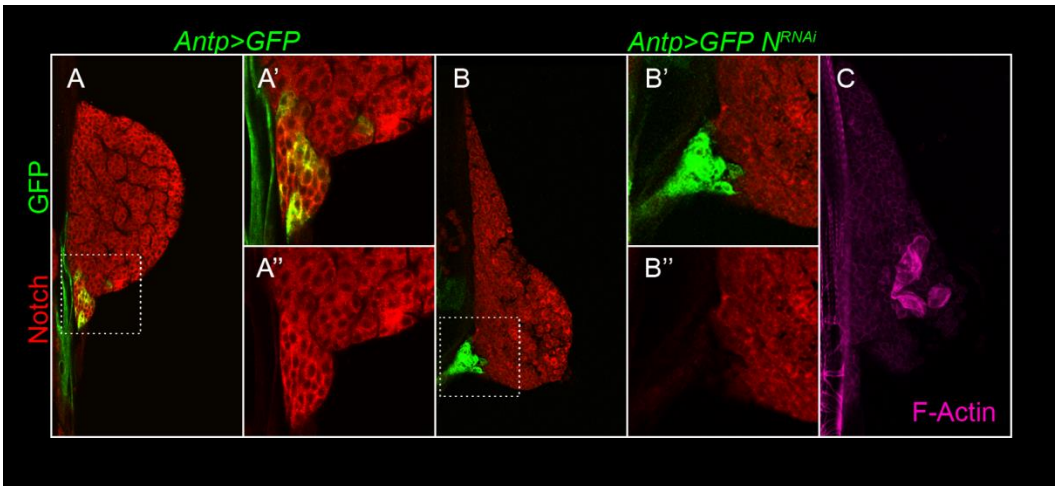

Done by Chiyedza Small. See Small and Ramroop *et al*., 2014

Figure S2. Cell-autonomous role for *N* in crystal cell differentiation in posterior lobes

(**A, B'**) *hsFLP; actin>NLS-GFP* control clones in a posterior lobe do not express pro-PO (red). (**B, B'**) Magnification of the region outlined in **A** and **A'**. (**C, D'**) Unlike the control lobes, *hsFLP; actin>NLS-GFP, NICD* posterior lobe produced clones that also express pro-PO. (**D, D'**) Magnification of the region outlined in panels **C** and **C'**. Hoechst stains DNA. For clarity, this channel is omitted in panels A', B', C', D'.

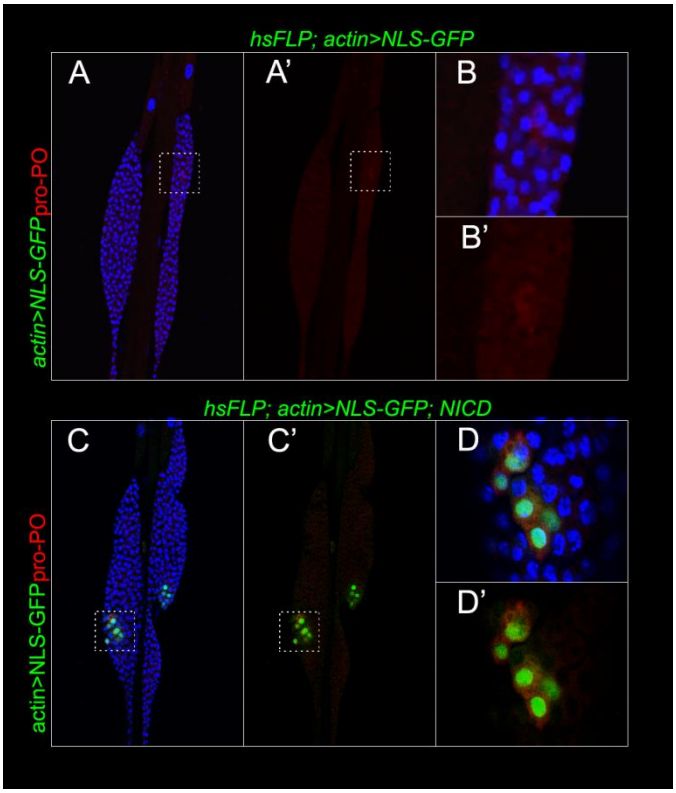

Done by Chiyedza Small. See Small and Ramroop *et al*., 2014

Figure S3. Wasp infection increases ROS in the niche

(**A-A’’**) ROS levels in the PSC of uninfected WT (*Antp>mCD8GFP*) lymph glands is low or undetectable (**A’’**) compared to infected (**B-B’’**). ROS levels were noticeably higher in the rest of the lymph gland lobe. Confocal settings of infected glands were turned down for clarity as the intensity of ROS (red) was extremely high.

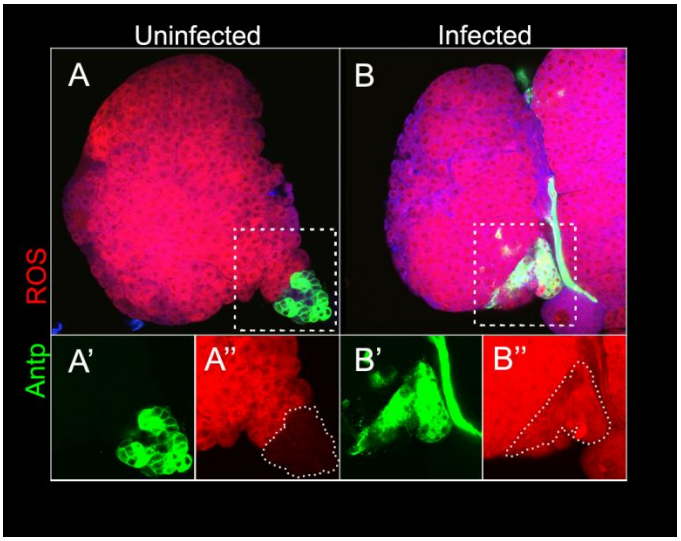

Table S1. The effects of N^{RNAi} in the wild type lymph glands

Dissected lymph glands were analyzed for the presence of three or more lamellocytes or signs of dispersal, both of which are criteria for immune activation. The Valium 10 construct elicited a stronger response than the Valium 1 construct. P value refers to student t test for the lymph gland dispersal response.

Valium	Genotype	Total Lymph Glands	Lymph Glands with Lamellocytes	Dispersed Lymph Glands	p-value
Valium 1	Antp>GFP	10	0	1	0.226
	Antp>N^{RNAi}	10	4	4	
	Hml>GFP	10	1	1	0.274
	Hml>N^{RNAi}	10	4	5	
Valium 10	Antp>GFP	35	5	2	0.001
	Antp>N^{RNAi}	35	21	30	
	Hml>GFP	35	2	4	0
	Hml>N^{RNAi}	35	17	31	

Quantification was done by Maria Otazo. See Small and Ramroop *et al*., 2014

Literature Cited

AVET-ROCHEX, A., K. BOYER, C. POLESELLO, V. GOBERT, D. OSMAN *et al.*, 2010 An in vivo RNA interference screen identifies gene networks controlling Drosophila melanogaster blood cell homeostasis. BMC Dev Biol **10:** 65.

BALABAN, R. S., S. NEMOTO and T. FINKEL, 2005 Mitochondria, oxidants, and aging. Cell **120:** 483-495.

BATAILLE, L., B. AUGE, G. FERJOUX, M. HAENLIN and L. WALTZER, 2005 Resolving embryonic blood cell fate choice in Drosophila: interplay of GCM and RUNX factors. Development **132:** 4635-4644.

BIGAS, A., T. D'ALTRI and L. ESPINOSA, 2012 The Notch pathway in hematopoietic stem cells. Curr Top Microbiol Immunol **360:** 1-18.

BRAY, S. J., 2006 Notch signalling: a simple pathway becomes complex. Nat Rev Mol Cell Biol **7:** 678-689.

CHRISTOPHIDES, G. K., E. ZDOBNOV, C. BARILLAS-MURY, E. BIRNEY, S. BLANDIN *et al.*, 2002 Immunity-related genes and gene families in Anopheles gambiae. Science **298:** 159-165.

CROZATIER, M., J. KRZEMIEN and A. VINCENT, 2007 The hematopoietic niche: a Drosophila model, at last. Cell Cycle **6:** 1443-1444.

CROZATIER, M., and M. MEISTER, 2007 Drosophila haematopoiesis. Cell Microbiol **9:** 1117-1126.

CROZATIER, M., J. M. UBEDA, A. VINCENT and M. MEISTER, 2004 Cellular immune response to parasitization in Drosophila requires the EBF orthologue collier. PLoS Biol **2:** E196.

DIAZ-BENJUMEA, F. J., and A. GARCIA-BELLIDO, 1990 Behaviour of cells mutant for an EGF receptor homologue of Drosophila in genetic mosaics. Proc Biol Sci **242:** 36-44.

DUVIC, B., J. A. HOFFMANN, M. MEISTER and J. ROYET, 2002 Notch signaling controls lineage specification during Drosophila larval hematopoiesis. Curr Biol **12:** 1923-1927.

EMERALD, B. S., and S. M. COHEN, 2004 Spatial and temporal regulation of the homeotic selector gene Antennapedia is required for the establishment of leg identity in Drosophila. Dev Biol **267:** 462-472.

FEHON, R. G., P. J. KOOH, I. REBAY, C. L. REGAN, T. XU *et al.*, 1990 Molecular interactions between the protein products of the neurogenic loci Notch and Delta, two EGF-homologous genes in Drosophila. Cell **61:** 523-534.

FOSSETT, N., 2013 Signal transduction pathways, intrinsic regulators, and the control of cell fate choice. Biochim Biophys Acta **1830:** 2375-2384.

GARCIA-OJEDA, M. E., R. G. KLEIN WOLTERINK, F. LEMAITRE, O. RICHARD-LE GOFF, M. HASAN *et al.*, 2013 GATA-3 promotes T-cell specification by repressing B-cell potential in pro-T cells in mice. Blood **121:** 1749-1759.

GHIGLIONE, C., O. DEVERGNE, E. GEORGENTHUM, F. CARBALLES, C. MEDIONI *et al.*, 2002 The Drosophila cytokine receptor Domeless controls border cell migration and epithelial polarization during oogenesis. Development **129:** 5437-5447.

GO, M. J., D. S. EASTMAN and S. ARTAVANIS-TSAKONAS, 1998 Cell proliferation control by Notch signaling in Drosophila development. Development **125:** 2031-2040.

GUEGUEN, G., M. E. KALAMARZ, J. RAMROOP, J. URIBE and S. GOVIND, 2013 Polydnaviral ankyrin proteins aid parasitic wasp survival by coordinate and selective inhibition of hematopoietic and immune NF-kappa B signaling in insect hosts. PLoS Pathog **In press**.

HAMANAKA, R. B., A. GLASAUER, P. HOOVER, S. YANG, H. BLATT *et al.*, 2013 Mitochondrial reactive oxygen species promote epidermal differentiation and hair follicle development. Sci Signal **6:** ra8.

HEITZLER, P., and P. SIMPSON, 1991 The choice of cell fate in the epidermis of Drosophila. Cell **64:** 1083-1092.

HONTI, V., G. CSORDAS, E. KURUCZ, R. MARKUS and I. ANDO, 2013 The cell-mediated immunity of Drosophila melanogaster: Hemocyte lineages, immune compartments, microanatomy and regulation. Dev Comp Immunol.

HONTI, V., G. CSORDAS, R. MARKUS, E. KURUCZ, F. JANKOVICS *et al.*, 2010 Cell lineage tracing reveals the plasticity of the hemocyte lineages and of the hematopoietic compartments in Drosophila melanogaster. Mol Immunol **47:** 1997-2004.

ITO, K., A. HIRAO, F. ARAI, K. TAKUBO, S. MATSUOKA *et al.*, 2006 Reactive oxygen species act through p38 MAPK to limit the lifespan of hematopoietic stem cells. Nat Med **12:** 446-451.

JANG, Y. Y., and S. J. SHARKIS, 2007 A low level of reactive oxygen species selects for primitive hematopoietic stem cells that may reside in the low-oxygenic niche. Blood **110:** 3056-3063.

JUNG, S. H., C. J. EVANS, C. UEMURA and U. BANERJEE, 2005 The Drosophila lymph gland as a developmental model of hematopoiesis. Development **132:** 2521-2533.

KALAMARZ, M. E., I. PADDIBHATLA, C. NADAR and S. GOVIND, 2012 Sumoylation is tumor-suppressive and confers proliferative quiescence to hematopoietic progenitors in Drosophila melanogaster larvae. Biol Open **1:** 161-172.

KOCH, U., R. LEHAL and F. RADTKE, 2013 Stem cells living with a Notch. Development **140:** 689-704.

KROEGER, P. T., JR., T. TOKUSUMI and R. A. SCHULZ, 2012 Transcriptional regulation of eater gene expression in Drosophila blood cells. Genesis **50:** 41-49.

KRZEMIEN, J., M. CROZATIER and A. VINCENT, 2010a Ontogeny of the Drosophila larval hematopoietic organ, hemocyte homeostasis and the dedicated cellular immune response to parasitism. Int J Dev Biol **54:** 1117-1125.

KRZEMIEN, J., L. DUBOIS, R. MAKKI, M. MEISTER, A. VINCENT *et al.*, 2007 Control of blood cell homeostasis in Drosophila larvae by the posterior signalling centre. Nature **446:** 325-328.

KRZEMIEN, J., J. OYALLON, M. CROZATIER and A. VINCENT, 2010b Hematopoietic progenitors and hemocyte lineages in the Drosophila lymph gland. Dev Biol.

KURUCZ, E., B. VACZI, R. MARKUS, B. LAURINYECZ, P. VILMOS *et al.*, 2007 Definition of Drosophila hemocyte subsets by cell-type specific antigens. Acta Biol Hung **58 Suppl:** 95-111.

LANOT, R., D. ZACHARY, F. HOLDER and M. MEISTER, 2001 Postembryonic hematopoiesis in Drosophila. Dev Biol **230:** 243-257.

LEBESTKY, T., T. CHANG, V. HARTENSTEIN and U. BANERJEE, 2000 Specification of Drosophila hematopoietic lineage by conserved transcription factors. Science **288:** 146-149.

LEBESTKY, T., S. H. JUNG and U. BANERJEE, 2003 A Serrate-expressing signaling center controls Drosophila hematopoiesis. Genes Dev **17:** 348-353.

LEE, C. Y., K. M. VOGELI, S. H. KIM, S. W. CHONG, Y. J. JIANG *et al.*, 2009a Notch signaling functions as a cell-fate switch between the endothelial and hematopoietic lineages. Curr Biol **19:** 1616-1622.

LEE, M. J., M. E. KALAMARZ, I. PADDIBHATLA, C. SMALL, R. RAJWANI *et al.*, 2009b Virulence factors and strategies of Leptopilina spp.: selective responses in Drosophila hosts. Adv Parasitol **70:** 123-145.

LUO, H., W. P. HANRATTY and C. R. DEAROLF, 1995 An amino acid substitution in the Drosophila hopTum-l Jak kinase causes leukemia-like hematopoietic defects. EMBO J **14:** 1412-1420.

MANDAL, L., U. BANERJEE and V. HARTENSTEIN, 2004 Evidence for a fruit fly hemangioblast and similarities between lymph-gland hematopoiesis in fruit fly and mammal aorta-gonadal-mesonephros mesoderm. Nat Genet **36:** 1019-1023.

MANDAL, L., J. A. MARTINEZ-AGOSTO, C. J. EVANS, V. HARTENSTEIN and U. BANERJEE, 2007 A Hedgehog- and Antennapedia-dependent niche maintains Drosophila haematopoietic precursors. Nature **446:** 320-324.

MINAKHINA, S., and R. STEWARD, 2010 Hematopoietic stem cells in Drosophila. Development **137:** 27-31.

MUKHERJEE, T., W. S. KIM, L. MANDAL and U. BANERJEE, 2011 Interaction between Notch and Hif-alpha in development and survival of Drosophila blood cells. Science **332:** 1210-1213.
NI, J. Q., L. P. LIU, R. BINARI, R. HARDY, H. S. SHIM *et al.*, 2009 A Drosophila resource of transgenic RNAi lines for neurogenetics. Genetics **182:** 1089-1100.
NI, J. Q., M. MARKSTEIN, R. BINARI, B. PFEIFFER, L. P. LIU *et al.*, 2008 Vector and parameters for targeted transgenic RNA interference in Drosophila melanogaster. Nat Methods **5:** 49-51.
OHLSTEIN, B., and A. SPRADLING, 2007 Multipotent Drosophila intestinal stem cells specify daughter cell fates by differential notch signaling. Science **315:** 988-992.
ORKIN, S. H., and L. I. ZON, 2008 Hematopoiesis: an evolving paradigm for stem cell biology. Cell **132:** 631-644.
OWUSU-ANSAH, E., and U. BANERJEE, 2009 Reactive oxygen species prime Drosophila haematopoietic progenitors for differentiation. Nature **461:** 537-541.
PADDIBHATLA, I., M. J. LEE, M. E. KALAMARZ, R. FERRARESE and S. GOVIND, 2010 Role for sumoylation in systemic inflammation and immune homeostasis in Drosophila larvae. PLoS Pathog **6:** e1001234.
PARMAR, K., P. MAUCH, J. A. VERGILIO, R. SACKSTEIN and J. D. DOWN, 2007 Distribution of hematopoietic stem cells in the bone marrow according to regional hypoxia. Proc Natl Acad Sci U S A **104:** 5431-5436.
PICCOLI, C., R. RIA, R. SCRIMA, O. CELA, A. D'APRILE *et al.*, 2005 Characterization of mitochondrial and extra-mitochondrial oxygen consuming reactions in human hematopoietic stem cells. Novel evidence of the occurrence of NAD(P)H oxidase activity. J Biol Chem **280:** 26467-26476.
R-DEVELOPMENT-CORE-TEAM, 2010 R: A language and environment for statistical computing. http://www.R-project.org/. R Foundation for Statistical Computing, Vienna, Austria. .
RADTKE, F., A. WILSON and H. R. MACDONALD, 2005 Notch signaling in hematopoiesis and lymphopoiesis: lessons from Drosophila. Bioessays **27:** 1117-1128.
SCHLENKE, T. A., J. MORALES, S. GOVIND and A. G. CLARK, 2007 Contrasting infection strategies in generalist and specialist wasp parasitoids of Drosophila melanogaster. PLoS Pathog **3:** 1486-1501.
SINENKO, S. A., E. K. KIM, R. WYNN, P. MANFRUELLI, I. ANDO *et al.*, 2004 Yantar, a conserved arginine-rich protein is involved in Drosophila hemocyte development. Dev Biol **273:** 48-62.
SINENKO, S. A., J. SHIM and U. BANERJEE, 2012 Oxidative stress in the haematopoietic niche regulates the cellular immune response in Drosophila. EMBO Rep **13:** 83-89.
SORRENTINO, R. P., Y. CARTON and S. GOVIND, 2002 Cellular immune response to parasite infection in the Drosophila lymph gland is developmentally regulated. Dev Biol **243:** 65-80.
SORRENTINO, R. P., J. P. MELK and S. GOVIND, 2004 Genetic analysis of contributions of dorsal group and JAK-Stat92E pathway genes to larval hemocyte concentration and the egg encapsulation response in Drosophila. Genetics **166:** 1343-1356.
STOFANKO, M., S. Y. KWON and P. BADENHORST, 2008 A misexpression screen to identify regulators of Drosophila larval hemocyte development. Genetics **180:** 253-267.
STOFANKO, M., S. Y. KWON and P. BADENHORST, 2010 Lineage tracing of lamellocytes demonstrates Drosophila macrophage plasticity. PLoS One **5:** e14051.
STRUHL, G., and A. ADACHI, 1998 Nuclear access and action of notch in vivo. Cell **93:** 649-660.
STRUHL, G., and K. BASLER, 1993 Organizing activity of wingless protein in Drosophila. Cell **72:** 527-540.
TARPEY, M. M., D. A. WINK and M. B. GRISHAM, 2004 Methods for detection of reactive metabolites of oxygen and nitrogen: in vitro and in vivo considerations. Am J Physiol Regul Integr Comp Physiol **286:** R431-444.
TERRIENTE-FELIX, A., J. LI, S. COLLINS, A. MULLIGAN, I. REEKIE *et al.*, 2013 Notch cooperates with Lozenge/Runx to lock haemocytes into a differentiation programme. Development **140:** 926-937.

TOKUSUMI, T., R. P. SORRENTINO, M. RUSSELL, R. FERRARESE, S. GOVIND *et al.*, 2009 Characterization of a lamellocyte transcriptional enhancer located within the misshapen gene of Drosophila melanogaster. PLoS One **4:** e6429.

TOKUSUMI, Y., T. TOKUSUMI, D. A. SHOUE and R. A. SCHULZ, 2012 Gene regulatory networks controlling hematopoietic progenitor niche cell production and differentiation in the Drosophila lymph gland. PLoS One **7:** e41604.

TOTHOVA, Z., R. KOLLIPARA, B. J. HUNTLY, B. H. LEE, D. H. CASTRILLON *et al.*, 2007 FoxOs are critical mediators of hematopoietic stem cell resistance to physiologic oxidative stress. Cell **128:** 325-339.

VINCENT, J. P., C. H. GIRDHAM and P. H. O'FARRELL, 1994 A cell-autonomous, ubiquitous marker for the analysis of Drosophila genetic mosaics. Dev Biol **164:** 328-331.

WANG, L. D., and A. J. WAGERS, 2011 Dynamic niches in the origination and differentiation of haematopoietic stem cells. Nat Rev Mol Cell Biol **12:** 643-655.

XU, T., and G. M. RUBIN, 1993 Analysis of genetic mosaics in developing and adult Drosophila tissues. Development **117:** 1223-1237.

ZHAO, H., S. KALIVENDI, H. ZHANG, J. JOSEPH, K. NITHIPATIKOM *et al.*, 2003 Superoxide reacts with hydroethidine but forms a fluorescent product that is distinctly different from ethidium: potential implications in intracellular fluorescence detection of superoxide. Free Radic Biol Med **34:** 1359-1368.

Chapter 2

Lethal effects of *L. heterotoma* infection on hematopoiesis and characterization of a SipD/IpaD-like protein from its virus-like particles

Abstract

In contrast to *L. boulardi* (*Lb*) that activates the humoral but suppresses cellular immunity, *L. heterotoma* (*Lh*) parasitizes *Drosophila* larvae using a sophisticated infection mechanism that blocks both humoral and cellular Toll-NF-κB-dependent immune arms of its fly hosts. Key to this attack are spiked virus-like particles (VLPs) produced in the female wasp's venom gland. Our previous work has shown that VLP spikes facilitate their entry into larval fly blood cells, where they kill both immature and mature hemocytes. To examine how the same host responds to differing in virulence strategies of *Lb* and *Lh* wasps, we (a) studied internalization of the *Lh* VLPs into plasmatocytes, lamellocytes, and crystal cells, (b) examined the cellular effects of *Lh* VLPs in hematopoietic cells, and (c) tracked VLP localization in hematopoietic cells and associated tissues of the larval circulatory system. We found that VLPs use a Rab5-dependent mechanism to enter plasmatocytes, whereas their entry into lamellocytes does not follow this pathway. VLPs do not appear to enter crystal cells. Cell death in plasmatocytes correlates with cleavage of Caspase 3, while lamellocytes die by lysis. In infected animals, VLPs are found in striking abundance not only in these hematopoietic cell types, but also around (but not within) the cells of the posterior signaling center (PSC), as well as within the dorsal vessel. Instead of being tightly clustered, PSC cells are dispersed in the body of the lobes, either singly or in smaller groups. Lymph glands remain non-responsive to wasps when

PSCs are ablated and VLP levels in the dorsal vessel and lymph glands were low. These studies highlight an immune function of the PSC and suggest that VLPs inactivate this function.

We also studied one of the most abundant *Lh* VLP proteins, p40, that is absent in the *Lb* venom. Previous studies have shown that p40 is a surface protein, also localized to VLP spike termini. p40 is synthesized in venom glands and enters the larval blood cells. Antibody inhibition experiments suggested that p40 mediates interaction of the VLP surface/spikes with host cell membranes and this interaction is pivotal to lamellocyte lysis. Here we show that p40 encodes a SipD/IpaD-like protein. The SipD/IpaD family of type 3 Gram negative bacterial secretion system proteins reside at bacterial needle tips and regulate protein secretion and needle insertion into host membranes. In preliminary experiments, bacterial extracts with the SipD/IpaD-like regions of p40 altered lamellocyte morphology, *in vitro*. These results further support the idea that p40, the first eukaryotic member of this protein family, may similarly function in protein secretion and efficient delivery of virulence factors into host hemocytes and mediate VLP entry into lamellocytes. These studies begin to explain how VLPs target and kill their host cells and the mechanisms underlying differing virulence strategies of the two wasp species.

Introduction

Parasitic wasps are engaged in an arms race with their hosts and are equipped with the armament for success. Members of a large group of insects, parasitic wasps have an obligatory relationship with their insect hosts. We are studying a unique *Drosophila*-parasitic wasp model to understand how this class of parasitic wasps overcomes their hosts' immunity. *Leptopilina heterotoma* (*Lh*) infects nearly all *Drosophila* species studied, but the specialist *L. boulardi* (*Lb*) infects only the melanogaster group flies (SCHLENKE 2007). Both wasps infect *Drosophila* larvae and hijack their developing bodies. Both *Lh* and *Lb* adult free-living females produce immune-suppressive virus like particles (VLPs) within their venom glands, but only *Lh*'s VLPs can completely suppress fly host immunity. In each case, 4-8 spikes (spike to spike ~300 nm) radiate from a central spherical/polygonal VLP core. Spikes mediate contact with host hemocytes. While not identical, both species' VLPs share notable morphological similarities even though the spikes of *Lb*'s VLPs are considerably longer (CHIU *et al.* 2006; CHIU 2006; GUEGUEN 2011).

VLPs enter the host larval hemolymph during oviposition, they bind to non-phagocytic lamellocytes, become internalized, and promote lamellocyte lysis (CHIU *et al.* 2006; RIZKI and RIZKI 1984; RIZKI and RIZKI 1992; RIZKI and RIZKI 1994; RIZKI *et al.* 1990). *Lh* VLPs enter circulating phagocytic plasmatocytes and lymph gland hemocyte progenitors and cause death via apoptosis (CHIU and GOVIND 2002). Different *Lh* strains tested on *D. melanogaster* are consistently highly virulent and harbor morphologically identical VLPs (our unpub. results). We proposed that VLPs carry effectors for ablation and silencing host immunity (CHIU *et al.* 2006; SCHLENKE *et al.* 2007).

In vitro incubation of plasmatocytes and lamellocytes from $hop^{Tum\text{-}l}$ larvae with venom of *Lh* or *L. victoriae* (*Lv* Leiden strain, sister species of *Lh* (SCHILTHUIZEN 1998)) wasp, but not

Lb's venom, results in apoptosis of plasmatocytes, but all lamellocytes rapidly become bipolar and lyse (CHIU and GOVIND 2002). Polyclonal antisera against the most abundant *Lh* VLP protein, p40 (that also reacts with a slightly larger p47.5 protein of *Lv* VLPs) neutralized VLP activity (CHIU *et al.* 2006). Antibody neutralization had a stronger effect on *Lh* VLPs (less than 10% bipolar lamellocytes) as compared to *Lv* VLP (less than 50% bipolar cells). When lamellocytes were treated with VLPs incubated with same concentration of serum from unimmunized mice, no significant effect was observed (87% bipolar cells). Immuno-EM staining of mature VLPs from both species localizes the p40 and p47.5 proteins largely to the periphery of the VLPs and along the VLP spike-like projections, and spike tips (CHIU *et al.* 2006). Thus, VLPs have at least two distinct cell-type-specific effects on hemocyte, apoptosis and lysis, and p40/p47.5 can be linked to lamellocyte lysis.

Although *Lb* infection activates humoral immunity in fly larvae (SCHLENKE 2007) and NF-κB target gene expression in the larval lymph gland PSC (GUEGUEN 2013) [posterior signaling center or PSC is a cluster of 25-50 cells of non-hematopoietic origin located at the posterior end of each anterior lobe and reprograms hematopoiesis upon *Lb* infection (BENMIMOUN *et al.* 2015; CROZATIER *et al.* 2004a; GUEGUEN 2013; KRZEMIEN *et al.* 2010a; KRZEMIEN *et al.* 2007; SINENKO *et al.* 2012; SMALL *et al.* 2014)], most *Lb* strains are quite virulent (COLINET 2013; DUBUFFET 2009; SCHLENKE 2007). *Lb* VLPs do not compromise hemocyte viability, although they modify lamellocyte shape and adhesion (COLINET 2013; COLINET 2010; SCHLENKE 2007). It is assumed that *Lb* VLPs enter hemocytes, but their uptake into host hemocytes has not been demonstrated experimentally (RIZKI 1990a). Thus, not only are *Lh* and *Lb* VLPs morphologically distinct, their interactions with plasmatocytes and lamellocytes also differ: *Lh* VLPs kill host hemocytes whereas *Lb* VLPs only appear to alter lamellocyte

properties (COLINET 2013; COLINET 2010; SCHLENKE 2007). These key differences underlie *Lh*'s differential immune suppression and greater virulence in comparison to *Lb* wasps.

Unlike viruses, bacteria, and eukaryotic organelles such as mitochondria, VLPs undergo morphogenesis and assembly extracellularly in the venom gland canals and lumen. VLPs are synthesized in the long gland and are first visible within efferent canals connecting secretory cells to the long gland lumen. Using confocal image reconstructions and scanning and transmission electron microscopy approaches, we found that in both *Lh* and *Lv*, (**1**) the canals originate in the cytoplasm of the secretory cells and, after passing through cells of the endothelial layer, open into the long gland lumen; (**2**) the region of the canal that is proximal to the secretory cell is surrounded by microvilli; (**3**) the region of the canal distal to the secretory cell is smooth; (**4**) the canals are lined with filamentous actin; (**5**) in three-dimensional reconstruction, solitary, unbranched canals exhibit roughly parallel orientation, directed towards the lumen; **(6**) these canals are found in equivalent glandular structures in other wasp species outside the *Leptopilina* genus and likely represent novel secretion structures for production of mature immune suppressive factors (FERRARESE 2009).

To delineate the molecular basis of *Lh* VLP bioactivity, we (1) characterized VLP proteomes from two *Lh* strains (*Lh14* and *LhNY*) and (2) scored the absence/presence of *Lh* VLP proteins in an *Lb* abdominal transcriptome. This analysis identified ~160 proteins some of which belong to the endomembrane/vesicular class, while others are related to infection, immunity and immune suppression (Govind lab, unpub.). Based on these studies, we propose that VLPs are novel fusion-active microvesicle-like compartments that transfer virulence cargo from the parasite to host. p40 is one among the few proteins present in the *Lh* venom, but not in the *Lb* venom (Govind lab, unpub.).

The goals of this study were to (a) identify the differences in the entry mechanisms of VLP into plasmatocytes and lamellocytes; (b) examine the localization of VLPs in the circulatory system; (c) examine the role of the niche in the infection process; and (d) identify the molecular structure of p40 and examine its role in lamellocyte function. We show that Entry into plasmatocytes but not in lamellocytes is mediated via Rab5. Furthermore, depletion of host hemocytes and hematopoietic progenitors in *Lh*-infected animals correlates with lamellocyte lysis, caspase-mediated cell death of plasmatocytes, changes in gene expression in the PSC cells, high levels of p40 signal in plasmatocytes, lamellocytes, but not in crystal cells, high p40 levels around PSC cells, as well as in the dorsal vessel. The PSC plays an immune function and *Lh* VLPs appear to inactivate this function by dispersing PSC cells. Sequence analysis and preliminary computational modeling of p40 suggests similarity with *Shigella*/*Salmonella* invasion proteins IpaD/SipD. This difference in *Lh* versus *Lb* venom may in part be responsible for their differing biological activities on host hemocytes. Our proteomic results of *Lh* VLPs, immunohistochemistry prediction of p40 structure support the notion that VLPs are microvesicle-like cellular products or secretion systems, and p40 likely directly mediates VLP entry into lamellocytes. p40 is encoded by a gene with four introns and five exons, and is likely to be part of the wasp genome, supporting a symbiotic relationship of the VLP with its wasp.

Virulence factors provide the armament for parasite success in the host/pathogen arms race, shaping their co-evolution and population structures. Our studies advance our understanding of a novel extracellular compartment produced in the wasp's venom gland and its relationship to its wasp host. The *Drosophila-Leptopilina* system offers opportunities to apply *Drosophila* genetics to explore why these generalist wasps succeed in a wide range of species worldwide.

Materials and Methods

Stocks, crosses, and wasp infections

All fly stocks and crosses were raised on standard fly medium (cornmeal flour 65 g/L, dry brewer's yeast (Sigma) 35g/L, sucrose 140g/L, and agar 10g/L) at 25ºC. Standard crosses were performed to obtain the desired genetic backgrounds.

Antp-GAL4 was received from S. Minakhina (EMERALD and COHEN 2004). The *Dome-MESO-GFP* (medulla is GFP-positive), (OYALLON *et al.* 2016) and *y w; Collier-Gal 4 / CyO y+* stocks were gifts of M. Crozatier. *D4-lacZ,* a gift from A. Courey, contains four tandemly repeated Dorsal/Dif binding sites (FLORES-SAAIB *et al.* 2001). *UAS-lz-NLS-GFP* mark mature crystal cells in the lymph glands and circulating populations (LEBESTKY *et al.* 2000). Hemocyte specific drivers (1) for plasmatocytes, *Pxn-Gal4,UAS-GFP* (LANOT *et al.* 2001), (2) for lamellocytes, $hop^{Tum\text{-}l}$ *msn-GAL4; UAS-mCD8-GFP* (recombinant 15.2 made in our lab) uses the *misshapen* driver (TOKUSUMI 2009). Pro-apoptotic gene *UAS-hid* was used for ablation of the PSC (IGAKI *et al.* 2000). *D. yakuba* was obtained from the University of California *Drosophila* species stock center. The following strains were also obtained from the Bloomington Stock Center; $Rab5^{RNAi}$ (#30518), $Rab7^{RNAi}$ (#27051), $Rab11^{RNAi}$ (#27703), $Toll^{RNAi}$ (#31044), $Toll7^{RNAi}$ (#30488), kn^{RNAi} (#31916), mys^{RNAi} (#27735), shi^{RNAi} (28513). All RNAi lines were valium 10 except for Tl^{RNAi} which was valium 1 (NI *et al.* 2009).

Unless otherwise stated, females from respective Gal4 driver stocks were crossed to males from respective UAS-RNAi stocks. Third instar larvae from 12 hour egg-lays were reared at 25^0C, matched for biological age and genotyped for immunohistochemistry and other analyses. PSC-less animals were made by crossing *UAS-hid* females with *y w*; *Collier-Gal 4 /*

CyO y+ males and screened by yellow mouth hooks. *CyO y+* (black mouth hooks) siblings served as the internal control (unaffected PSC animals).

y w D. melanogaster was used as wild type stock for rearing of wasps. Wasp infections were performed as follows: from a twelve-hour egg-lay, second instar wild type or mutant larvae were subjected to infection by *L. boulardi* 17 (*Lb17*) or *L. heterotoma* 14 (*Lh14*) (SCHLENKE 2007) or *L. heterotoma* NY (*LhNY*) (CHIU 2006), *L. victoriae Unk* (*Lv*) (Dr. T. Schlenke, via Dr. M. Mateos). Ten to twelve trained female wasps were introduced with hosts for eight to twelve hours, after which wasps were removed and host larvae were allowed to recover and develop to third instar stage. Uninfected controls followed the same growth regimen.

Immunohistochemistry

Mid third instar larvae were used in all antibody staining experiments. Staining was performed according to (PADDIBHATLA *et al.* 2010). Primary antibodies: mouse anti-p40 (CHIU 2006) 1:1000, rabbit anti-cleaved caspase 3 (Cell Signaling Technology) 1:200, mouse anti-integrin-β PS (CF6G11; Developmental Studies Hybridoma Bank) 1:10, mouse anti-Antennapedia (8C11-s; Developmental Studies Hybridoma Bank) 1:20, chicken anti-β galactosidase (Immunology Consultants, Inc.) 1:200. Secondary antibodies: Cy3 AffiniPure donkey anti-chicken (Jackson Immuno Research) 1:500, Cy3 AffiniPure donkey anti-mouse, Cy3 AffiniPure donkey anti-rabbit and FITC-AffiniPure goat anti-mouse (all from Jackson Immuno Research) 1:200. Rhodamine-or Alexa Fluor 488-tagged Phalloidin and nuclear dye Hoechst 33258 (all from Invitrogen) were used to examine cell morphology.

Lamellocytes were visualized by (a) their cell shape (Phalloidin detected filamentous actin); or (b) by expression of integrin-β (STOFANKO *et al.* 2008); or (c) by the *misshapen* transcriptional enhancer *msnf9* linked to GFP expression (TOKUSUMI 2009).

Confocal imaging

Samples were imaged with Zeiss laser scanning confocal microscopes LSM 510 or LSM710. Optical section images were gathered at 0.8 µm -1.5 µm and recorded at 8 bit. Images were analyzed according to (GUEGUEN 2013). Images for each experiment were scanned on the same microscope using the same software scan settings. A negative control (identical staining protocol but without primary antibody) was used to find the amplifier gain/offset cut-off value. Images were processed for analysis using Zeiss LSM image browser and Zen lite 2012 software. All images were assembled using Microsoft PowerPoint 2010.

***In situ* melanization assay**

Third instar larvae (10-15) were heated in 1xPBS, pH 7.4 at 70°C for 20 minutes in a heating block. Animals were dried with Kim wipes and placed on microscope slide oriented the same way, dorsal side up. Posterior segments of animals were imaged with a Leica MZFL III stereomicroscope at 63x magnification. Melanized cells in the three posterior-most larval segments visible through the cuticle were counted manually. Infection status of individual animals was confirmed after the imaging step was complete by physically opening each animal and scoring wasp eggs in the hemocoel. Data were analyzed with Microsoft Excel 2010.

Peptide analysis of p40

p40 protein from *LhNY* VLPs (estimated to be roughly 0.4 mg on 9% SDS-PAGE, stained with Coomassie Blue) was sequenced at the Harvard Microchemistry Facility by microcapillary reverse phase HPLC nano-electrospray tandem mass spectrometry on a Finnigan LCQ quadrupole ion trap mass spectrometer. Three partial peptide sequences obtained are as follows: **S[Q/G]VV[S/A]NLE[E]AN[T/L][K]** (8 possible sequences), **[M/N]INEL[N/T]VGT[K] ,** (4 possible sequences), and **FYNSI[K/P]** (2 possible sequences). In addition, we also obtained p40 peptide sequences from mass spectrometry of all VLP proteins (all the bands were subjected to sequencing at the Proteomics Facility at the Icahn School of Medicine at Mount Sinai). There was overlap of peptide sequences for these two independent proteomic analyses. These peptides from the Mount Sinai proteome data were "BLASTed" against *Lh14* abdominal transcripts (GOECKS 2013). These efforts lead to the identification of GAJC01013394 as a candidate p40 cDNA that was then used in primer design.

RNA extraction, cDNA preparations, p40 cloning, expression, and Western analysis

Total RNA was isolated/extracted with TRIZOL reagent (Invitrogen) from (1) ~50 abdomens of *Lh14* or *Lv* females, (2) ~600 *Lh14* venom glands, and (3) total hemocytes of ~50 uninfected or *Lh14* wasp-infected $hop^{Tum\text{-}l}$ *msn>mcd8GFP* larvae. cDNA was synthesized using ProtoScript M-MuLV first strand synthesis kit (New England Biolabs Inc.) following manufacturer's protocol. The presence of host cells cDNA was confirmed by PCR of a reference ribosomal gene, *rp49*. RNA was stored at -80ºC and cDNA was stored at -20ºC.

Specific primers (5'UTR and 3'UTR GAJC01013394; Supplementary Table 1) and *Lh14* venom gland cDNA template were used to amplify the full-length p40 sequence (Figure S9 B)

For this, Phusion Hot Start II high-fidelity DNA polymerase (Thermo Scientific) was used. 3' A-overhangs were generated by Taq polymerase (home-made; gift from Dr. C. Li). This full-length p40 sequence was cloned into pCRII TOPO Dual (Invitrogen) and transformed into BL21 competent cells. The sequence of clone # 9 was verified by Sanger sequencing (Genewiz).

The internal helical p40 domain was amplified not from clone # 9, but from a full length (5'UTR and 3" UTR primers) clone # M1, also prepared from amplified venom gland cDNA template (Li lab, Taq polymerase) in pCR 2.1-TOPO (Invitrogen) in *DH5α* (NEB). Internal primers (*Bam* HI site in the forward and *Eco* RI site in the reverse directions and an in-frame stop codon, Supplementary Table 1) and clone # M1 template were used to amplify this region which was cloned into the pTrcHisA vector in *DH5α* (New England Biolabs Inc.). Clone # 36 was transferred to BL21 cells for protein induction. Potential clones were screened by colony PCR and selected clone sequences were verified by Sanger sequencing (Genewiz).

pTrcHisA has the following properties: (*trp-lac* promoter) (AMANN *et al.* 1983), an N-terminal peptide that codes for a translation initiation codon, a series of six histidine residues for metal binding in the translated protein, the bacteriophage T7 gene 10 translation enhancer, and an enterokinase cleavage recognition sequence to remove the histidine tag. p40 protein was induced with addition of 1mM IPTG (Thermo Scientific) and protein extracts were prepared by freeze thawing and lysing *E. coli* BL21 cells in lysis buffer (10% triton X, 150 mM NaCl, 1 mM EDTA and 50 mM Tris HCl, pH 6.8). Loading dye composition was 50 mM Tris-HCl (pH6.8), 5% SDS, 20% glycerol, 5% beta mercaptoethanol (Acros Organics), and 0.05% bromophenol blue. Protease inhibitors (Fermentas Proteoblock Protease inhibitor) cocktail (#R1321: AEBSF-HCl 100 mM, aprotinin 80 µM, bestatin 5 mM, E-64 1.5 mM, leupeptin 2 mM, pepstatin A 1mM) or (Sigma# P8340, same composition) was used in some experiments.

Proteins were separated by SDS-PAGE (5% stacking gel and 12% resolving gel). Following electrophoresis (100 volts), proteins were transferred onto nitrocellulose membrane (HyBond, Amersham Life Science), blocked with PBS (pH 7.4) containing 0.1 % Tween 20, 5% nonfat dry milk, and 3% BSA for 1 hour at room temperature. Blots were incubated with mouse anti-p40 antibody (1:1000) or mouse anti-His antibody (Invitrogen 1:1000) at 4ºC overnight, followed by the secondary alkaline-phosphatase-linked anti-mouse antibody 1:2,500 (Promega) at room temperature for 1 hour. Protein was detected by incubating the blots in alkaline phosphatase buffer (NTM 9.5: 100 mM Tris pH 9.5, 100mM NaCl, and 50 mM $MgCl_2$) containing substrate [5 µL of 25 µg/µL BCIP (Amresco), and 5 µL of 50 µg/µL NBT (Biotium) per 1 mL of NTM]. Blots were rinsed in water to stop color development.

Bipolar cell assay

Thirty third instar (uninfected or *Lh14*-infected; $hop^{Tum\text{-}l}$ *msn>mcd8GFP* each) larvae were washed in 70% ethanol followed by 1xPBS (pH 7.4). Hemolymph was collected by puncturing the cuticle with a dissecting forceps and pipetting into 200 µL of 7% BSA in PBS in a glass depression slide. 20 µL of 7% BSA and 20 µL of live cells were aliquoted directly onto a microscope slide and allowed to adhere to the slide for 1 hour. Fresh BSA was added to cells, and they were next incubated for 2 hours with (a) phosphate buffer (no treatment control with no lysates or venom gland extracts, (b) *Lh14* venom gland extract, (c) bacterial lysates with truncated p40 from IPTG-induced, or (d) lysates from uninduced *E. coli* BL21 cells. The pellet and supernatant fractions were processed separately. Venom gland extract and bacterial protein extracts were collected and lysed in 20 mM phosphate buffer (pH 7.0) without triton X or Tris,

frozen (dry ice) and thawed (42°C) several times with vortexing in between. GFP positive lamellocytes were imaged with a fluorescent Nikon Eclipse TS100 microscope at 100x.

Results

Differential effects of *Lb17* and *Lh14* on the lymph gland

We compared effects of *Lb* and *Lh* infection on lymph gland homeostasis in two different genetically wild type background animals, *Antp>GFP* and *Dome-Meso-GFP* where the PSC or the medullary zone cells express GFP, respectively. Infection by *Lb17* results in lamellocyte differentiation in the cortical zone, and by mid-third instar stage, lymph glands are dispersed (Figure 1, A, B, D E; (SMALL *et al.* 2014). Although at earlier time points, a few lamellocytes are sometimes observed after *Lh* infection (not shown), by mid-third instar, lobes of *Lh* infected glands are significantly smaller; the overall numbers of lobe cells in both the cortex and medulla are reduced considerably (Figure 1 G and H). Moreover, the PSC (*Antp>GFP* positive cells) is disorganized (Figure 1 G) and unlike PSC from *Lb*-infected animals (Figure 1 D). PSC expression of *D4-LacZ* reporter increases and Antp protein signal remains unchanged (Figure 1 C, F), these PSC markers are reduced in *Lh* infected lymph glands (Figure 1 C, I). Thus, both wasp species have drastically different effects on the various regions of the anterior lobes. A similar loss of hematopoietic progenitors was observed in *Lh* infected *D. yakuba* (Figure S1 A, C) suggesting that the lymph gland is a primary target of *Lh* in different *Drosophila* species.

p40 localization in hematopoietic cells

We used a mouse polyclonal antibody against the VLP surface marker (CHIU 2006) as proxy for VLPs in hemocyte populations and associated tissues. Control experiments for specificity were: (1) lack of staining signal in *Lb* infected cells (not shown); (2) no signal in *Lh* infected tissues without primary antibody (Figure 7 A and D, 8 A and A', S1 A-B', S2 A and C).

To detect VLPs (or the p40 antigen) in all three cell types, we infected wild type (*lz-NLS-GFP*) and mutant (*hop^{Tum-l} msn>mcd8GFP*) larvae with two different *Lh* strains (*Lh14* or *LhNY*). In the *hop^{Tum-l}* background, numerous lamellocytes form due to constitutive JAK-STAT signaling (LUO *et al.* 1995). Furthermore, only lamellocytes but not plasmatocytes or crystal cells express GFP under the control of the *misshapen* (*msn*) promoter. In the infected larvae, p40 signal is high in cells of lymph gland lobes, dorsal vessel, as well as in circulating hemocytes. Furthermore, p40 staining is different in plasmatocytes and lamellocytes regardless of whether they are in the lymph glands (Figure 2 A-A' ') or in circulation (Figure 2 B-B''). In plasmatocytes, p40 staining is bright, cytoplasmic and punctate (arrows), while in lamellocytes, it is diffuse and nuclear (arrowheads) (Figure 2 A-B"). This dichotomous cytoplasmic/nuclear localization of p40 in plasmatocytes versus lamellocytes is also observed in anterior (Figure S1 C-C'') and posterior lobes of *D. yakuba* (Figure S1 D-D''). Wild type *D. melanogaster* infected with another *Lh* wasp strain, *LhNY* showed the same p40 staining pattern in anterior and posterior lobes and the dorsal vessel (Figure S2 A-D'').

Like *Lb* infection, *Lh* infection results in a reduction of circulating and sessile crystal cells as visualized by *in situ* melanization of infected larvae (Figure S3). This reduction appears not to be due to direct destruction by VLPs as the p40 signal in *Lh14* infected *lz>NLS-GFP* larvae (mature crystal cells express GFP (LEBESTKY *et al.* 2000)) did not coincide with GFP expression either in the lymph gland crystal cells (Figure 2 C-C'') or in circulating crystal cells (Figure D-D').

VLP entry into host hemocytes

We next investigated the mode of VLP entry into plasmatocytes and lamellocytes. Since plasmatocytes are macrophage-like phagocytic cells (KURUCZ 2007), we investigated the requirements of endosomal proteins Rab5, Rab7, and Rab11 for *Lh14* VLP uptake. Rab5 mediates trafficking from the plasma membrane to early endosomes, Rab7 mediates late endosome formation controlling trafficking between late endosomes and lysosomes, and Rab11 is involved in transport from the Golgi network to recycling endosomes (BHUIN and ROY 2014). In contrast to *Pxn>GFP* plasmatocytes, where the VLP signal is punctate and distributed in the cytoplasm (peripheral to perinuclear, Figure 2 A" and B" arrows) $Rab5^{RNAi}$ knockdown (*Pxn>GFP,* $Rab5^{RNAi}$) plasmatocytes show only peripheral localization of p40, presumably of intact VLPs, trapped in early endosomes (Figure 3 A-B''). This peripheral localization was observed for both GFP-positive phagocytic cells in the lymph gland anterior lobes (Figure 3 A-A'') and in circulation (Figure 3 B-B''). Surprisingly however, unlike Rab5, Rab7 and Rab11 knockdown plasmatocytes remained competent in VLP uptake, even though knockdown plasmatocytes for all three genes compromised phagocytosis of fluorescently-labeled surrogate bacteria (not shown). Knockdown of *shibiri* in plasmatocytes ($Pxn>shi^{RNAi}$) did not compromise VLP uptake. Some (<5%) unusual $Pxn>shi^{RNAi}$ hemocytes were polyploid and multinucleate; these cells however failed to take up VLPs (not shown). Similarly, knockdown of two candidate receptors Toll1 (PADDIBHATLA *et al.* 2010) and Toll7 (NAKAMOTO *et al.* 2012) did not compromise VLP uptake and normal distribution of the p40 signal was observed (Figure S4 A-E", arrowheads).

Unlike plasmatocytes, lamellocytes are not phagocytic and do not internalize bacterial particles (Govind lab unpub.). A knockdown of Rab5 in lamellocytes of $hop^{Tum\text{-}l}$ background

using the *msn-Gal4* driver shows no effect on p40 staining and distribution and the signal remains diffuse and nuclear (compare Figures 2 A-B'' and 3 C-D'' arrowheads).

Lamellocytes can be distinguished from plasmatocytes by higher levels of integrin-β (STOFANKO 2010) (Figure S5 A-A'). To investigate if integrin-β might mediate VLP binding or internalization, we infected $hop^{Tum\text{-}l}$ *msn>mCD8GFP,* $Int\beta^{RNAi}$ animals. However, the p40 staining and distribution remains diffuse and nuclear (Figure S5 D-E', arrowheads) and bipolar lamellocytes were observed.

The cell-killing effects of *Lh14* VLPs is hemocyte-specific

It has previously been shown that *Lh* infection leads to apoptosis as detected by TUNEL staining (CHIU 2002). *In vitro* studies with VLP-containing venom gland extracts induce morphological changes of lamellocytes, causing them to become bipolar, leak cytoplasm and lyse (CHIU *et al.* 2006; MORALES 2005; RIZKI 1990b). We used an independent approach to confirm these differential effects of *Lh* VLPs on hematopoietic tissues. We applied anti-cleaved caspase 3 antibody to plasmatocytes, lamellocytes and lymph gland cells. A preparation of circulating hemocytes from $hop^{Tum\text{-}l}$ *msn>mCD8GFP* animals (Figure 4 A-C') shows that lamellocytes become bipolar and lose their broad, flattened morphology (Figures 4 A-A''), but do not react with cleaved caspase 3 antibody (Figure 4 C-C'). However, many plasmatocytes (Figure 4 B) from the same hosts express the cleaved caspase 3 antigen (arrows), confirming a caspase-dependent cell death mechanism. Strikingly, many plasmatocytes appear to have internalized GFP-positive cell debris, presumably from VLP-mediated lamellocyte lysis (Figure 4 B). This GFP-positive cell debris also exhibits high levels of integrin-β (red) (see also Figure S5 A-A').

Many hematopoietic cells of both anterior (not shown) and posterior lymph gland lobes (Figure 4 D-E') exhibit the cleaved caspase 3 fluorescence signal (Figure 4 D-D') which colocalizes with the p40 staining signal (Figure 4 E-E' arrows) suggesting a direct effect of VLPs on cell viability. Furthermore, evidence of significant cell death in this population is also marked by cell morphological changes such as blebbing, cell shrinkage, and nuclear chromosomal DNA fragmentation (Figure 4 A', C, D' and E'). Thus, both caspase-dependent and caspase-independent cell death pathways are utilized to eliminate effector innate immune cells as well as progenitors, leaving the host defenseless.

p40 staining of the lymph gland PSC and the role of the PSC in cell killing

Previous studies (CROZATIER *et al.* 2004b; GUEGUEN 2013; SMALL *et al.* 2013) have demonstrated that the PSC reprograms hematopoietic development and induces massive lamellocyte differentiation upon *Lb* infection (Figure 1 D, E), and that PSC-less lymph glands are unable to induce lamellocyte differentiation (BENMIMOUN *et al.* 2015). We found that after *Lh14* infection, loss of PSC integrity as a tight unit (Figure 5 A, B) is accompanied by high p40 signal around but not within the PSC cells (Figure 5 C-C''). PSCs of *LhNY* infected animals show similarly dispersed PSCs with high p40 levels around but not within the PSC cells (Figure S6 A-A''). This disruption of the PSC appears to be distinct mechanism by which *Lh* blocks host response in addition to inducing rapid hemocyte cell death.

Intrigued by PSC dispersal (Figures 1G, 5 B-C'', S6) we investigated the role of the PSC in mediating *Lh*-induced cell death by (1) removing the PSC with the pro-apoptotic gene *hid* (*Col>hid*; PSC ablation was confirmed by loss of Antp staining of *Col>hid* lymph glands (Figure 6 A, C'), and (2) knocking down PSC function in *Antp-Gal4>col*^{RNAi} lymph glands.

In third instar larvae, Antp and Col promoters are expressed in embryonic PSC (CROZATIER *et al.* 2004b; MANDAL *et al.* 2007). While the *Antp* promoter activity is limited to the PSC and cardiomyocytes (MANDAL *et al.* 2007), *Col-Gal4* is expressed in the PSC and at lower levels in the MZ (BENMIMOUN *et al.* 2015; OYALLON *et al.* 2016) in third instar larvae. Like wild type lobes, control *Lh* infected *UAS-hid* lobes showed loss of progenitors and disrupted PSCs (Figure 6 A- B'), but the *Lh* infected PSC-less *Col>hid* lymph glands remained intact (Figure 6 C-C') and without signs of cell death or lamellocyte differentiation (Figure 7 A-C). Unlike controls, p40 staining of these *Lh14* infected PSC-less lymph glands was ubiquitously low (compare Figure 7 B' to C').

Without infection, *Antp-Gal4>col*^{RNAi} had no obvious effects on the organization or size of the PSC or on the *Antp>mCD8GFP* intensity (Figure S7 A-B'). Infection of *Antp-Gal4>col*^{RNAi} resulted in PSC dispersal (Figure 8 A-B') and loss of anterior lobe (Figures 8 B and S8 A, B) or posterior lobe (Figures 8 C and S8 C-C'') progenitors but this dispersal/loss of cells is not as severe as in wild type (Figures 1G, 5 B-C'', S6). Furthermore, the overall VLP signal in the lobes and the dorsal vessel of these *Lh14* infected *Antp>mCD8GFP, col*^{RNAi} lymph glands is also significantly lower compared to control *Antp>mCD8GFP* lymph glands (Figure 8 B', D'). Like the *UAS>hid* lymph glands in infected animals, these *Antp>mCD8GFP, col*^{RNAi} lymph glands remain intact. Taken together, these results suggest that the PSC has a general role in protecting the host and *Lh* VLPs appear to inactivate this function.

The identity and structure of p40

Tryptic digests of SDS gel-purified p40, followed by N-terminal sequencing (Govind lab, unpub.) resulted in partial amino acid sequence information, which matched with a transcript in

the published *Lh14* abdominal transcriptome (GOECKS 2013). This transcript encodes ~30 kDa protein and also showed several perfect matches to peptides in our unpublished *Lh* VLP proteomes. The discrepancy between the predicted 30 kDa protein versus observed 40 kDa protein (CHIU 2006)) is likely due to post-translational modification in wasp cells. This transcript is not expressed in the *Lb17* or *Ganaspis 1* abdomens (GOECKS 2013; MORTIMER 2013). Domain architecture analysis of p40 predicts an N-terminal signal sequence, a C-terminal transmembrane helix, and a highly helical central domain (Figure 9 A). A preliminary *in silico* model of the highly helical region of p40 reveals similarity to the three-dimensional structure of the IpaD/SipD family of tip proteins present on T3SS needles (Figure 9 B) (Govind and Singh labs, unpub.). IpaD/SipD-like proteins mediate needle contact with host intestinal cells in the T3SS-producing Gram negative bacteria (SCHIAVOLIN *et al.* 2013).

Amplification of full length p40 sequence from venom gland using specific primers allowed amplification of the internal IpaD-like helical p40 domain. This domain was cloned into the pTrcHisA vector and expressed in *E. coli* BL21 cells. Western blot analysis of IPTG-induced cell extracts confirmed the identity of p40 (Figure 9 C). The size of the predicted protein (~29 kDa) matched the observed major band at ~29 kDa, the pellet fraction being more enriched than the supernatant (Figure 9 C arrow). This 29 kDa protein also reacted with anti-His antibody on western blots (not shown). In addition, a doublet of 24 kDa and 23 kDa bands was observed in both fractions with anti-p40, but not with anti-His antibody. This protein profile remained unaltered even under unreduced conditions or if protein samples were treated with protease inhibitors before loading (not shown). Protein samples prepared from uninduced bacteria did not show these protein bands (Figure 9 C). *Lh* infected $hop^{Tum\text{-}l}$ *msn>mCD8GFP* host cells showed protein at the expected 40 kDa (Figure 9 D, arrow) as well as bands of higher molecular size.

These proteins were present at higher levels in the pellet than in the supernatant. The identity of larger sized bands is not known, these could be heterodimers of full-length p40 and/or truncated forms. None of these proteins were detected in samples from uninfected *hop*$^{Tum\text{-}l}$ *msn>mCD8GFP* host cells. Venom gland extracts from *Lh14* and *Lv* revealed proteins of the appropriate sizes (Figure 9 E); 40kDa for *Lh* and 47.5kDa for *Lv* (CHIU 2006).

Genomic sequencing of the p40 locus and comparison with the cDNA sequence revealed 4 introns and 5 exons (Figure S9 A, B). Specific primers (from (a) the UTRs, or (b, c) internal to both UTRs, Supplementary Table 1) failed to amplify any p40 product from a cDNA template prepared from *Lh14* infected *hop*$^{Tum\text{-}l}$ *msn>mCD8GFP* hemocytes suggesting that the p40 gene is not expressed in host hemocytes (not shown).

Truncated p40 promotes morphological changes in host lamellocytes *ex vivo*

Exposure to venom gland extracts induces lamellocytes to become spindle-shaped or bipolar. Lamellocytes lose membrane integrity and lyse (Figure 10 A, B, (RIZKI and RIZKI 1990) and Govind lab unpub)). To investigate if truncated p40 (with the central IpaD-like helical domain but lacking the signal sequence and the transmembrane domain), expressed in *E. coli* BL21 cells, might similarly affect lamellocyte morphology *ex vivo*, we introduced either the pellet or the supernatant fraction of IPTG-induced bacterial lysates onto live lamellocytes from *hop*$^{Tum\text{-}l}$ *msn>mCD8GFP* animals. Preliminary results show that both fractions from induced cells (but not from uninduced *E. coli* cells (Figure 10 C and C') promoted cell shape changes, causing lamellocytes to become spindle-shaped or bipolar (Figure 10 D and D').

Discussion

In this study we investigated the cellular effects on and localization of *Lh* VLPs in hematopoietic tissues and associated cells in the larval circulatory system. We found that unlike *Lb* infection that activates innate immunity in fly larvae (SCHLENKE 2007; SMALL *et al.* 2013), *Lh* VLPs abolish cellular immunity. They have strong cytolytic effects on plasmatocytes and lamellocytes, the two major effector cell types for host defense. VLPs were found in striking abundance not only in the hematopoietic cells, but also in the PSC and the dorsal vessel of the larval lymph gland regardless of whether the *Lh14* or *LhNY* strain was used for infecting *D. melanogaster* or *D. yakuba* hosts. Characterization of the *Lh* VLP proteomes, peptide analysis of p40, and western analysis of bacterially-expressed p40 allowed identification of the p40 sequence. The primary sequence of p40 is not highly similar to any protein in the database, although protein-domain analyses identified similarities with Gram negative bacterial proteins engaged in delivering virulence effectors into mammalian cells. Comparative transcriptomic/proteomic approaches revealed that p40 is not expressed in *Lb*. This difference in *Lh* versus *Lb* may in part be responsible for their differing biological activities on host hemocytes. Our immunohistochemistry results and structural prediction of p40 support a role for p40 in mediating entry into lamellocytes.

The lymph gland PSC is essential for an immune response and *Lh* VLPs appear to inactivate this PSC function

We were surprised to observe significantly high VLP levels in circulation, in the dorsal vessel, and around the PSC in addition to observing the VLP signals in most plasmatocytes and lamellocytes suggesting that the wasp venom produces an overabundance of VLPs that

overwhelm the host's target tissues. Interestingly, PSCs of most lobes from infected animals were dispersed and single or multiple PSC cells were found scattered in the body of the anterior lobes and the VLP signal was extremely intense in the extracellular spaces around but not within the PSC cells.

Finally, unlike *Lb* infected glands where *D4-lacZ* (a target of the Toll/Dorsal (NF-κB) pathway) is activated (GUEGUEN *et al.* 2013), *Lh* infection has the opposite effect and it turns down constitutive moderate levels of *D4-lacZ* expression. These results suggest that *Lh* VLP uptake into host cells is selective, *Lh* VLP proteins/enzymes act to dissociate the tightly-packed PSC cell clusters, and the integrity and/or function of the PSC is disrupted by VLPs. Proteomic analyses of *Lh* VLPs have identified neprilysin-like membrane endopeptidases (Govind lab unpub.) and it is possible that such VLP proteins disrupt the PSC integrity or affect PSC function by acting in the intercellular spaces.

Early studies (LANOT *et al.* 2001; SORRENTINO *et al.* 2002) showed that the lymph gland itself is immune-responsive to *Lb* infection and lamellocytes differentiate from hematopoietic progenitors. Lamellocyte differentiation occurs only in third instar larvae when encapsulation of wasp egg or embryo occurs (SORRENTINO *et al.* 2002). Subsequent studies revealed the existence and function of the PSC in the anterior lobes and showed its role in crystal cell development (via Serrate expression and Notch signaling (LEBESTKY *et al.* 2003)) as well as in lamellocyte differentiation (via Collier expression and function in the PSC (CROZATIER *et al.* 2004b; JUNG *et al.* 2005). The PSC plays an essential role in mounting an anti-parasite response against *Lb* infection by encouraging lamellocyte differentiation and inhibiting crystal cell development (BENMIMOUN *et al.* 2015; CROZATIER and MEISTER 2007; CROZATIER *et al.* 2004b; KRZEMIEN *et*

al. 2010b; OYALLON *et al.* 2016). *L. boulardi* infection also activates ROS production in the PSC (SINENKO *et al.* 2012; SMALL *et al.* 2013) and NF-κB signaling in the PSC (GUEGUEN 2013).

Our PSC ablation experiments with pro-apoptotic gene *hid* confirms the anti-parasite function of the PSC in registering the presence of the wasp; PSC-less lymph gland lobes (*Col>Hid*) exhibit normal lobe size without cells with DNA damage, no dispersal and low levels of VLPs in progenitors or in the dorsal vessel. Inactivating the niche by removing Collier in the PSC ($Antp>Col^{RNAi}$) however only has a partial effect and although VLP levels in these lymph glands is low, signs of cell death in the lobes is observed in both anterior and posterior lobes.

In sum, we have identified key differences between *Lb* and *Lh* wasps' VLPs. Chief among these is the presence of the p40 protein in *Lh* VLPs and its absence from *Lb* VLPs. Furthermore, *Lh* VLPs inactivate its host's immune system by inactivating the PSC and killing or lysing the effector cell populations.

p40: the first eukaryotic member of the SipD/IpaD family of proteins

p40 is encoded by a gene with four introns and five exons. Even though its protein structure resembles bacterial proteins (see below), the presence of introns in its gene suggests that the genetic information for p40 is integrated in the wasp genome. This scenario suggests that VLPs may be true endosymbionts of their wasps, as one or more VLP proteins may be encoded in the wasp genome. Ongoing experimental and comparative genomic analyses of VLP proteins and wasp genome sequences will shed more light on the relationship of VLPs with their wasps.

Algorithms for signal sequence (PETERSEN *et al.* 2011) identify a 27-amino acid secretion signal for p40. This finding is consistent with p40's intra- and extra-cellular localization inside and immediately outside venom gland secretory cells as revealed with confocal microscopy

(FERRARESE 2009) and immuno-electron microscopy (CHIU 2006). Curiously however, a transmembrane domain and short cytoplasmic tail are also encoded at the C-terminus of p40. These observations present a cell biological dilemma: how does p40, a predicted membrane protein, appear in the extracellular space? Our interpretation is that membrane-bound p40 exits the venom gland secretory cells, not by the process of secretion, but instead via a mechanism similar to microvesicle formation, in which either (a) membrane vesicles are released from the plasma membrane by budding, or (b) exocytosis of multivesicular bodies. This interpretation is consistent with p40's constant localization around (but rarely inside) VLPs at all stages of biogenesis, indicating that p40 is tethered to the pre-VLP vesicle membrane (CHIU 2006). In this scenario, anti-p40 antibodies likely detect the extracellular epitopes of p40 on mature VLPs (CHIU 2006).

The interpretation that VLPs are microvesicle-like organelles that shuttle cargo of virulence factors is further supported by the presence of various other proteins predicted to function in endocytosis or membrane fusion (Govind lab, unpub.). It is likely that VLPs use these proteins to enter host hemocytes modify retrograde transport and/or assist with delivery of virulence factors into the right subcellular compartments.

The secondary structure of p40 is predicted to be almost entirely α-helical, with multiple long helices of more than twenty-five residues. An IpaD superfamily domain has been identified in p40**,** based on sequence conservation and matrix scoring (Govind and Singh labs, unpub.) (PICKING *et al.* 2005). This domain is found in T3SS needle tips from pathogenic *Shigella flexneri* and *Salmonella enteric* bacteria (COLLAZO and GALAN 1997a; COLLAZO and GALAN 1997b; MEGHRAOUI *et al.* 2014; PICKING *et al.* 2005; SCHIAVOLIN *et al.* 2013). The T3SS bacterial domains interact with mammalian host-cell plasma membranes to inject virulence

effector proteins (SCHIAVOLIN *et al.* 2013). The majority of results from both classic full-length and iterative partial-protein p40 fold threading also identify pathogenic virulence factors. *S. flexneri* IpaD regulates both protein secretion as well as insertion of pores into target membranes (PICKING *et al.* 2005). Similar activities for p40 would be consistent with its localization on VLP spike tips (CHIU 2006), as spike tips, like bacterial needles, contact host cells (CHIU 2006). Significantly, inhibition of p40 by pre-incubation of VLPs with anti-p40 antibodies reduces host blood cell lysis (CHIU 2006).

A function for p40 in mediating VLP entry into lamellocytes?

VLPs use different mechanisms to enter plasmatocytes and lamellocytes: They use the Rab5-dependent phagocytic pathway to enter plasmatocytes, as Rab5 knockdown leads to a restricted distribution of VLPs adjacent to the plasma membrane. In lamellocytes however, Rab 5 entry is not via endocytosis, which is not surprising given that these cells are not phagocytic and do not take up pH-Rodo-labeled *E. coli* bioparticles (our unpub. results). But one EM study (RIZKI and RIZKI 1994) revealed complete or partial VLPs/VLP substructures within lamellocytes. Our studies do not show strong cytoplasmic signal in the cytoplasm; instead, the p40 signal is consistently diffuse and nuclear in lamellocytes whether they are from *D. melanogaster* or *D. yakuba*, and in the lymph gland or circulating populations.

Based on our previous work, i.e., (a) scanning electron microscopy (VLP spikes contact lamellocyte surface, (b) immuno-electron microscopy (surface localization of p40 to spike length and tips, and (c) immuno-inhibition (anti-p40 antibody blocks lamellocyte lysis) experiments, we hypothesized p40's role in lamellocyte entry(CHIU *et al.* 2006). Computational modeling of p40 (above) further supports this function for p40. Additional experimental support also comes from

our preliminary observations that bacterial extracts containing the p40 core with SipD/IpaD-like helices (excluding N-terminal signal sequence and C-terminal transmembrane domain) are able to induce cell shape changes in live lamellocytes, much like what is observed with the complete wasp venom. While additional experiments will ascertain the biochemical functions of p40 in either contacting lamellocyte membranes and/or in efficient delivery of VLP effectors into lamellocytes, our initial results point to fundamental reason for differences in *Lb* and *Lh* virulence: absence/presence of p40 likely dictates differences in the ways these VLPs initiate interaction or target delivery of virulence proteins. Such key differences are bound to underlie differential immune suppression strategies of the two wasps affecting their natural host range.

Systematic application of state-of-the art sequencing and bioinformatics methods to VLP components and parasite virulence will also deepen our understanding of the evolution of virulence proteins in generalist parasites. Because of extensive molecular conservation in the core NF-κB signaling components in insects, it is also likely that inhibitory strategies identified in our system will be experimentally transferrable to other insect species to restrict the spread of disease or plant pests.

Figures

Figure 1. Differential effects of *Lb17* and *Lh14* on the larval lymph gland

Third instar lymph glands are shown with either the PSC (**A, D and G** *Antp>mCD8GFP*) or the medullary zone (**B, E and H** *Dome-Meso-GFP*) labeled with GFP. PSC is also detected by β-Gal (red) and Antp antibody (green) (**C, F and I** *D4-lacZ*). (**A and B**) Intact lymph glands without lamellocytes from uninfected animals. (**D and E**) *L. boulardi* attack results in robust lamellocyte differentiation. (**G and H**) *L. heterotoma* attack leads to loss of cells in the anterior lobes and cells in the PSC appear displaced. (**C-C'''**) PSC of lymph glands from uninfected animals with moderate levels of β-Gal and Antp. (**F-F'''**) *L. boulardi* attack results in higher levels of β-Gal but Antp levels remains high. (**I-I'''**) *L. heterotoma* attack leads to reduced levels of both β-Gal and Antp relative to uninfected controls. Lamellocytes are labeled with rhodamine-phalloidin which also labels the dorsal vessel. Hoechst stains DNA (blue). Scale bars indicate 20 μm (panels A-I) and 10 μm (panels C'-C''', F'-F''' and I'-I''').

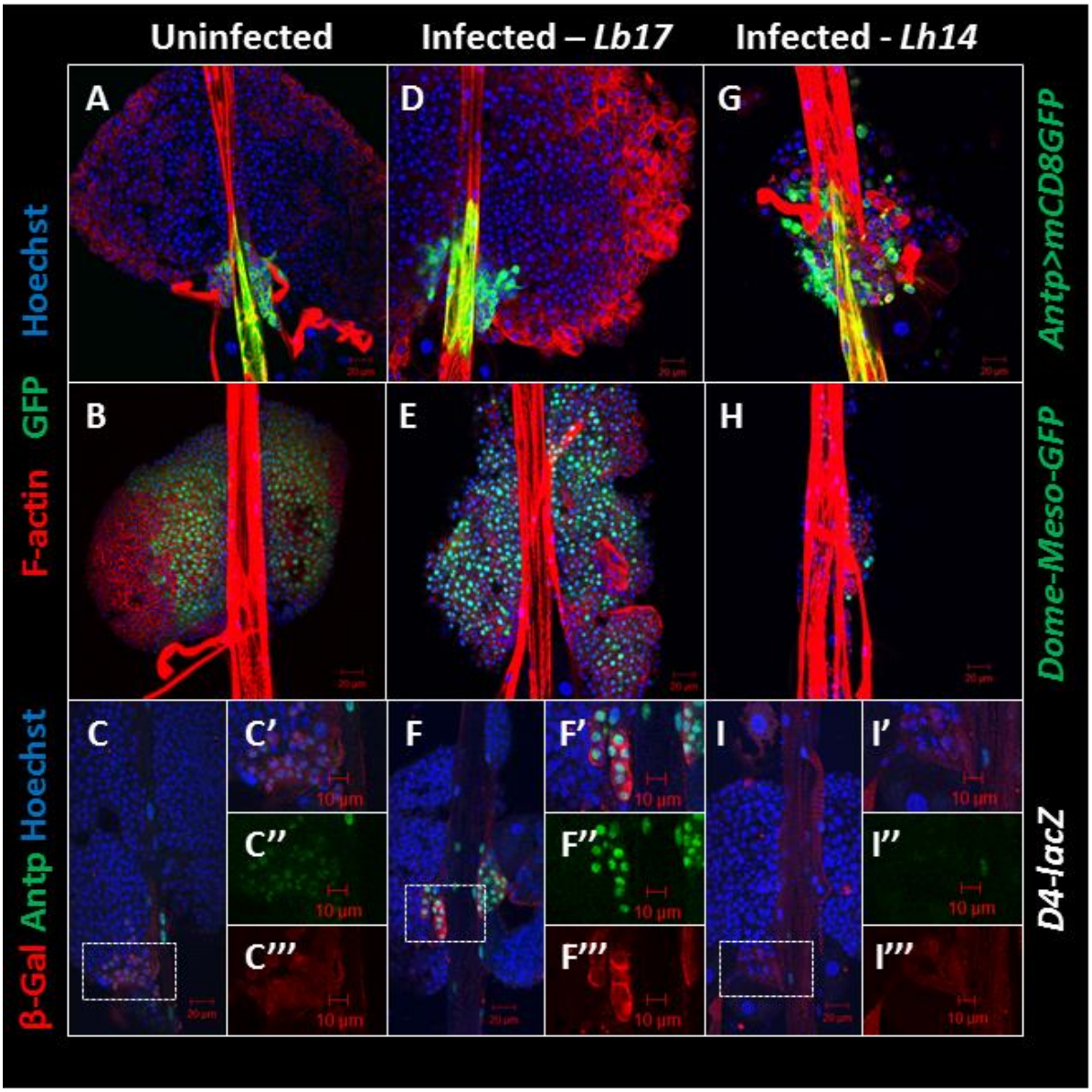

Immunohistochemistry and imaging for panels C – I''' was done by Mary Ellen Heavner, Unpublished data.

Figure 2. p40 localization in *Drosophila* hematopoietic cells

(**A-B"**) p40 antibody staining of lymph gland (**A-A''**) and circulating hemocytes (**B-B''**) from *hop*$^{Tum\text{-}l}$ *msn>mcd8GFP* animals. GFP positive cells are lamellocytes. Magnification (**A' and A''**) of lymph gland cells and (**B' and B''**) of circulating hemocytes, shows high punctate cytoplasmic staining in plasmatocytes (arrows) and diffuse nuclear staining in lamellocytes (arrowheads). (**C-D'**) *lz-NLS-GFP* positive lymph gland crystal cells (**C-C''**) and circulating crystal cells (**D-D'**) are devoid of the p40 signal. (**C'-D'**) Results shown at high magnification. Hoechst stains DNA (blue). Scale bars indicate 20 µm (panels A-C), 10 µm (panels C' to D') and 5 µm (panels A'-A'' and B'-B').

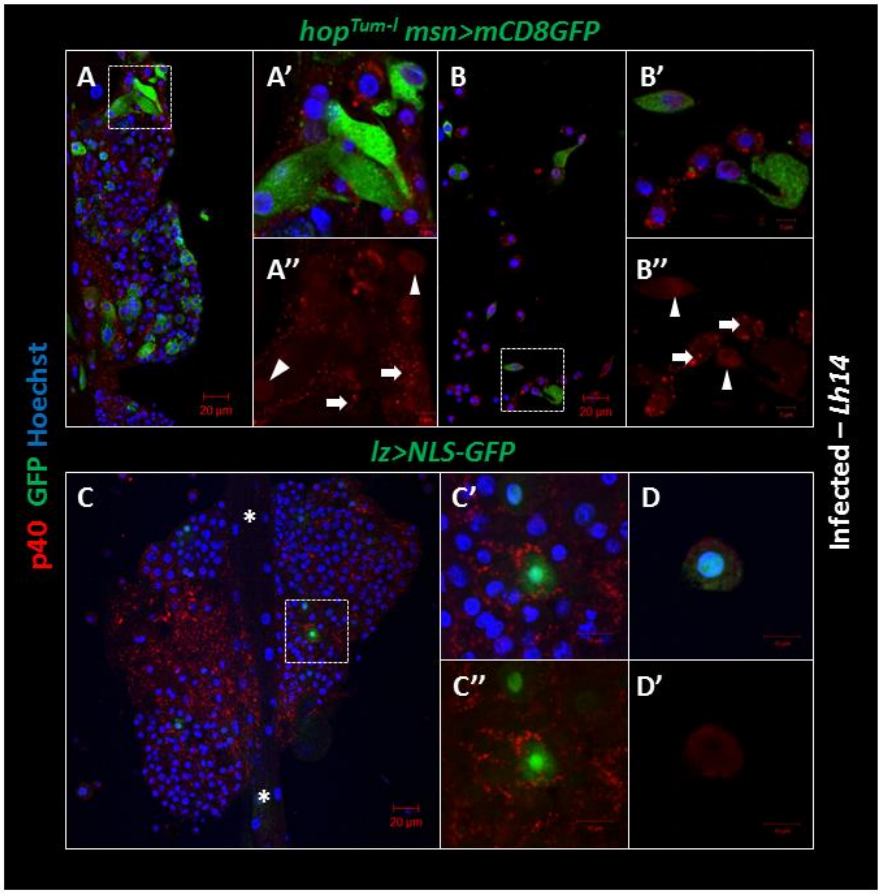

Figure 3. Rab5 is needed for VLP entry into plasmatocytes but not into lamellocytes

(**A-D''**) p40 antibody stained lymph gland anterior lobe (**A-A''**) and circulating hemocytes (**B-B''**) from *Pxn>GFP, Rab5*^{RNAi} animals shows localization of p40 to the inner periphery of Pxn>GFP-positive cells and are not completely internalized into the cytoplasm. (**C-C''**) Lymph gland anterior lobe and (**D-D''**) circulating hemocytes from *hop*$^{Tum-l}$ *msn>mCD8GFP, Rab5*^{RNAi} animals shows nuclear localization of p40 in *msn>GFP* positive lamellocytes (arrowheads, see also Figure 2 A'' and B'', arrowheads). Hoechst stains DNA (blue). Scale bars indicate 20 µm (panels A-D) and 10 µm (panels A'- B'' and C'- D'').

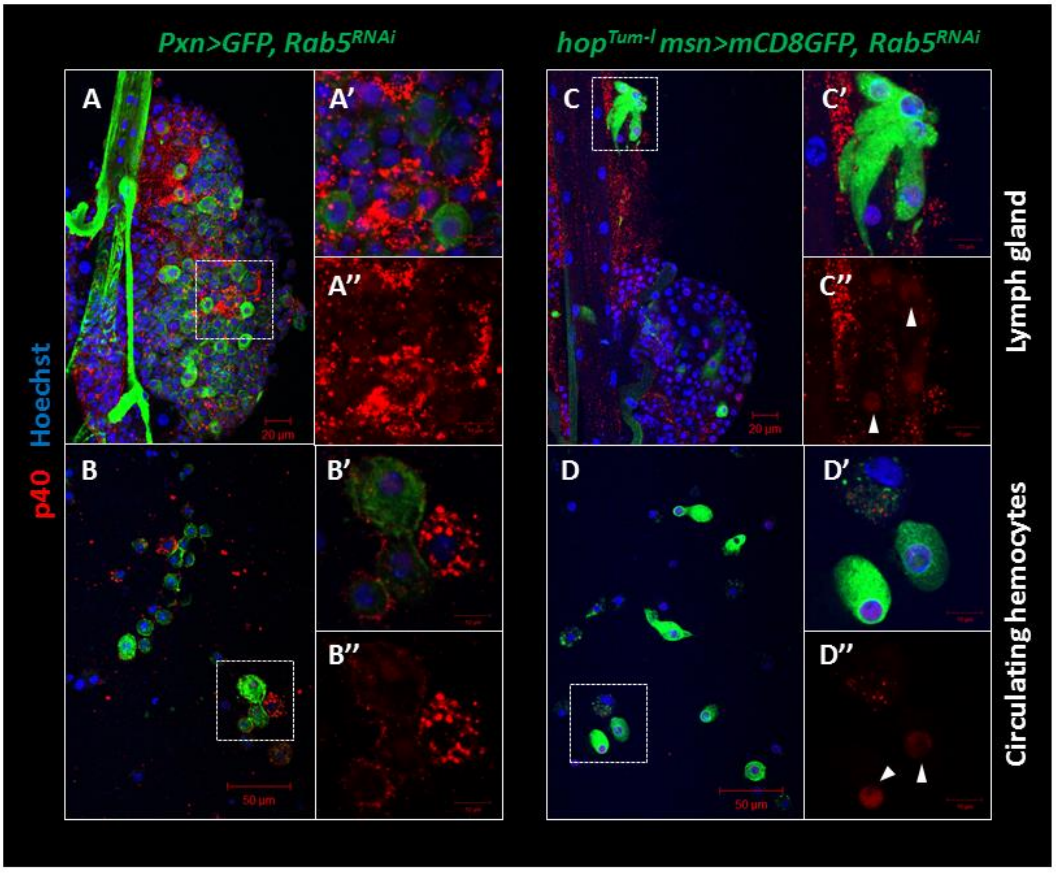

Figure 4. Cell-killing effects of *Lh14* VLPs

(**A-C'**) Circulating hemocytes from *hop*$^{Tum-l}$ *msn>mCD8GFP* animals shows bipolar GFP-positive lamellocytes (**A-A'' and C-C'**) losing their broad, flattened morphology. GFP-negative plasmatocytes (**B**) are cleaved caspase 3 positive (arrows), while lamellocytes (**C-C'**) remain caspase negative. Plasmatocytes engulf dying lamellocytes as evidenced by GFP specks in their cytoplasm. **(D-E')** Caspase 3 positive cells in the posterior lobes (**D-D'**) also show high p40 signal (**E-E'** arrows). VLP signal is also very high in the lumen of the dorsal vessel. Hoechst stains DNA (blue). Scale bars indicate 20 µm (panels A, D and E), 10 µm (panels A'-B and E') and 5 µm (panels C-C' and D').

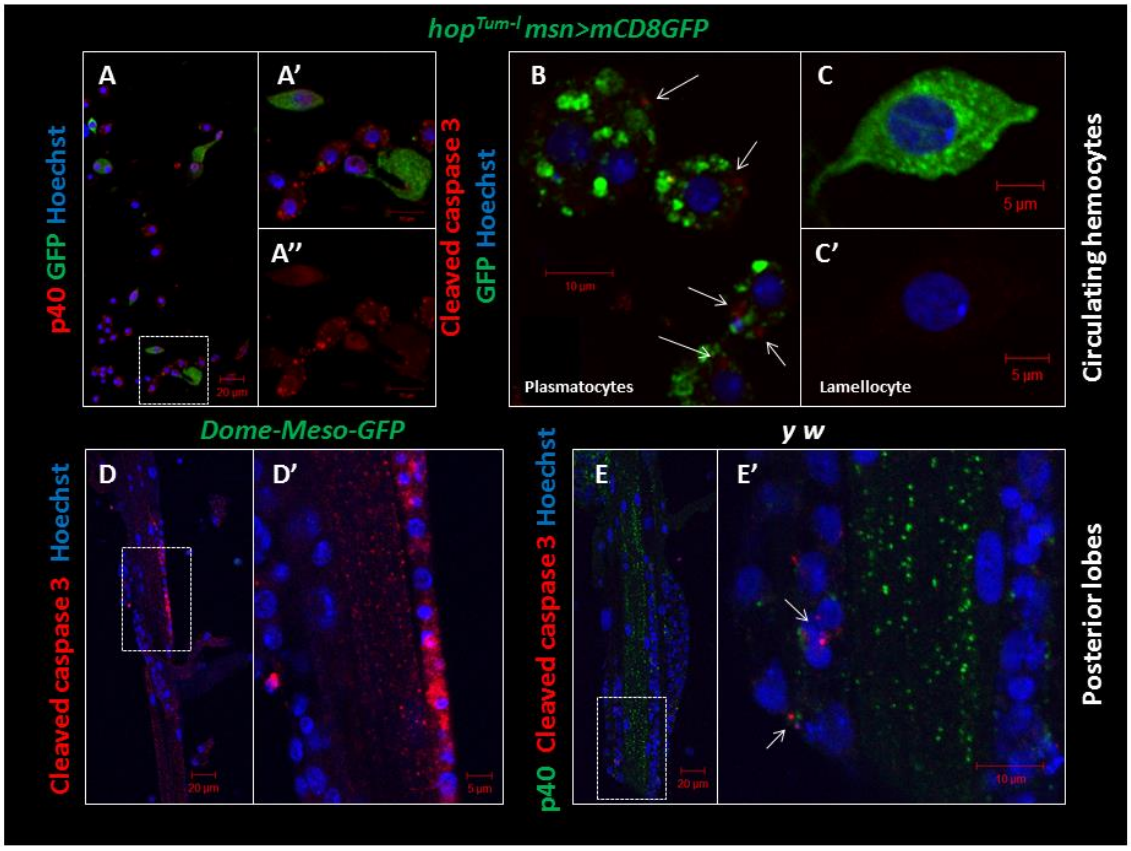

Figure 5. The effect of the niche post *Lh14* infection

(**A-C’’**) The PSC is dispersed and cells are devoid of p40 staining post *Lh14* infection. (**A-B**) Lymph glands from *Antp>mCD8GFP* animals shows a disrupted organization of the PSC post *Lh14* infection. The rest of the anterior lobe is depleted of progenitors post infection. (**C-C’’**) The dispersed GFP positive PSC cells do not react with the p40 antibody (red) however p40 appears concentrated in the extracellular spaces between PSC cells. Hoechst stains DNA (blue). Scale bars indicate 20 µm (panels A-C) and 10 µm (panels C’-C’’).

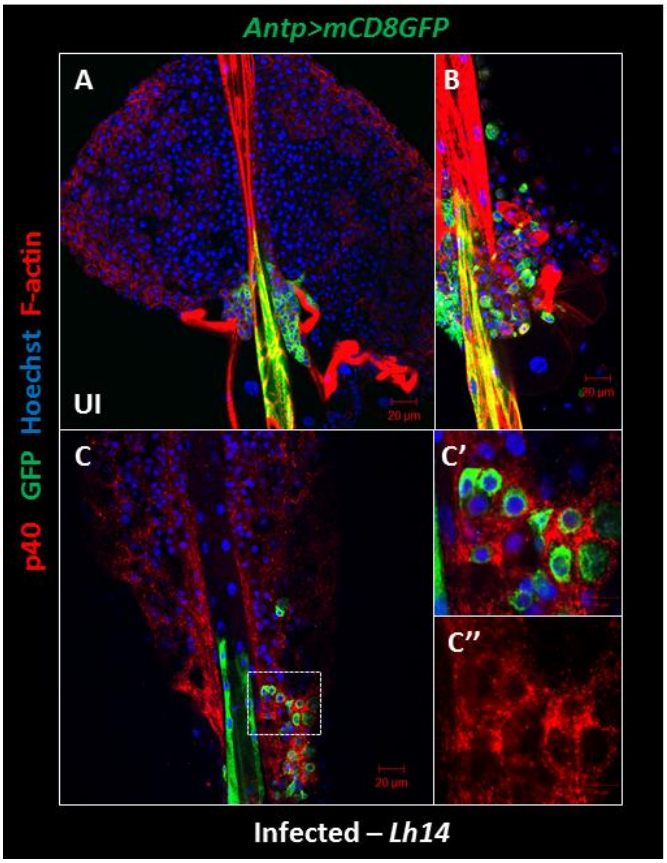

Figure 6. PSC-less lymph glands do not respond to *Lh14* infection

(**A-A'**) In a wild type *UAS-hid* background, the PSC is present, intact and Antp positive. (**B-B'**) Post *Lh14* infection, the lymph gland anterior lobes are depleted, and the Antp positive cells are also in a disorganized state. Antp staining is nuclear and reduced in some nuclei in lymph glands from infected animals (**B'**, arrow). (**C-C'**) The PSC-less lymph gland from *Col>Hid* animals are Antp negative and remain intact and whole even after *Lh14* infection. Panel A', B' and C' show Antp (red) staining only. Hoechst stains DNA (blue). Scale bars indicate 50 µm.

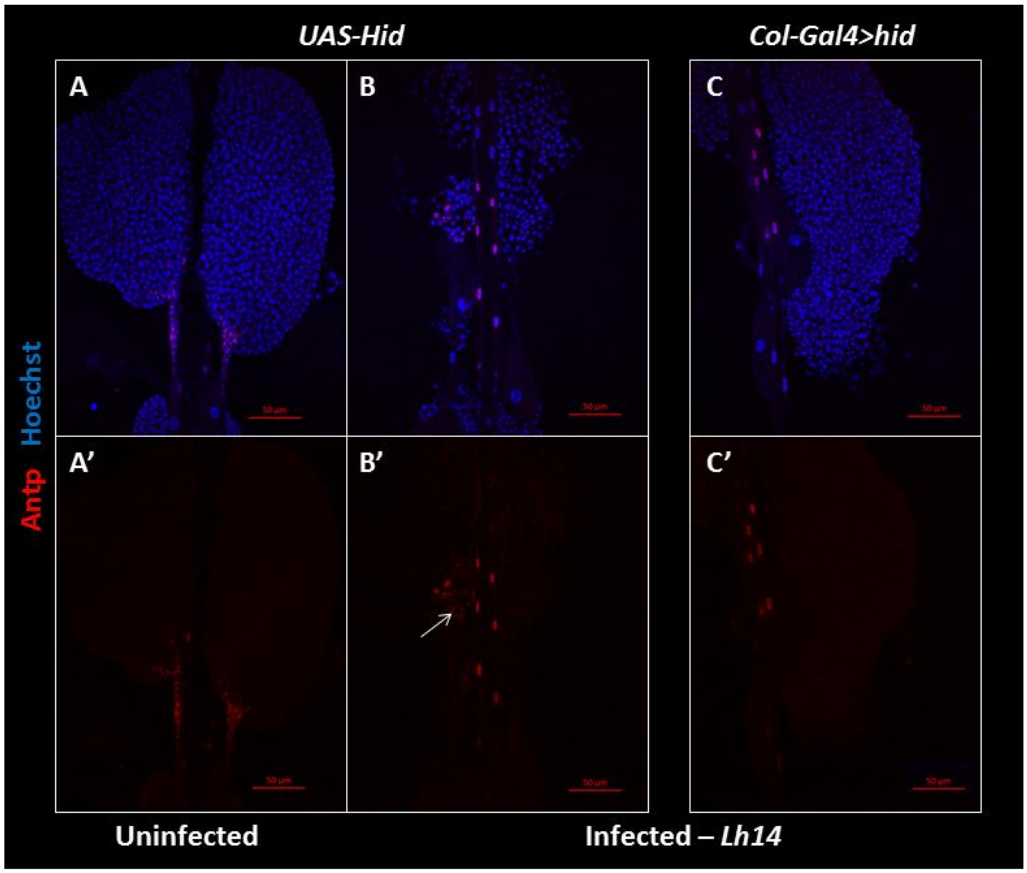

Figure 7. PSC-less lymph glands from *Lh14* infected animals show reduced p40 signal

(**A and D**) Lymph gland from uninfected wild type *UAS-hid* background are intact, p40 negative and contains no lamellocytes; anterior lobes (**A**) and posterior lobes (**D**). Post *Lh14* infection, wild type lymph gland anterior lobes are depleted of cells, dispersed and heavily stained with p40, anterior lobes (**B-B'**) and posterior lobes (**E-E'**). (**C-F'**) The *Col>hid* PSC-less lymph gland post *Lh14* infection is intact, does not show lamellocyte differentiation, and p40 staining is weak; anterior lobes (**C-C'**) and posterior lobes (**F-F'**). Panel B', C', E' and F' show p40 (red) staining only. Hoechst stains DNA (blue). Scale bars indicate 50 µm.

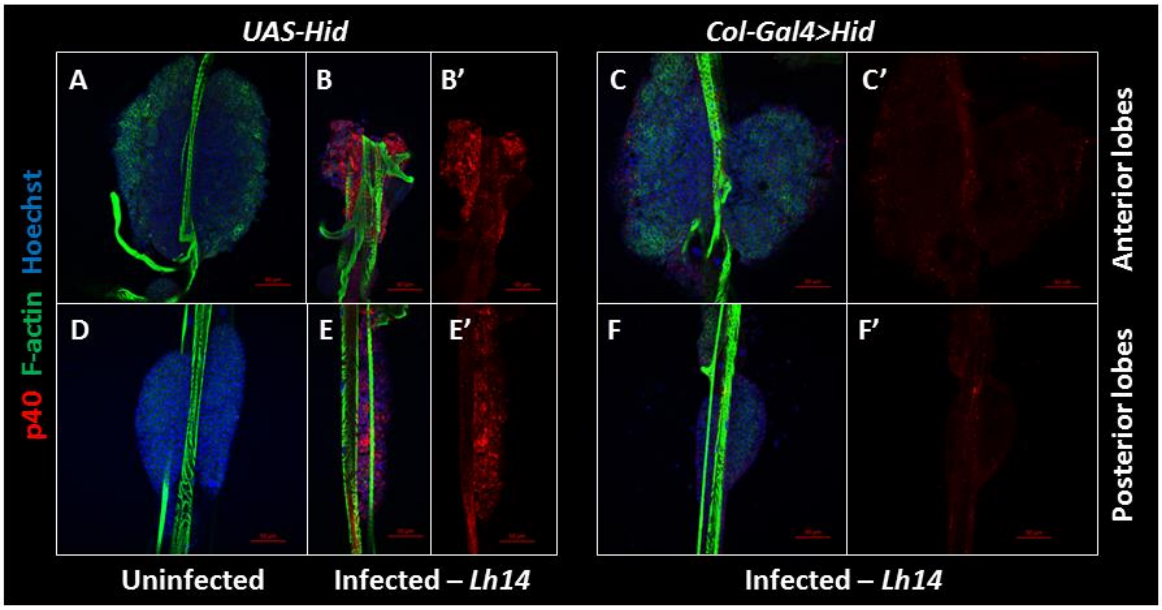

Figure 8. Knockdown of *col* in the PSC and the effect post *Lh14* infection

(**A-C'**) *Antp> mCD8GFP, Col*^{RNAi} lymph glands have low p40 staining (red) in anterior lobes (AL), posterior lobes (PL) and the dorsal vessel (C' asterisks) compared to *Antp>mCD8GFP* lymph glands (compare panels B' and C' to panel D'). (**A', B' and D'**) *Antp>mCD8GFP* marks the PSC (green). The tightly held PSC structure is slightly disrupted (compare A' to B') see also Figure 6Sb. Some nuclei in posterior lobes are fragmented (**C-C'**) see also Figure 6Sb C-C''. Hoechst channel has been removed from panels A'-D' to show p40 staining. Lymph glands from uninfected animals are negative for p40 staining (**A-A'**). Hoechst stains DNA (blue). Scale bars indicate 50 µm.

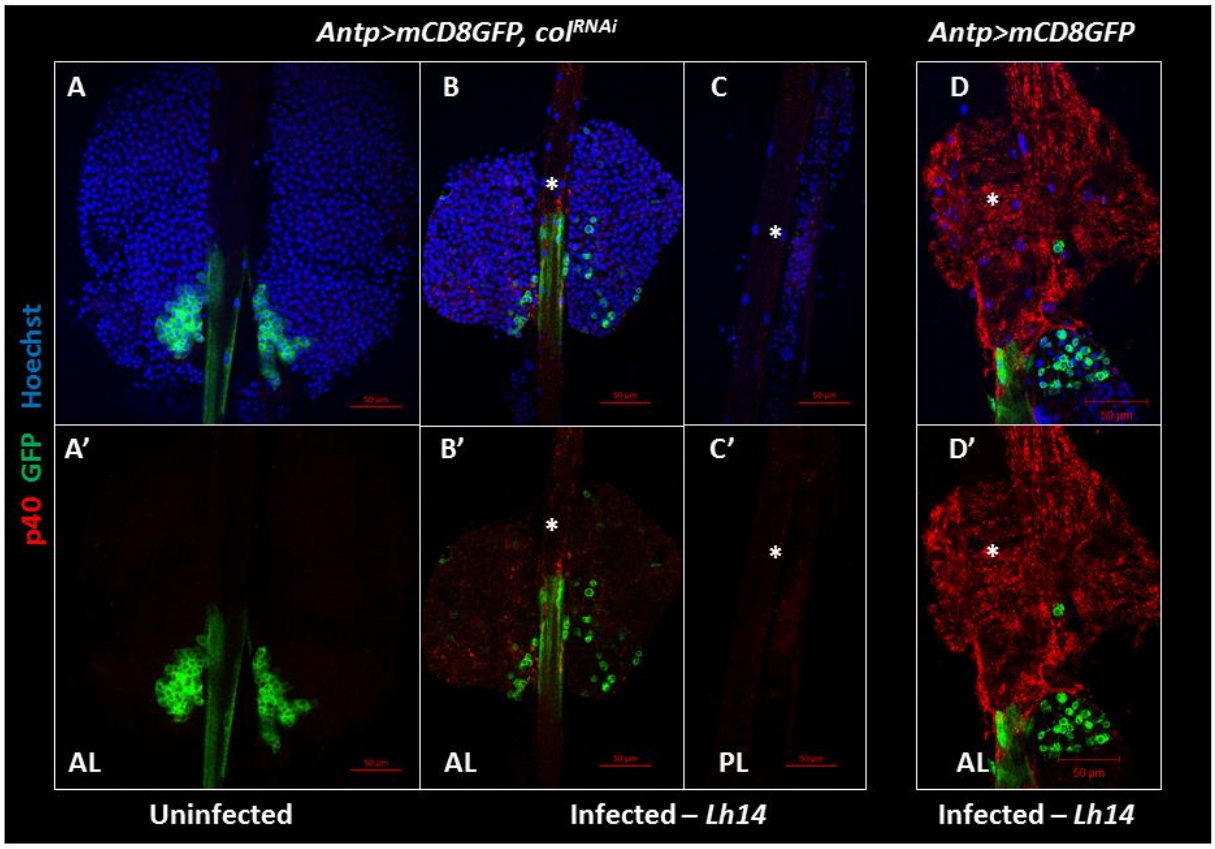

Figure 9. The structure and identity of p40

(**A**) Domain architecture of p40 showing the signal sequence (ss), transmembrane domain (TM), and intron insertion sites (arrows). (**B**) Cartoon based comparison of the structural fold of the truncated IpaD protein (PDB ID:4E3D), missing the N-terminal self-chaperoning domain (green) and the modeled IpaD-like domain of *Lh14* p40 (cyan) The N-termini are colored red and the C-termini are colored blue. (**C-E**) Western blot analyses of bacterially expressed truncated p40 with only the IpaD-like domain (3 hours after induction, reduced conditions) (**C**), host cells post *Lh14* infection (**D**), and venom gland extracts from *Lh14* and *Lv* wasps (**E**).

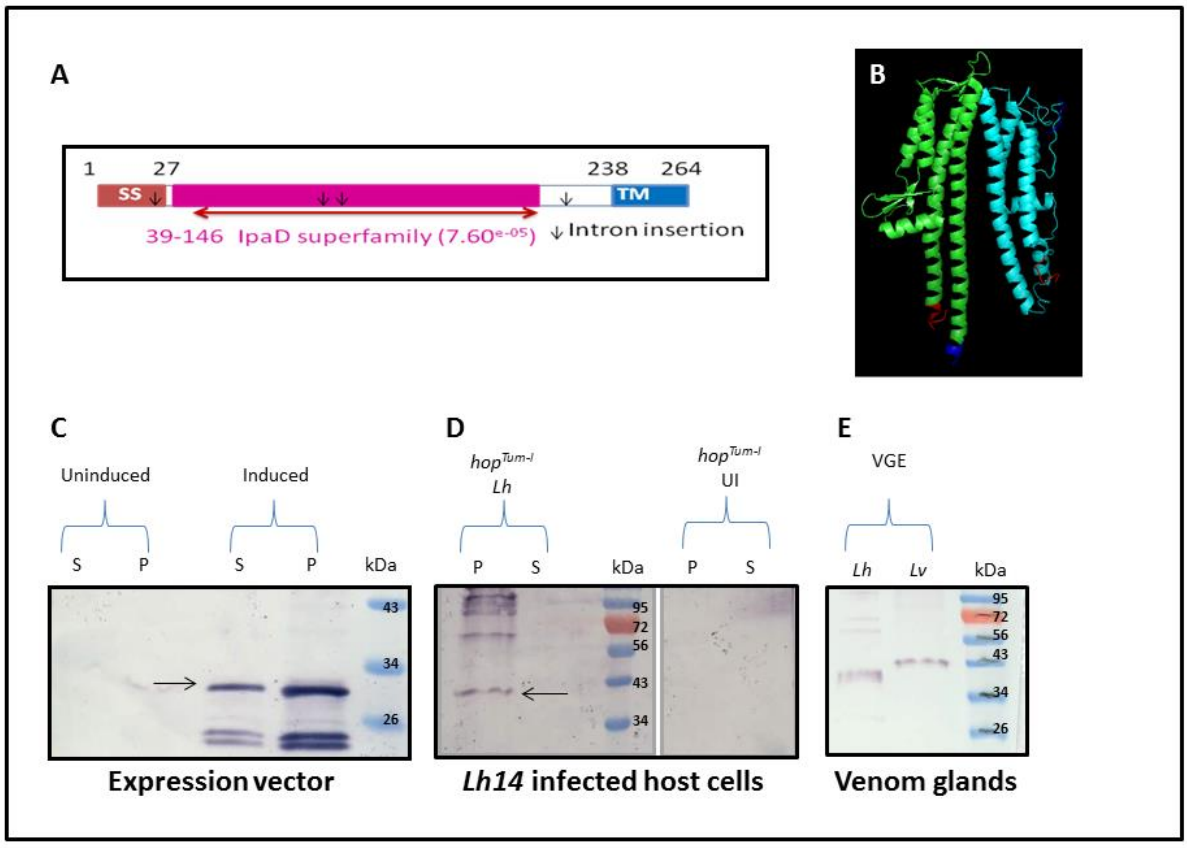

Mary Ellen Heavner deduced the putitive identity and the intron insertion sites in the p40 coding region, panel A.

Dr. S. Singh, Brooklyn College, constructed the preliminary p40 *in silico* model, panel B

Figure 10. Bacterially expressed p40 protein promotes lamellocyte morphological changes (**A**) Untreated cells remain unaffected whereas treatment with *Lh14* venom gland extract (**B**) results in lysis of lamellocytes. (**C-C'**) Uninduced bacterial cell lysates did not promote morphological changes while lysates from IPTG-induced bacteria (**D-D'**) promote lamellocyte morphological changes similar to the *Lh14* venom gland extract positive control.

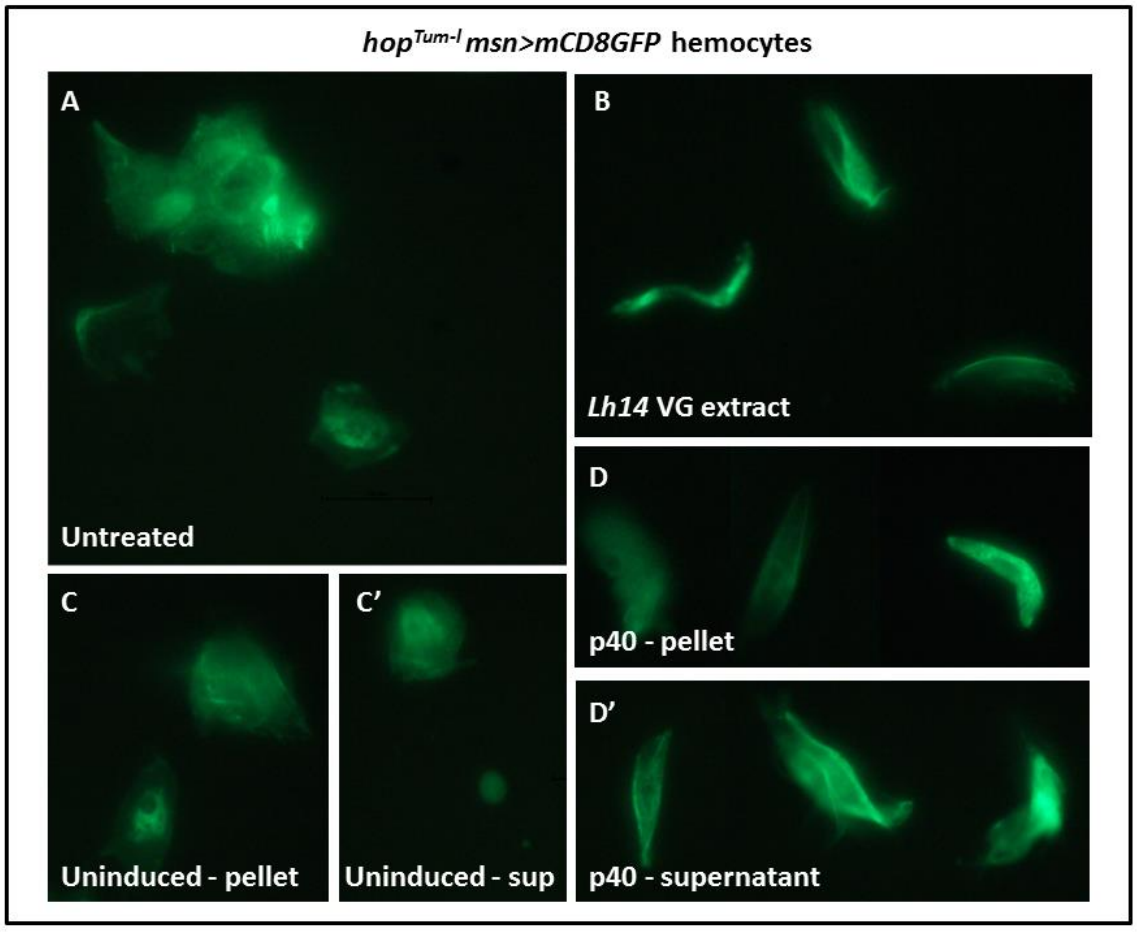

Supporting Figures

Figure S1. Effect of *Lh14* attack on *D. yakuba* lymph glands

(**A, B**) Anterior lobes (**A**) and posterior lobes (**B**) from uninfected animals. Anterior lobes are large and contain numerous lamellocytes (arrow heads). (**C-D''**) *L. heterotoma* attack reduces lobe size (**C**) with p40 signal high in anterior lobes and nuclear in putative lamellocytes (**C'-C''** arrowheads). (**D-D''**) posterior lobes and dorsal vessel (asterisk) also show high p40 signal. Nuclei of posterior lobes appear fragmented. Hoechst stains DNA (blue). Scale bars indicate 20 µm (panels A-B', C and D) and 5 µm (panels C'-C'' and D'-D'').

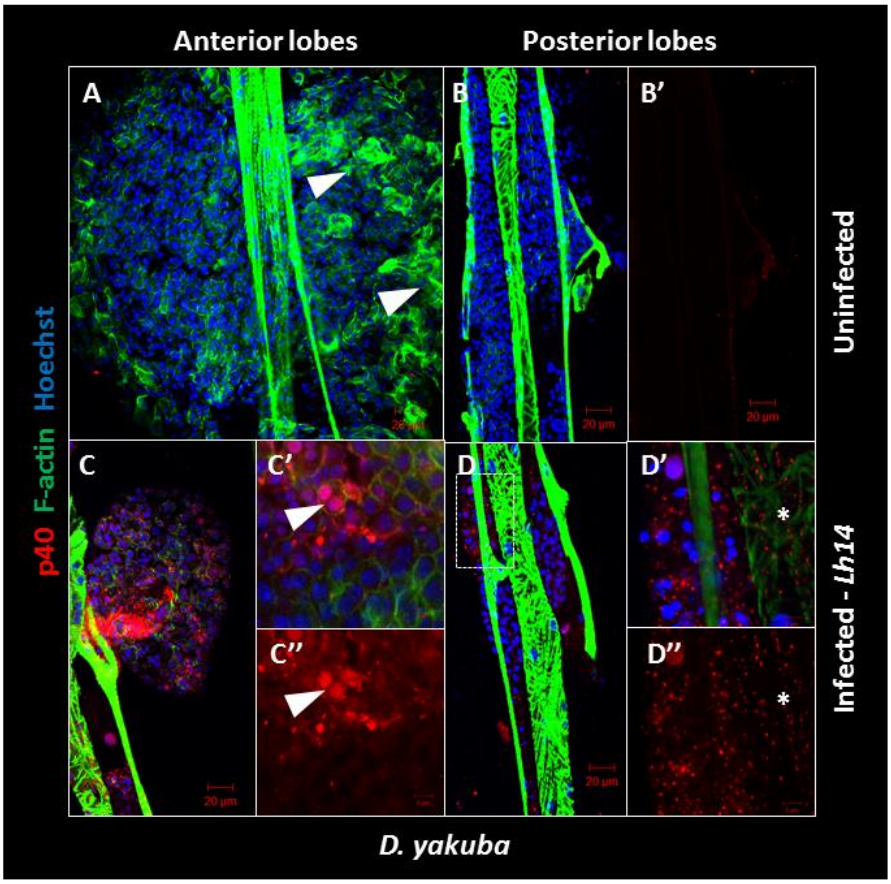

Figure S2. p40 localization of *LhNY* infected *D. melanogaster* lymph glands

(**A-D’’**) *y w* wild type background lymph glands anterior and posterior lobes shows p40 signal in anterior lobes (**A-B’’**) and in posterior lobes (**C-D’’**) post *LhNY* infection. Magnifications show punctate staining in plasmatocytes (**B’** arrowhead) and nuclear staining in putative lamellocytes (**B’’** arrow) of anterior lobes. (**D-D’’**) show speckled staining in posterior lobe cells and the dorsal vessel (**D’-D’’** asterisk). Hoechst stains DNA (blue). Scale bars indicate 20 µm (panels A, B, C and D) and 10 µm (panels B’-B’’ and D’-D’’).

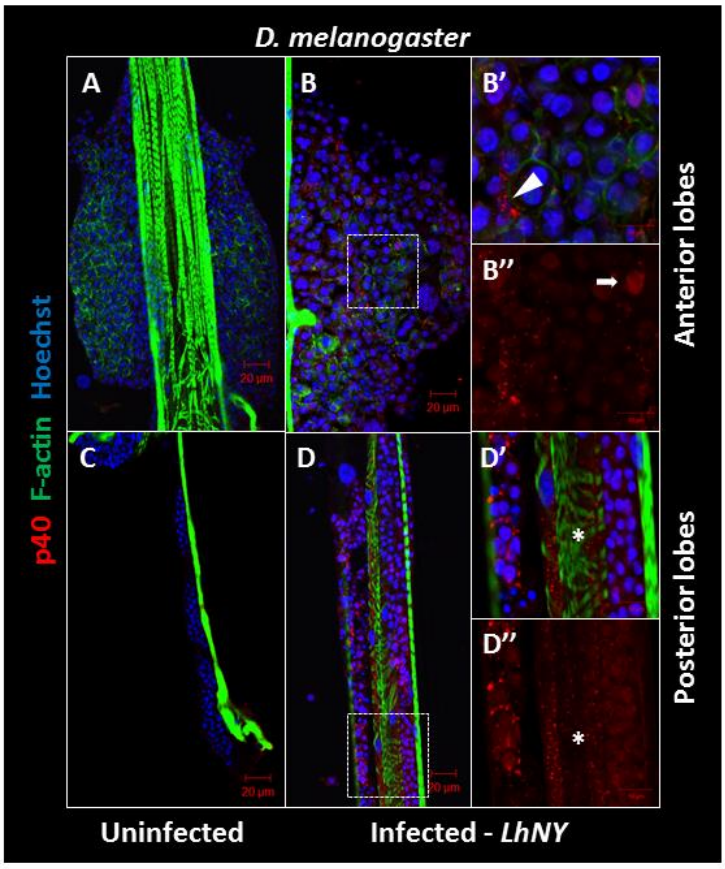

Figure S3. Effect of *Lb17* and *Lh14* infection on crystal cell development

(**A-D**) Crystal cell numbers in the three posterior larval segments decrease post infection. (**A**) Uninfected animals (n=10) have a significantly higher number of sessile population crystal cells compared to infection by *Lb17* (n=13) (**B and D**) or *Lh14* (n=13) (**C and D**). Bars in graph indicate standard deviation. Stars indicate that the difference is statistically significant from the controls (*** for $p<0.001$).

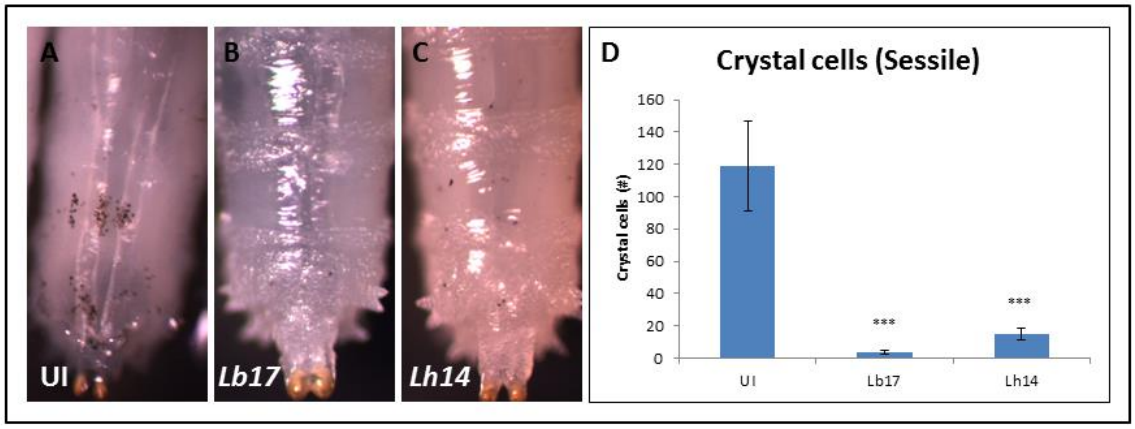

Figure S4. VLP uptake into plasmatocytes is Toll1 and Toll7 independent

Plasmatocyte specific knockdown of Toll1 (**A-C'**) and Toll7 (**D-E''**) has no impact on VLP uptake. (**A-C'**) *Pxn>Toll1* knockdown hemocytes internalize VLPs. (**D-E''**) *Pxn>Toll7* knockdown lymph gland posterior lobes cells and hemocytes internalize VLPs. Magnifications (**B-E''**) shows p40 signal in the dorsal vessel (asterisks), and internalization of the p40 signal in knockdown hemocytes (arrowheads). (**B', C', D'', and E'**) Only p40 (red) staining is shown. Hoechst stains DNA (blue). Scale bars indicate 50 µm (panels A and D), 20 µm (panel E) and 10 µm (panels B-C', D'-D'' and E-E'').

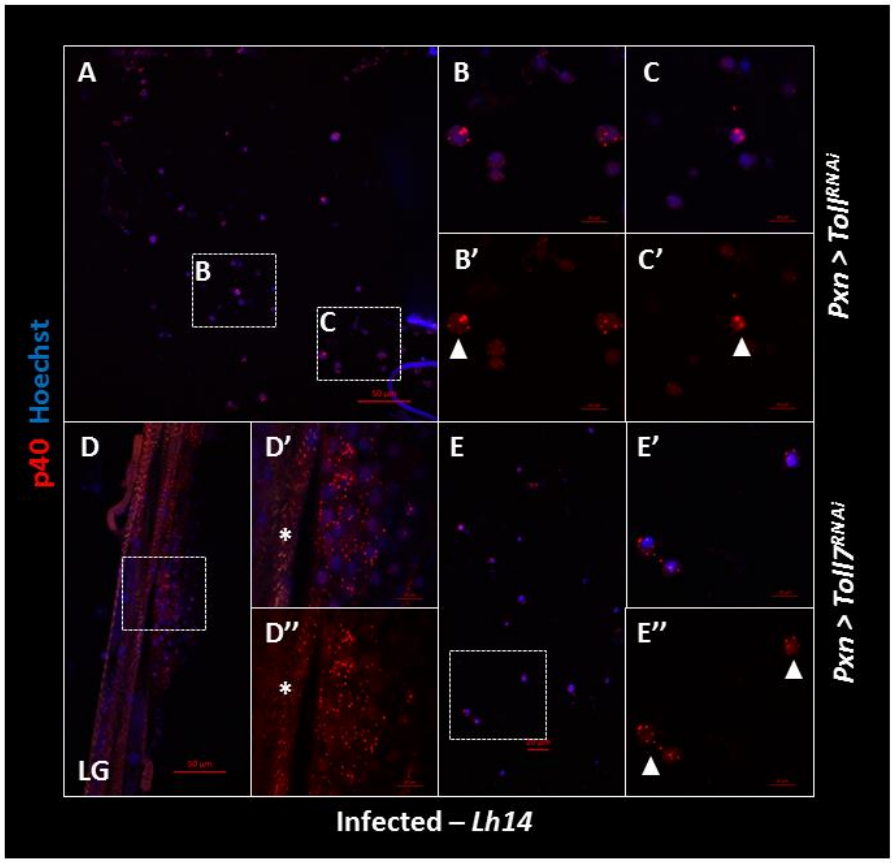

Figure S5. VLP entry into lamellocytes is integrin-β independent

(**A-A'**) Integrin-β antibody (red) signal overlaps with the specific GFP expression in lamellocytes produced in *hop*$^{Tum\text{-}l}$ animals. (**B-C'**) *hop*$^{Tum\text{-}l}$ *msn>mCD8GFP ,Intβ*^{RNAi} leads to significant knockdown of Integrin-β (compare B' to panel C') without affecting lamellocyte differentiation. (**D-E'**) p40 staining and distribution is diffuse and nuclear (arrowheads) in *hop*-$^{Tum\text{-}l}$ msn> *mCD8GFP Intβ*^{RNAi} in cells. Hoechst stains DNA (blue). Scale bars indicate 50 µm (panels A and B-C') and 10 µm (panels A' and D-E').

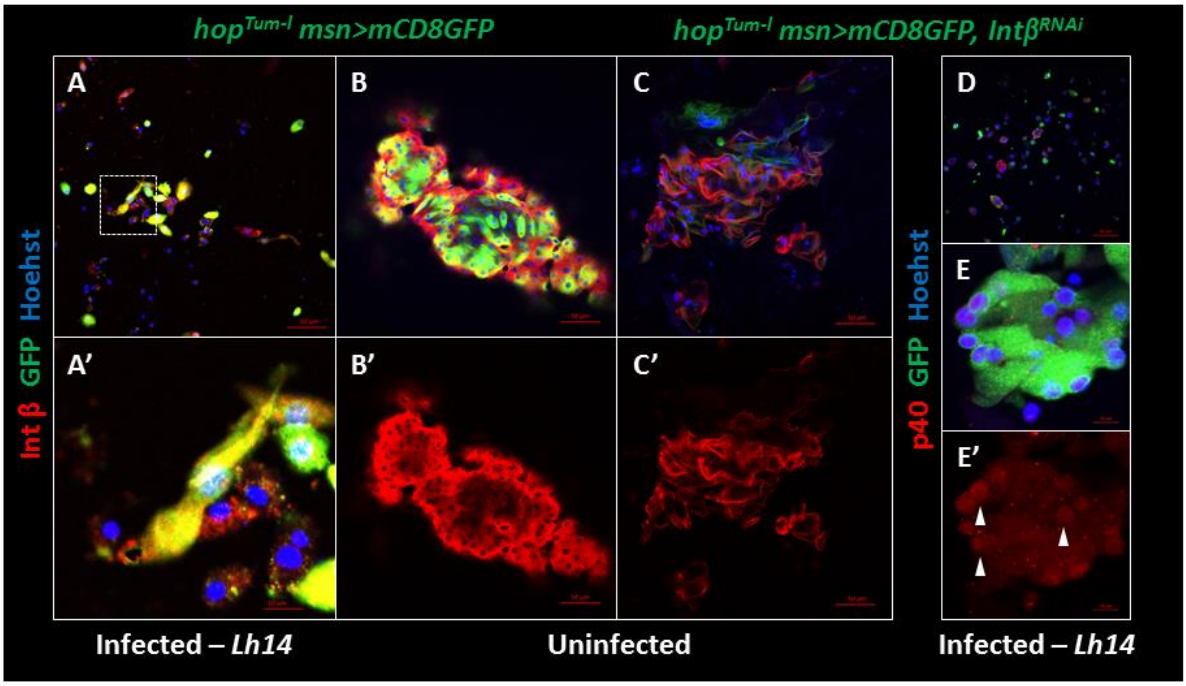

Figure S6. The effect of the niche post *LhNY* infection

(**A-A’’**) p40 staining and effect on the PSC organization from *LhNY* infected *D. melanogaster* is similar to that observed post *Lh14* infection (compare to Figure 5). The rest of the anterior lobe is also reduced as previously seen (see Figure 1, Figure 5 and Figure S2). Hoechst stains DNA (blue). Scale bars indicate 20 µm (panel A) and 10 µm (panels A’-A’’).

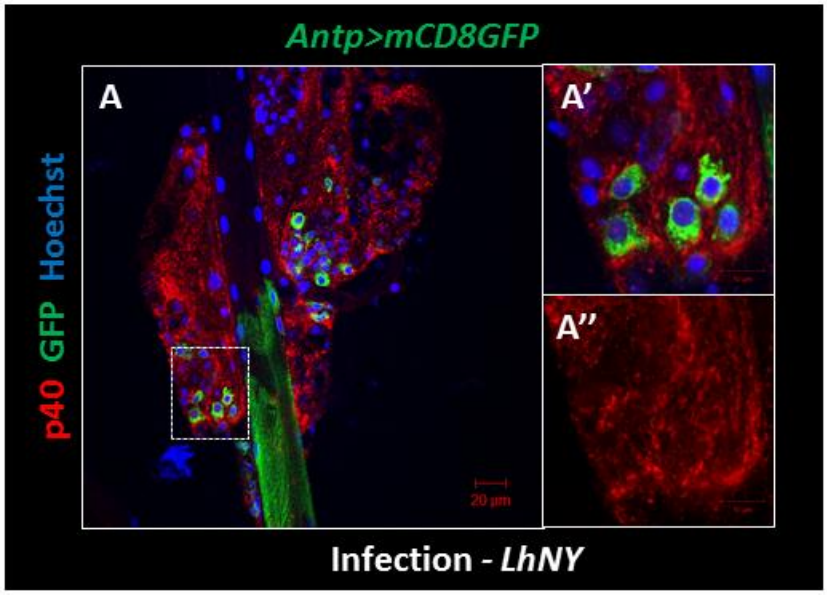

Figure S7. Knockdown of *col* in the PSC

(**A-B'**) In uninfected animals, *Antp>mCD8GFP col*^{RNAi} knockdown PSCs show no apparent effect on PSC organization or cell count (**compare panel A to panel B**). Hoechst stains DNA (blue). Scale bars indicate 20 µm.

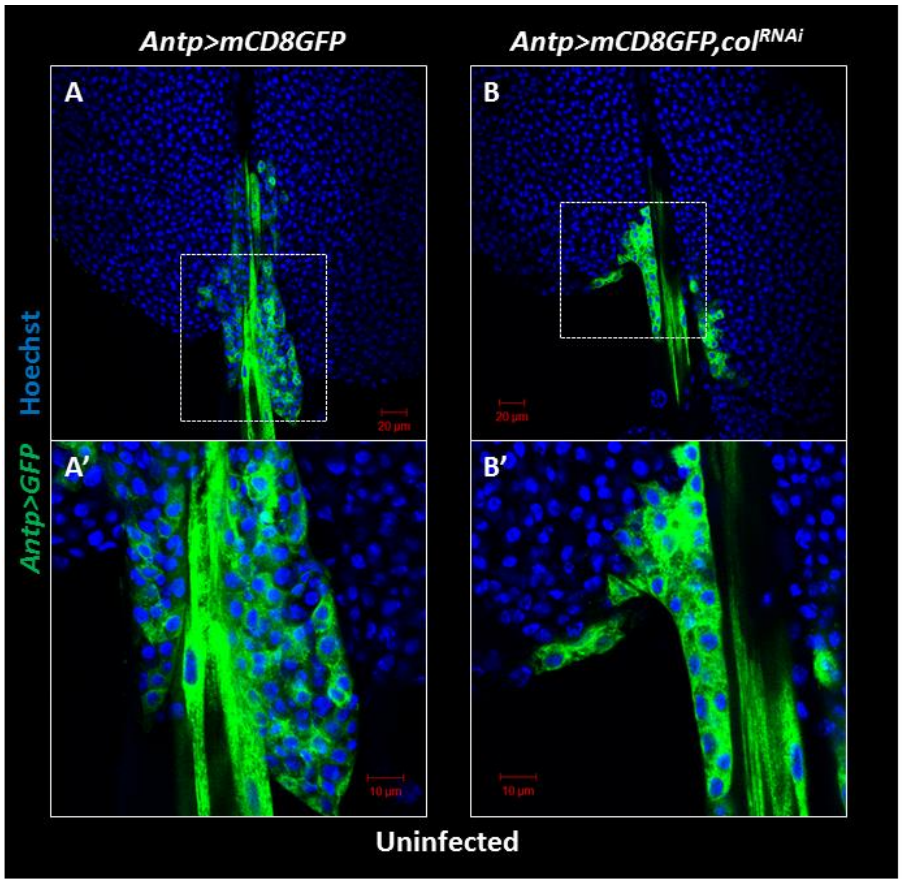

Figure S8. Knockdown of *col* in the PSC and the effect post *Lh14* infection

(**A-B'**) The compact organization of PSC cells is only slightly affected in *Lh-14* infected animals, *Antp>mCD8GFP col*^{RNAi} knockdown lymph glands (**Compare panel A to panel B**). *Antp>mCD8GFP* marks the PSC (green). Anterior lobes are reduced and cells of anterior and posterior lobes contain fragmented DNA (**C-C''**). Hoechst stains DNA (blue). Scale bars indicate 20 µm (panel A-C) and 10 µm (panels C'-C'').

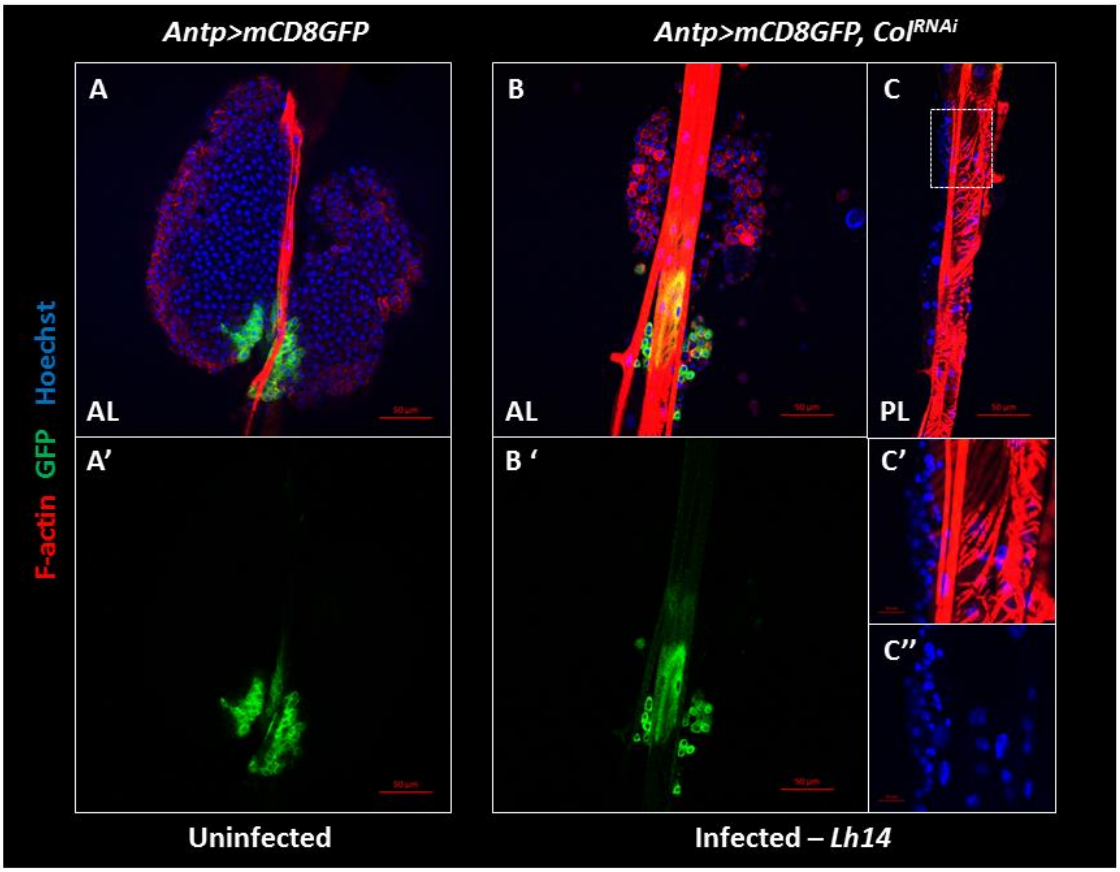

Figure S9. Annotation of predicted p40 nucleotide and amino acid sequences

(A) Blue, green and purple amino acids show mass spectrometric peptides from the p40 gel band (Chiu and Govind, unpub.). Underlined sequences were identified from the VLP proteome data (Mount Sinai). Alternate regular and yellow highlighted regions correspond to the 5 exons. (B) cDNA nucleotide sequence (GAJC01013394) aligned with predicted protein sequence shows from 5' to 3': (1) 5'UTR (gray), (2) N-terminal signal sequence, amino acids 1-27, (bold blue), start codon (green), (3) internal helical IpaD-like p40 domain (yellow), (4) C-terminal transmembrane domain, amino acid 238-264 (bold blue) with stop codon (red), and (5) 3' UTR (gray). Sequence-specific primers are underlined and arrows point to the intron insertion sites.

A

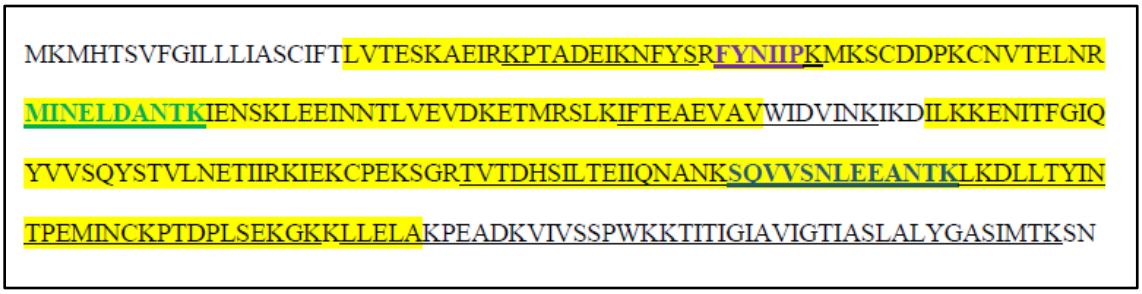

B

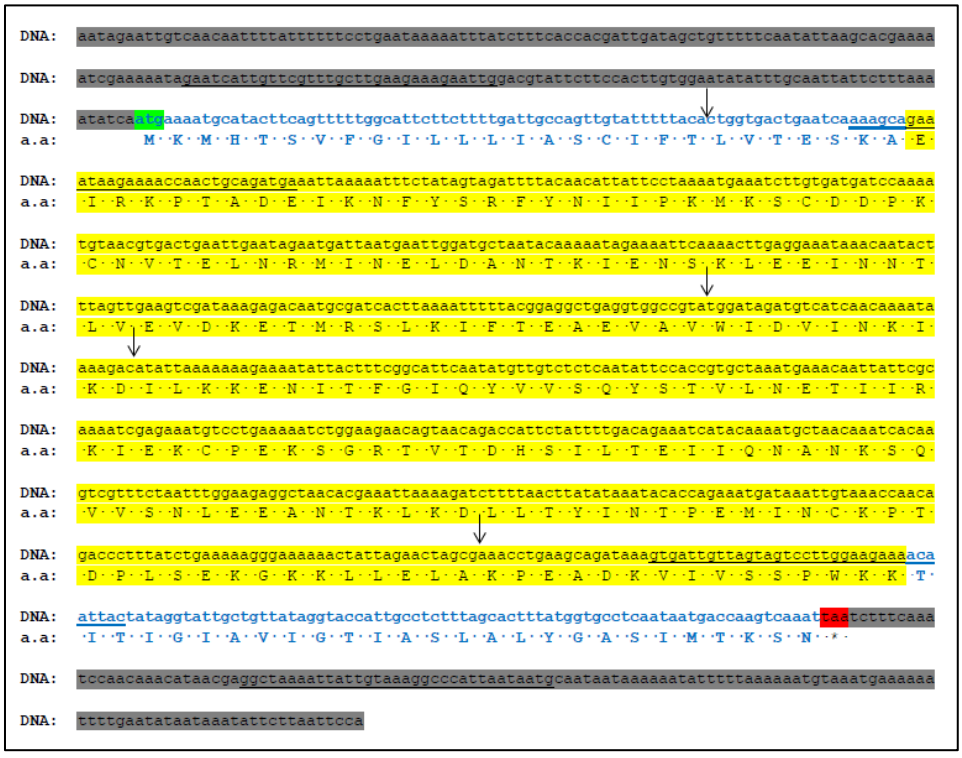

Supplementary Table 1

Template and purpose	Primers (5' to 3')	PCR conditions	Reference
Venom gland cDNA template Full length p40 cloned into pCRII Topo Dual Clone # 9 obtained	Forward – (5'UTR) GAATCATTGTTCGTTTGCTTGAAGAAA GAATTGG Reverse – (3'UTR) CATTATTAATGGGCCTTTACAATAATT TTAGCC	35 cycles Tm = 56°C	This study
Clone M1 with full-length p40 sequence in Topo2.1 DNA template (PCR errors in sequence outside the helical domain) IpaD like internal domain of p40 cloned into pTrcHisA vector. Clone #36 obtained	Forward – (p40BHI-F) ATCGCGGGATCCAAAGCAGAAATAAG AAAACCAACTGCAGATGA Reverse – (p40ERI-R) TAAGCCGAATTCCTAAGTAATTGTTTT CTTCCAAGGACTACTAACAATCAC	40 cycles Tm = 60°C	This study
Hemocyte cDNA template *p40* – IpaD like internal domain Check expression in host, no product obtained	Forward – (260F) GTGATGATCCAAAATGTAACGTGACTG Reverse – (469R) GAATGGTCTGTTACTGTTCTTCCAGA	40 cycles Tm = 56°C	This study
Hemocyte cDNA template *p40* – IpaD like internal domain Check expression in host, no product obtained	Forward – (260F) GTGATGATCCAAAATGTAACGTGACTG Reverse – (Stop-R) GACTTGGTCATTATTGAGGCACCAT	40 cycles Tm = 56°C	This study
Hemocyte cDNA template Host *rp49* control, correctly amplified	Forward – (RP-F) GACGCTTCAAGGGACAGTATCTG Reverse – (RP-R) AAACGCGGTTCTGCATGAG	40 cycles Tm = 59°C	(GUEGUEN 2013; PADDIBHATLA *et al.* 2010)

Literature Cited

AMANN, E., J. BROSIUS and M. PTASHNE, 1983 Vectors bearing a hybrid trp-lac promoter useful for regulated expression of cloned genes in Escherichia coli. Gene **25:** 167-178.

BENMIMOUN, B., C. POLESELLO, M. HAENLIN and L. WALTZER, 2015 The EBF transcription factor Collier directly promotes Drosophila blood cell progenitor maintenance independently of the niche. Proc Natl Acad Sci U S A **112:** 9052-9057.

BHUIN, T., and J. K. ROY, 2014 Rab proteins: the key regulators of intracellular vesicle transport. Exp Cell Res **328:** 1-19.

CHIU, H., and S. GOVIND, 2002 Natural infection of D. melanogaster by virulent parasitic wasps induces apoptotic depletion of hematopoietic precursors. Cell Death Differ **9:** 1379-1381.

CHIU, H., J. MORALES and S. GOVIND, 2006 Identification and immuno-electron microscopy localization of p40, a protein component of immunosuppressive virus-like particles from Leptopilina heterotoma, a virulent parasitoid wasp of Drosophila. J Gen Virol **87:** 461-470.

COLINET, D., DELEURY, E., ANSELME, C., CAZES, D., POULAIN, J., AZEMA-DOSSAT, C., BELGHAZI, M., GATTI, J.-L., POIRIE, M., 2013 Extensive inter- and intraspecific vemon variation in closely related parasites targeting the same host: The case of Leptopilina parasitoids of Drosophila. Insect Biochem and Mol Biol **43:** 601-611.

COLINET, D., SCHMITZ, A., CAZES, D., GATTI, J.-L., POIRIE, M., 2010 The origin of intraspecific variation of virulence in an eukaryotic immune suppressive parasite. PLoS Pathog **6:** e1001206.

COLLAZO, C. M., and J. E. GALAN, 1997b The invasion-associated type III system of Salmonella typhimurium directs the translocation of Sip proteins into the host cell. Mol Microbiol **24:** 747-756.

CROZATIER, M., B. GLISE and A. VINCENT, 2004a Patterns in evolution: veins of the Drosophila wing. Trends Genet **20:** 498-505.

CROZATIER, M., and M. MEISTER, 2007 Drosophila haematopoiesis. Cell Microbiol **9:** 1117-1126.

CROZATIER, M., J. M. UBEDA, A. VINCENT and M. MEISTER, 2004b Cellular immune response to parasitization in Drosophila requires the EBF orthologue collier. PLoS Biol **2:** E196.

DUBUFFET, A., COLINET, D., ANSELME, C., DUPAS, S., CARTON, Y., POIRIE, M., 2009 Variation of Leptopilina boulardi success in Drosophila hosts: What is inside the black box?, pp. 147-188 in *Advances in Parasitology*, edited by G. PREVOST. Academic Press.

EMERALD, B. S., and S. M. COHEN, 2004 Spatial and temporal regulation of the homeotic selector gene Antennapedia is required for the establishment of leg identity in Drosophila. Dev Biol **267:** 462-472.

FERRARESE, R., MORALES, J., FIMIARZ, D., WEBB, B., GOVIND, S., 2009 A supracellular system of actin-lined canals controls biogenesis and release of virulence factors in parasitoid venom glands. J Exp Biol **212:** 2261-2268.

FLORES-SAAIB, R. D., S. JIA and A. J. COUREY, 2001 Activation and repression by the C-terminal domain of Dorsal. Development **128:** 1869-1879.

GOECKS, J., MORTIMER, N.T., MOBLEY, J.A., BOWERSOCK, G.J., TAYLOR, J., SCHLENKE, T.A., 2013 Integrative approach reveals composition of endoparasitoid wasp venoms. PLoS One **8:** e64125.

GUEGUEN, G., KALAMARZ, M.E., RAMROOP, J., URIBE, J., GOVIND, S., 2013 Polydnaviral ankyrin proteins aid parasitic wasp survival by coordinate and selective inhibition of hematopoietic and immune NF-kappa B signaling in insect hosts. PLoS Pathog **In Press**.

GUEGUEN, G., RAJWANI, R., PADDIBHATLA, I., MORALES, J., GOVIND, S., 2011 VLPs of Leptopilina boulardi share biogenesis and overall stellate morphology with VLPs of the heterotoma clade. Virus Res **160:** 159-165.

IGAKI, T., H. KANUKA, N. INOHARA, K. SAWAMOTO, G. NUNEZ *et al.*, 2000 Drob-1, a Drosophila member of the Bcl-2/CED-9 family that promotes cell death. Proc Natl Acad Sci U S A **97:** 662-667.

JUNG, S. H., C. J. EVANS, C. UEMURA and U. BANERJEE, 2005 The Drosophila lymph gland as a developmental model of hematopoiesis. Development **132:** 2521-2533.
KRZEMIEN, J., M. CROZATIER and A. VINCENT, 2010a Ontogeny of the Drosophila larval hematopoietic organ, hemocyte homeostasis and the dedicated cellular immune response to parasitism. Int J Dev Biol **54:** 1117-1125.
KRZEMIEN, J., L. DUBOIS, R. MAKKI, M. MEISTER, A. VINCENT *et al.*, 2007 Control of blood cell homeostasis in Drosophila larvae by the posterior signalling centre. Nature **446:** 325-328.
KRZEMIEN, J., J. OYALLON, M. CROZATIER and A. VINCENT, 2010b Hematopoietic progenitors and hemocyte lineages in the Drosophila lymph gland. Dev Biol **346:** 310-319.
KURUCZ, E., VÁCZI, B., MÁRKUS, R., LAURINYECZ, B., VILMOS, P., ZSÁMBOKI, J., CSORBA, K., GATEFF, E., HULTMARK, D., ANDÓ, I., 2007 Definition of Drosophila hemocyte subsets by cell-type specific antigens. Act Biol Hung **58 Suppl:** 95-111.
LANOT, R., D. ZACHARY, F. HOLDER and M. MEISTER, 2001 Postembryonic hematopoiesis in Drosophila. Dev Biol **230:** 243-257.
LEBESTKY, T., T. CHANG, V. HARTENSTEIN and U. BANERJEE, 2000 Specification of Drosophila hematopoietic lineage by conserved transcription factors. Science **288:** 146-149.
LEBESTKY, T., S. H. JUNG and U. BANERJEE, 2003 A Serrate-expressing signaling center controls Drosophila hematopoiesis. Genes Dev **17:** 348-353.
LUO, H., W. P. HANRATTY and C. R. DEAROLF, 1995 An amino acid substitution in the Drosophila hopTum-l Jak kinase causes leukemia-like hematopoietic defects. EMBO J **14:** 1412-1420.
MANDAL, L., J. A. MARTINEZ-AGOSTO, C. J. EVANS, V. HARTENSTEIN and U. BANERJEE, 2007 A Hedgehog- and Antennapedia-dependent niche maintains Drosophila haematopoietic precursors. Nature **446:** 320-324.
MEGHRAOUI, A., L. SCHIAVOLIN and A. ALLAOUI, 2014 Single amino acid substitutions on the needle tip protein IpaD increased Shigella virulence. Microbes Infect **16:** 532-539.
MORALES, J., CHIU, H., OO, T., PLAZA, R., HOSKINS, S., GOVIND, S., 2005 Biogenesis, structure, and immune-suppressive effects of virus-like particles of a Drosophila parasitoid, Leptopilina victoriae. J Insect Physiol **51:** 181-195.
MORTIMER, N. T., GOECKS, J., KACSOH, B.Z., MOBLEY, J.A., BOWERSOCK, G.J., TAYLOR, J., SCHLENKE, T.A., 2013 Parasitoid wasp venom SERCA regulates Drosophila calcium levels and inhibits cellular immunity. PNAS.
NAKAMOTO, M., R. H. MOY, J. XU, S. BAMBINA, A. YASUNAGA *et al.*, 2012 Virus recognition by Toll-7 activates antiviral autophagy in Drosophila. Immunity **36:** 658-667.
NI, J. Q., L. P. LIU, R. BINARI, R. HARDY, H. S. SHIM *et al.*, 2009 A Drosophila resource of transgenic RNAi lines for neurogenetics. Genetics **182:** 1089-1100.
OYALLON, J., N. VANZO, J. KRZEMIEN, I. MORIN-POULARD, A. VINCENT *et al.*, 2016 Two Independent Functions of Collier/Early B Cell Factor in the Control of Drosophila Blood Cell Homeostasis. PLoS One **11:** e0148978.
PADDIBHATLA, I., M. J. LEE, M. E. KALAMARZ, R. FERRARESE and S. GOVIND, 2010 Role for sumoylation in systemic inflammation and immune homeostasis in Drosophila larvae. PLoS Pathog **6:** e1001234.
PETERSEN, T. N., S. BRUNAK, G. VON HEIJNE and H. NIELSEN, 2011 SignalP 4.0: discriminating signal peptides from transmembrane regions. Nat Methods **8:** 785-786.
PICKING, W. L., H. NISHIOKA, P. D. HEARN, M. A. BAXTER, A. T. HARRINGTON *et al.*, 2005 IpaD of Shigella flexneri is independently required for regulation of Ipa protein secretion and efficient insertion of IpaB and IpaC into host membranes. Infect Immun **73:** 1432-1440.
RIZKI, R. M., and T. M. RIZKI, 1984 Selective destruction of a host blood cell type by a parasitoid wasp. Proc Natl Acad Sci U S A **81:** 6154-6158.
RIZKI, R. M., and T. M. RIZKI, 1990 Parasitoid virus-like particles destroy Drosophila cellular immunity. Proc Natl Acad Sci U S A **87:** 8388-8392.

RIZKI, T. M., and R. M. RIZKI, 1992 Lamellocyte differentiation in Drosophila larvae parasitized by Leptopilina. Dev Comp Immunol **16:** 103-110.

RIZKI, T. M., and R. M. RIZKI, 1994 Parasitoid-induced cellular immune deficiency in Drosophila. Ann N Y Acad Sci **712:** 178-194.

RIZKI, T. M., R. M. RIZKI and Y. CARTON, 1990 Leptopilina heterotoma and L. boulardi: strategies to avoid cellular defense responses of Drosophila melanogaster. Exp Parasitol **70:** 466-475.

SCHIAVOLIN, L., A. MEGHRAOUI, Y. CHERRADI, L. BISKRI, A. BOTTEAUX *et al.*, 2013 Functional insights into the Shigella type III needle tip IpaD in secretion control and cell contact. Mol Microbiol **88:** 268-282.

SCHILTHUIZEN, M., NORDLANDER, G., STOUTHAMER, R., VAN ALPHEN, J., 1998 Morphological and molecular phylogenetics in the genus Leptopilina (Hymenoptera: Cynipoidea: Eucoilidae). Syst Entomol **23:** 253-264.

SCHLENKE, T., MORALES, J., GOVIND, S., CLARK, A., 2007 Contrasting infection strategies in generalist and specialist wasp parasitoids of Drosophila melanogaster. PLoS Pathog **26:** 1486-1501.

SINENKO, S. A., J. SHIM and U. BANERJEE, 2012 Oxidative stress in the haematopoietic niche regulates the cellular immune response in Drosophila. EMBO Rep **13:** 83-89.

SMALL, C., J. RAMROOP, M. OTAZO, L. H. HUANG, S. SALEQUE *et al.*, 2014 An unexpected link between notch signaling and ROS in restricting the differentiation of hematopoietic progenitors in Drosophila. Genetics **197:** 471-483.

SORRENTINO, R. P., Y. CARTON and S. GOVIND, 2002 Cellular immune response to parasite infection in the Drosophila lymph gland is developmentally regulated. Dev Biol **243:** 65-80.

STOFANKO, M., S. Y. KWON and P. BADENHORST, 2008 A misexpression screen to identify regulators of Drosophila larval hemocyte development. Genetics **180:** 253-267.

STOFANKO, M., KWON, S.Y., BADENHORST, P., 2010 Lineage tracing of lamellocytes demonstrates Drosophila macrophage plasticity. PLoS ONE **5:** e14051.

TOKUSUMI, T., SORRENTINO, R.P., RUSSELL, M., FERRARESE, R., GOVIND, S., SCHULZ, R.A., 2009 Characterization of a lamellocyte transcriptional enhancer located within the misshapen gene of Drosophila melanogaster. PLos ONE **4:** e6429.